Dissertation

Regulation of PU.1 in normal blood development and core binding factor leukemia: Role of chromatin structure and antisense transcription

Steuerung des Transkriptionsfaktors PU.1 in der Blutentwicklung: Einfluss von Chromatinstruktur und noncoding Transkription

submitted by

Priv. Doz., Dr. med. Univ.

Philipp Bernhard Staber

for the Academic Degree of

Doctor of Medical Science

(Dr. scient. med.)

at the

Medical University of Graz

Institute of Pathology

under the Supervision of

Prof. Dr. Gerald Höfler & assoc.Prof. Barbara Gürtl

Submission: 2014

Eidesstattliche Erklärung

Ich erkläre ehrenwörtlich, dass ich die vorliegende Arbeit selbständig angefertigt und abgefasst, und jene Personen und Institutionen, die am Zustandekommen der Forschungsdaten beteiligt waren, namentlich genannt habe. Andere als die angegebenen Quellen habe ich nicht verwendet und die den benutzten Quellen wörtlich oder inhaltlich entnommenen Stellen habe ich als solche kenntlich gemacht. Die Arbeit an der Dissertation und daraus entstandener Publikationen wurde gemäß den Regeln der „Good Scientific Practice“ durchgeführt.

for Lilo and Gabriela

ACKNOWLEDGEMENTS:

Many thanks to the following people for substantially contributing to the research: Pu Zhang[1], Min Ye[1], Robert Welner[1], César Nombela-Arrieta[4], Christian Bach[1], Marc Kerenyi[1,5], Elena Levantini[1], Annalisa Di Ruscio[1], Alexander K. Ebralidze[1] Boris A. Bartholdy[1], Hong Zhang[1], Merixell Alberich-Jorda[1], Sanghoon Lee[6], Henry Yang[6], Felicia Ng[7], Junyan Zhang[1], Mathias Leddin[8], Leslie E. Silberstein[4], Gerald Hoefler[9], Stuart H. Orkin[1,5], Berthold Gottgens[7], Frank Rosenbauer[8,10], Gang Huang[11], and Daniel G. Tenen[1,6].

I want to thank Christopher Hetherington for expert assistance with quantitative 3C analysis, the Dartmouth Transgenic Facility directed by Steven Fiering, and the BIDMC Flow Cytometry Facility. I want to thank Dr. Wenyi Wei and Dr. Peter Sicinski for providing reagents (Anti-Cdc25a antibody, Cdk1 expression construct respectively). I am grateful to the members of the Tenen laboratory for helpful discussions, especially Deepak Bararia. This work was supported by NIH grant R01HL112719 to D.G. Tenen and by fellowships from the Austrian Research Foundation (to P.B. Staber / Erwin Schrödinger Stipendium: J2876-B12) and the Austrian Academy of Science (to P.B. Staber / APART Stipendium: 11379). Starting January 2012 P.B. Staber has received a Marie Curie International Outgoing Fellowship from the European Union (PIOF-254486).

[1] Harvard Stem Cell Institute, Harvard Medical School, Boston, MA, USA

[2] Division of Hematology, Medical University Graz, Austria

[3] Division of Hematology and Hemostaseology, Medical University of Vienna, Austria

[4] Division of Transfusion Medicine, Children's Hospital, Boston, MA

[5] Division of Hematology/Oncology; Children's Hospital and Dana Farber Cancer Institute, Harvard Medical School, Boston, MA, USA

[6] Cancer Science Institute, National University of Singapore, Singapore

[7] Cambridge Institute for Medical Research and Wellcome Trust and MRC Stem Cell Institute, Cambridge, UK

[8] Max Delbrueck Center for Molecular Medicine, Berlin, Germany

[9] Institute of Pathology, Medical University Graz, Austria

[10] Institute of Molecular Tumor Biology, University of Münster, Germany

[11] Division of Experimental Hematology and Cancer Biology, Cincinnati Children's Hospital Medical Center, Cincinnati, OH, USA

TABLE OF CONTENTS

1 Abstract

1.1 Zusammenfassung (Deutsch)

Blutentwicklung wird über die Konzentration des Transkriptionsfaktors PU.1 gesteuert. Während der myeloischen Differenzierung muss die intrazelluläre PU.1 Konzentration ansteigen, andernfalls entsteht eine akute myeloische Leukämie (AML). Im Gegensatz dazu muss die Expression von PU.1 komplett gestoppt werden um T-Lymphozyten zu bilden. Die Mechanismen wie PU.1 abgeschaltet werden kann sind bislang unbekannt. In der vorliegenden Arbeit können wir zeigen, wie ausgewählte Transkriptionsfaktoren (Runx und, in einem positiven Vorwärtsregulationskreis, PU.1) die Chromatinstruktur des PU.1 Genlokus verändern und damit einen fundamentalen Einfluss auf die Funktion sowohl von normalen Blutstammzellen als auch leukämischen Stammzellen haben. Wir fanden heraus, das PU.1 ein Meisterregulator von Zellzyklusgenen in Stammzellen ist und dass eine verringerte Menge von PU.1 zu einer exzessiven Stammzellproliferation und konsekutiv zur Stammzellerschöpfung führt. Wir zeigen weiters, dass ein langes nicht-codierendes Antisense- Transkript von PU.1 (PU.1 AS) eine zentrale Rolle spielt um die PU.1 Expression abzudrehen. Wir vermuten außerdem, dass die 3-dimensionale Chromosomen-Architektur festlegt, ob PU.1 mRNA oder PU.1-AS transkribiert wird. Unsere Daten zeigen, dass Runx Transkriptions Faktoren einen direkten Einfluss auf die PU.1-AS Transkription haben. Runx Faktoren sind häufig verändert in verschiedenen Formen von Akuter Myeloischer Leukämie, wie in den Core Binding Factor (CBF) Leukämien t(8;21) und inv(16). PU.1 ist auch funktional defizient in diesen Leukämien. Wir zeigen, dass die Mutationen der CBF Leukämien einen Mechanismus ausnützen, der physiologisch für die T-Zell Reifung notwendig ist. CBF-Mutationen stellen eine höher geordnete Chromatinstruktur her, die die PU.1 AS Transkription ermöglicht und PU.1 mRNA abschaltet. Bisherige Studien konzentrierten sich hauptsächlich auf Mechanismen, wie Transkriptionsfaktoren eingeschaltet werden, und PU.1 wurde diesbezüglich sehr gründlich untersucht. Hier untersuchen wir das genaue Gegenteil und vermuten, dass das Abschalten von PU.1 ein aktiver Prozess ist, der eine spezifische drei-dimensonale Chromosomenformation und ein langes nicht-codierendes Antisense-transkript benötigt.

1.2 Abstract (English)

Blood development is regulated by levels of transcription factor PU.1 (encoded as *SPI1/Sfpi1*). During myeloid differentiation PU.1 levels need to increase to avoid a differentiation block, which would lead to leukemia. In contrast PU.1 expression needs to stop completely to develop T-cells. So far the mechanisms of PU.1 suppression, physiologic as for T-cell differentiation or pathologic as for leukemia development are unknown. Here we demonstrate how binding of selected transcription factors (Runx and PU.1) change the chromatin structure of PU.1 with fundamental impact on the function of normal hematopoietic stem cells (HSC) and leukemic stem cells (LSC). We found that PU.1 is a master regulator of cell cycle genes in stem cells and that a decrease of PU.1 levels results in excessive HSC proliferation and consecutively to HSC exhaustion. We further show that expression of a long noncoding antisense RNA plays a central role in silencing the expression of PU.1. We provide evidence that specific 3-dimensional chromosome architectures facilitate expression of either PU.1 mRNA or PU.1 antisense transcription by locating distal enhancer- or modifier- segments either to the proximal or the antisense promoter. Our data suggest that the tight interplay between Runx factors and PU.1 directly influences PU.1 antisense expression. Runx function is frequently affected in various leukemias such as the core-binding factor (CBF) leukemias t(8;21) and inv(16) and, importantly, PU.1 is functionally deficient in these diseases. We thus conclude that fusion oncoproteins of CBF leukemias hijack a mechanism, which is required for normal T-cell development. They establish a specific higher-order chromatin structure leading to PU.1 antisense transcription and active PU.1 silencing. Former studies have mainly focused on mechanism how transcription factors are up-regulated and regulation of PU.1 is particularly well studied in this respect. Here, we also studied the opposite suggesting that silencing transcription factor PU.1 is an active process that requires a specific chromosome formation and transcription of a non-coding antisense transcript.

2 Introduction

2.1 The transcription factor PU.1 : Importance of tight regulation in hematopoiesis

PU.1 is a hematopoietic lineage-specific transcription factor of the ETS family that is absolutely required for normal hematopoiesis (Moreau-Gachelin et al., 1988, Tenen, 2003). The level of PU.1 expression is critical for specifying cell fate and, even modest decreases in PU.1 can lead to leukemias and lymphomas or loss of hematopoietic stem cells (Moreau-Gachelin et al., 1988, Tenen, 2003, Cook et al., 2004, Dahl et al., 2003, DeKoter and Singh, 2000, Huang et al., 2008, Rosenbauer et al., 2006, Rosenbauer et al., 2004, Rothenberg and Anderson, 2002, Staber et al., 2013). PU.1 transcripts are upregulated at day 7 of hematopoiesis, around the time of appearance of myeloid precursors in the murine embryonic stem cell model (Voso et al., 1994). Recent examples of dose-dependent PU.1 functions are the differentiation choices of dendritic cells versus macrophages, neutrophils versus macrophages, and B2 versus B1 B cells (Dahl et al., 2003, Bakri et al., 2005, Ye et al., 2005, Rosenbauer et al., 2006, Carotta et al., 2010). PU.1 gene expression is strictly regulated through the proximal promoter (prPr) (Chen et al., 1995) and an upstream regulatory element (URE) located –14kb or –17kb upstream of the transcription start site in mice and humans, respectively (Li et al., 2001, Rosenbauer et al., 2004). Removal of this URE results in 80% reduction of PU.1 expression in bone marrow compared to wild-type mice and leads to the development of leukemias or lymphomas (Rosenbauer et al., 2004, Rosenbauer et al., 2006). These results emphasize that tight regulation of PU.1 levels is critical for specifying cell fate and tumor suppression and establish that PU.1 mediates its functions via gradual expression level changes rather than binary on/off states.

2.2 PU.1 in hematopoietic stem cells

So far, dose-dependency of PU.1 functions has not been considered in any study of HSCs. Previous studies using fetal liver HSCs reported a lack of homing related integrins in PU.1 complete knock out cells which resulted in defects to colonize bone marrow in transplantation assays preventing further functional testing (Fisher et al., 1999, Kim et al., 2004, Iwasaki et al., 2005). Therefore, besides the importance for HSC homing after transplantation no further

functional role of PU.1 in HSCs could be retrieved from these models. Interestingly, when bypassing the homing defect in adult mice (through PU.1 deletion after engraftment of transplanted HSCs had occurred) erythro-myeloid repopulation capacity persisted suggesting that PU.1 might not have a role in adult HSC maintenance (Dakic et al., 2005). However, we here have developed a mouse model with decreased PU.1 levels specifically in phenotypic HSCs, which preserved normal bone marrow homing capabilities. HSCs with decreased PU.1 levels are functionally compromised in competitive repopulation and serial transplantation assays, and are insufficient to regenerate bone marrow after injuries. Mechanistically we found that in HSCs PU.1 acts as a master regulator of multiple cell cycle genes, restricting disproportionate HSC proliferation and sustaining HSC functional integrity. Moreover, we present direct evidence that positive autoregulation is necessary to establish and maintain normal PU.1 levels in HSCs of adult mice. Our study further provides the experimental proof to connect binding of a single transcription factor, PU.1 to changes in chromosome structure and gene expression.

2.3 PU.1 and Runx transcription factors

As the DNA-binding subunit of the heterodimeric transcription factor CBF (core binding factor), the three isoforms of the RUNX family, RUNX1 (AML1/CBFA2/PEBP2aB), RUNX2 (AML3/CBFA1/PEBP2aA), and RUNX3 (AML2/CBFA3/PEBP2aC), regulate normal cell specification during development and are commonly altered in many forms of leukemia and cancer [reviewed in (Ito, 2008, Blyth et al., 2005)]. Runx1 and CBFβ, the heterodimeric partner of all three Runx proteins, are the most frequent mutational targets in acute myeloid leukemia. They are disrupted either by chromosomal translocations creating oncogenic fusion proteins such as AML1-ETO and CBFB-MYH11, or by intragenic loss of function mutations and loss of heterozygosity (Miyoshi et al., 1991, Tang et al., 2009, Schnittger et al., 2011, Gaidzik et al., 2011, Silva et al., 2003). In leukemia with chromosomal translocations, a dominant negative effect of the fusion protein and inactivation of the Runx downstream target PU.1 has been considered as a critical mechanism of leukemia development (Vangala et al., 2003, Goyama and Mulloy, 2011, Huang et al., 2011, Huang et al., 2008, Meyers et al., 1995, Yergeau et al., 1997, Okuda et al., 1998, Castilla et al., 1996).

Runx1 knockout mice lack definitive hematopoiesis (Okuda et al., 1996), mainly due to the essential role of Runx1 in the endothelial to hematopoietic cell transition during embryonic development (Chen et al., 2009, Hoogenkamp et al., 2009, Lancrin et al., 2009, Eilken et al., 2009). However, studies on its function in adult hematopoietic stem cells (HSCs) have been inconsistent, with some demonstrating that Runx1 deficiency results in HSC defects (Ichikawa et al., 2008, Jacob et al., 2010), and others suggesting minimal impact on HSCs (Cai et al., 2011, Ichikawa et al., 2004). Partial and varying compensation by other Runx family members might explain the discrepancies of these reports, given that all three Runx family members bind directly to a conserved nucleotide sequence (-TGNGGTA-). Indeed, it was shown recently that Runx3 has an antiproliferative function in HSC/progenitors of aged mice (Wang et al., 2013). In this report, utilizing a knock-in mouse model in which binding of all Runx factors at the -14kb upstream enhancer of PU.1 is abolished (Huang et al., 2008), we could rule out any compensatory effects of individual Runx family members. Using this model, we here observe mayor importance of the Runx-PU.1 pathway for HSC function. Mechanistically, Runx binding facilitated chromosomal loop formation between the PU.1 enhancer and its proximal promoter, thereby promoting transcription. Importantly, we further found that Runx induced PU.1 expression is essential for leukemic initiating cell (LIC) function in AML/ETO9a leukemia. These findings point to the importance of PU.1 in both normal and leukemia stem cells.

2.4 Chromatin structures and transcription.

The spatial organization of the genome is fundamental for transcriptional regulation. Chromatin loops bring enhancers or insulator elements into close physical proximity with promoters, thereby activating or repressing gene transcription, respectively (Engel and Tanimoto, 2000, Staber et al., 2013, Kagey et al., 2010, Zhao et al., 2006). These interactions occur in cis along the same chromosome or in trans between different chromosomes and occupy distinct chromosome territories within the nucleus (Schardin et al., 1985, Schoenfelder et al., 2010, Zhao et al., 2006). Recent advances in genomic high-throughput technologies, such as the 4-C and Hi-C method, led to identify chromatin interactions of particular regions with interacting elements at a genome wide range (Zhao et al., 2006, Dixon et al., 2012, Duan et al., 2010, Dekker et al., 2002, Sexton et al., 2012). Using these technologies recent studies have uncovered networks of interactions that are specific to

embryonic stem cells (ESC) or induced pluripotent stem cells (iPSC) (Apostolou et al., 2013, Phillips-Cremins et al., 2013, Wei et al., 2013, Zhang et al., 2013). Since time course studies during iPSC generation or ESC differentiation observed changes of chromatin interactions days before transcriptional changes occurred it is more likely that specific genome configurations are the functional cause rather than a byproduct of transcription (Apostolou et al., 2013, Wei et al., 2013). Chromatin interactions are established and maintained by two classes of proteins: First, "architectural" proteins, which are non-cell-type-specific factors without sequence specific binding properties like the insulator-binding protein CTCF (Splinter et al., 2006), the cohesin complex and Mediator (Kagey et al., 2010). Second, transcription factors which mediate chromatin interactions in cell-type-specific and sequence-specific manner (Staber et al., 2013). Since CTCF, cohesin and Mediator do not have sequence binding properties, transcription factors may generally function by recruitment of these factors (Sexton and Cavalli, 2013).

2.5 Noncoding RNAs: another component of epigenetic regulation.

Stem cells express unusually high numbers of genes compared to more differentiated cells, and precisely regulated timing and levels of gene expression appear to be critical to cell fate determination. This concept is particularly well demonstrated in hematopoiesis, which is controlled by finely tuned combinations of transcription factors in a stage-specific context, and dose-dependent manner (Tenen, 2003). Clearly, multiple mechanisms of gene regulation function to determine stem cell fate, among those many are imposed on the epigenetic level. The latter is characterized by formation of the inheritable "active" or "silent" chromatin states. The important marks of these two opposite states of chromatin structure are covalent histone modifications, such as acetylation, methylation and phosphorylation, DNA cytosine methylation, and nucleosome positioning (Schubeler and Elgin, 2005, Rando and Ahmad, 2007, Plass et al., 2008, Mendenhall and Bernstein, 2008, Bonifer, 2005). Introduction of microarrays, chromatin immunoprecipitation, and high throughput genome-wide sequencing revealed a quite unexpected result: Existence of bidirectional transcription of eukaryotic genes and the widespread occurrence of long noncoding RNA transcripts (longer than 200 nucleotides) (Carninci, 2009, Carninci et al., 2005, Katayama et al., 2005, Okazaki et al., 2002, Olivarius et al., 2009, Cheng et al., 2005, Mendenhall and Bernstein, 2008, Guttman et

al., 2009, Lee and Bartolomei, 2013, Rinn and Chang, 2012). Noncoding RNAs have been reported to associate with chromatin-modifying complexes like the polycomb repressive complex, PRC2 and the LSD1/REST/coREST compexes, histone methyltransferase, G9a and DNA methyl transferases (1, 3a, 3b) indicating their role as epigenetic regulators (Lee, 2012, Zhao et al., 2008, Sado et al., 2005, Nagano et al., 2008, Rinn et al., 2007, Khalil et al., 2009, Tsai et al., 2010, Di Ruscio et al., 2013).

2.6 Chromatin architecture of the PU.1 gene locus

Proving a causal relationship between binding of transcription factors and formation of chromatin loops has been difficult. However, using genetically engineered transcription factor binding-site-mutants of the PU.1 gene locus we recently could demonstrate that transcription factor binding is essential for chromatin loop formation as measured by quantitative chromosome conformation capture (3C) (Staber et al., 2013). Together with in vivo footprinting experiments using MNase, DNase I, and DMS we learned that the proximal promoter and the upstream regulatory element (URE) of PU.1 adopt differential patterns of chromatin fine structure in primary macrophages (active chromatin; high PU.1 expression) and T cells (silent chromatin but open chromatin conformation; no PU.1 expression) (Hoogenkamp et al., 2007). Also, histone H3 acetylation occurs over the PU.1 gene regulatory regions as well as a significant level of H3 lysine4 trimethylation (Hoogenkamp et al., 2007). The latter was correlated with the induction of the gene expression. Furthermore, an extensive nucleosome remodeling over the transcription start site was observed in PU.1 expressing cells and pronounced differences in nucleosome positioning between PU.1 expressing and nonexpressing cell types (Hoogenkamp et al., 2007). The PU.1 locus remains open and accessible already at early phase of hematopoiesis, and thus its tight regulation needs active mechanisms to control the wide range from very high expression to complete repression.

2.7 Noncoding RNAs occurring in the PU.1 gene locus

Dr. Tenen's laboratory has discovered naturally occurring antisense transcripts overlapping the PU.1 coding region. (Figure 1). These transcripts were found in a variety of

PU.1 expressing and non-expressing human and murine tissue culture and primary hematopoietic cells. 5'- RACE experiments revealed the antisense transcription start site (ATSS) within an evolutionarily conserved cis-element in intron 3, the homology region H3 (Ebralidze et al., 2008). To test for a potential regulatory role of the antisense RNAs on PU.1 expression, RNA interference experiments were performed with siRNAs targeting human PU.1 antisense RNAs. Strikingly, H3-specific siRNAs induced increases in PU.1 protein levels of ~210%, and increases in PU.1 mRNA levels of ~145% ($p<0.001$). However, antisense transcripts themselves were only decreased in cytoplasmic and polysomal fractions. Similar results have been obtained with siRNAs specifically targeting murine PU.1 antisense RNAs in the murine cell line RAW 264.7 (Ebralidze et al., 2008). Altogether, these siRNA experiments provided evidence that one way of action of antisense noncoding RNAs of the PU.1 locus is interference with PU.1 mRNA translation. On the other hand due to technical limitations and the lack of nuclear knock down of antisense noncoding RNAs their function in the nucleus remains unclear.

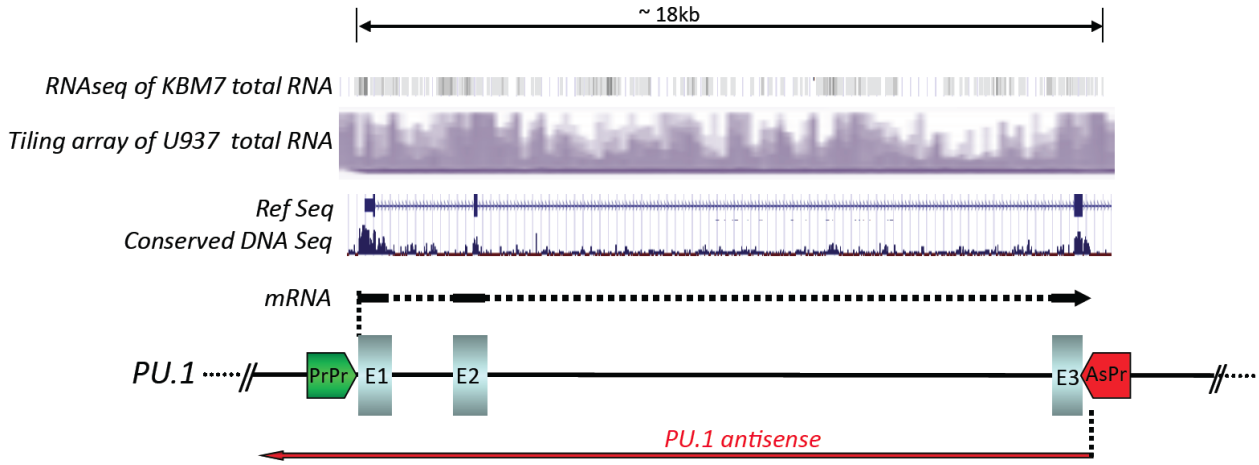

Figure 1. PU.1 mRNA and PU.1 antisense RNA expression. Scheme localizing transcripts at the PU.1 locus (PrPr-proximal promoter, AsPr-antisense promoter, E-exon). Expression is indicated by RNA-sequencing of the haploid cell line KBM7 (Burckstummer et al., 2013) and high resolution tiling array data of the myeloid cell lone U937 (own preliminary data in collaboration with Roche Nimblegen).

3 Methods

3.1 Mice

All mice were kept in a sterile barrier facility approved by the Beth Israel Deaconess Medical Center Institutional Animal Care and Use Committee. To generate mutant PU.1 site knock-in mice ($PU.1^{ki/ki}$) we used the pPNT-(–14 kb URE) targeting vector (Rosenbauer et al., 2004) and introduced a GGAA to TCGC mutation by site directed mutagenesis (Okuno et al., 2005). Figure S1A indicates the exact position of the binding site mutation. 20µg of the linearized (Not1) construct was used to transfect R1 embryonic stem cells. Generation, identification, and conformation of positive embryonic stem cell clones, chimera mice and heterozygous mice was performed as previously reported (Rosenbauer et al., 2004). Non-conditional and Mx1Cre conditional PU.1 knockout mice, as well as transgenic mice with human PU.1 BAC used in this study have been described previously (Iwasaki et al., 2005, Leddin et al., 2011, Back et al., 2004). Generation of PU.1-URE-mRunx mice was previously reported (Huang et al., 2008). Supplemental Figure S1A indicates the exact position of binding site mutations. Mx-1Cre conditional Runx1 knockout mice as well as transgenic mice with a human PU.1 BAC used in this study have been described previously (Growney et al., 2005, Leddin et al., 2011). All mouse strains were crossed into C57B6 mice for at least 6 generations. Primer sequences for genotyping PCRs are listed in Supplementary Table S3. All mice used in this study were 3-4 months of age.

3.2 Bone Marrow Transplantations

For Limiting dilution long-term competitive reconstitution assays HSCs were collected from CD45.2+ mice (WT and PU.1ki/ki), indicated number of cells were re-sorted into individual wells of a 96-well plate containing $2x10^5$ CD45.1+ whole bone marrow cells in PBS, and transferred i.v. into lethally irradiated CD45.1+ recipients (650 rads twice with a 4-hour interval). Peripheral blood and bone marrow was obtained from each mouse after 6 months and analyzed by FACS. A recipient mouse was considered positive if CD45.2+CD45.1- cells are present in myeloid and B and T cells, comprise more than 0.3% of cells in peripheral blood and if CD45.2+CD45.1- HSC were detectable in bone marrows.

Serial and competitive long-term total bone marrow transplantations were performed as described in the figure legends.

3.3 Cell Cycle Analysis

BrdU incorporation was measured by flow cytometry using an APC BrdU Flow Kit (BD Pharmingen) following the manufacturer's protocol on gated Lin^-, $Sca1^+$, $c\text{-}kit^+$, $CD150^+$, $CD48^-$ cells or cultured LSKs (sh-RNA knockdown studies). For Hoechst/Pyronin Y staining, sorted HSCs (lin-sca1+ckit+CD150+CD48-) were suspended in phosphate-citrate buffer solution with 0.02% saponin for permeabilization, and then incubated with Hoechst 33342 (Invitrogen) and Pyronin Y (Sigma-Aldrich).

3.4 Chromosome Conformation Capturing (3c)

Bone marrow of 4 individual animals (either $PU.1^{ki/ki}$ or WT) was pooled and $2x10^5$ sorted cells were used (Macrophages [Mac], Lin^-, $Sca1^+$, $c\text{-}kit^+$ [HSC]). We used a modified protocol of Dostie and Dekker (Dostie and Dekker, 2007) to reduce the amount of cellular material needed and to quantify interactions of the -14kb URE (H2 region) or proximal promoter (prPr) with other genetic elements of the PU.1 locus (detailed protocol as Supplementary Table S4). Fig. 6A demonstrates localization of Bgl2 restriction sites. A TaqMan probe was designed for the H2 fragment of the -14kb URE containing the PU.1 autoregulatory site. As a "housekeeping gene", we used an amplicon within two Bgl2 restriction sites in intron 3 of the PU.1 gene. Exact sequence information of all primers and probes used are shown in Supplementary Table S3. 3C experiments were performed as two independent biological and two technical replicates.

3.5 Flow Cytometry

Single-cell suspensions were analyzed by flow cytometry using the following monoclonal antibodies (mAbs) conjugated with phycoerythrin (PE), PE-CY7, fluorescein isothiocyanate (FITC), allophycocyanin (APC), APC-Cy7 or eFluor 450 obtained from BD Pharmingen (BD), BioLegend (San Diego, CA) or eBioscience (San Diego, CA): Mac-1/CD11b (M1/70), Gr-1 (8C5), CD3 (KT31.1), CD4 (GK1.5), CD8 (53-6.7), B220 (RA3-6B2), CD19 (1D3),

TER119 (TER-119), Sca1 (E13-161-7), c-Kit (2B8), CD16/32 (2.4G3), Thy-1.2 (53-2.1), CD135 (AF2 10.1), CD48 (HM48-1), Ly5.1 (A20), Ly5.2 (104), and CD150 (TC15-12F12.2). Viable cells were identified either by propidium iodide (PI) or 4',6-diamidino-2-phenylindole (DAPI) exclusion. Cells were analyzed by LSRII flow cytometer or sorted by FACSAria (BD Biosciences, San Jose, CA). Diva software (BD) or FlowJo (Tree Star) was used for data acquisition and analysis.

3.6 Laser Scanning Cytometry Analysis Of Femoral Bone Marrow Cryosections

Femoral bones were isolated, fixed in PLP (paraformaldehyde-lysine-periodate) for 4-8 hours, rehydrated in 30% sucrose for 48 hours and snap frozen in OCT (TissueTek). Bones were sectioned using the Cryojane tape transfer system (Leica microsystems). Single cell-thick (5µm) sections were immunostained. In brief, sections were blocked with PBS 10% donkey serum, and stained with goat anti c-kit (R&D systems) followed by donkey anti goat DyLight488 (Jackson Immunoreseach). Excess purified goat IgG was then used to block. Biotynilated antibodies against lineage markers, CD48 and CD41 were then added (rat anti-B220, rat anti-Ter119, rat anti-Gr-1, rat anti-CD41, hamster anti-CD3 and hamster anti-CD48, from eBiosciences), together with rabbit anti-Laminin (Sigma-Aldrich). After washing, sections were stained with biotinylated goat anti-hamster (Jackson Immunoresearch) followed by Donkey anti-rabbit DyLight649 (Jackson Immunoresearch), Streptavidin AF555 and DAPI (Invitrogen). In between all staining steps sections were washed in PBS/0.1%Tween20 3x 5mins. Sections were then dehydrated in ethanol gradients, mounted using Vectashield mounting media (Vector Labs) and kept at 4 °C until imaged. Laser Scanning Cytometry was performed with a iCys Research Imaging Cytometer 4-laser system (Compucyte), equipped with 4 laser lines (405, 488, 561 and 633 nm) and 4 detectors with the following filter sets 450/40, 521/15, 575/50 and 650/LP. Sections were scanned with a 10x objective using the 405nm laser to generate low resolution images of the DAPI stained nuclei and obtain a general view of the BM. Subsequently, sections were divided in small regions that were scanned with a 40x dry objective lens at a spatial resolution of 0.25 mm stage step size to create high resolution field images of the whole BM cavity. Lasers scanned BM sections in independent passes. Detector levels were set according to background fluorescence of isotype control stained sections, which were always scanned in parallel to

stained samples. Data was analyzed post-acquisition using iCys Cytometric Analysis Software (Compucyte). Images were exported into Photoshop (Adobe Inc) for processing.

3.7 Real-Time PCR

RNA was purified using RNeasy Micro Kit (Qiagen) after cells were directly sorted into a tube containing 350µl of RLT buffer (Qiagen). RNA was either directly used in Taqman RT-PCR or reverse-transcribed and subsequently amplified with a Rotor-Gene 6000 RT-PCR machine (Corbett). Transcript levels of tested genes were normalized to 18S (Applied Biosystems), or GAPDH. Sequence information of primers and Taqman probes is listed in Supplementary Table S3.

3.8 Microarray Gene Expression Analysis

RNA of sorted HSCs (lin-sca1+ckit+CD150+CD48-) was purified using an RNeasy Micro Kit (Qiagen). Quality of RNA (10ng per sample) was tested using bioanalyzer Pico –Chip (Agilent) with RIN (RNA Integrity Number) > 6.7 as threshold. RNA/cDNA amplification was performed with an Ovation Pico WTA System (NuGen) resulting in > 5µg cDNA per sample. Mouse430_2 arrays (Affymetrix) were used for hybridizations. Original raw data (CEL files) were stored at the gene expression repository at the Harvard Stem Cell Institutes (bloodprogram.hsci.harvard.edu) and in the gene expression omnibus database (http://www.ncbi.nlm.nih.gov/geo/query/acc.cgi?acc=GSE33031) according to MIAME standards. All raw data were preprocessed using RMA (Irizarry et al., 2003) to obtain expression intensities at gene levels and then normalized using the cross-correlation method(Chua et al., 2006) to minimize chip-to-chip or sample-to-sample variations. Differential expression was called based on the mean log2 fold changes (≥1.5-fold) and p value ($p \leq 0.05$) of modified t-statistics between mutants and their corresponding controls. Gene Ontology analysis was performed for the differentially expressed genes using DAVID (Database for Annotation, Visualization and Integrated Discovery). Enriched categories were obtained in comparison to the whole mouse genome as background. All *P*-values were calculated based on Fisher exact test and further corrected using the Benjamini & Hochberg method. All heatmaps were generated using hierarchical clustering with average linkage, and

genes were sorted based on the mean fold changes. GSEA analysis were performed as described in legends of Supplementary Figures S2 and S5.

3.9 Western Blot

Antibodies for immunoblotting were mouse monoclonal anti-Hsp90 (catalog number 610418, BD Biosciences, San Jose, CA), rabbit polyclonal anti-PU.1, donkey anti-rabbit IgG-HRP, and goat anti-mouse IgG-HRP (catalog numbers sc-352 X, sc-2313, and sc-2031, respectively; all from Santa Cruz Biotechnology, Santa Cruz, CA). Total cell extracts were prepared from murine bone marrow cells by direct lysis in SDS sample buffer and subsequent denaturation. Antibodies for detection were used at dilutions ranging from 1:2000 to 1:10,000. To test knockdown efficiency of Cdk1 and Cdc25a, total cell lysates of cotransfected HEK293T cells were blotted and probed with either mouse monoclonal anti-flag M2 (1:20,000, catalog number F3165, Sigma-Aldrich, St Louis, MO) or mouse monoclonal anti-Cdc25A (F-6) (Santa Cruz, catalog number sc-7389, 1:2,500).

3.10 ChIP-Seq Analysis

Data source and processing

H3K4me3 and H3K27me3 ChIP-Seq data for LSK cells were obtained from (Adli et al., 2010). SRA files were downloaded from the Gene Expression Omnibus website. These files were converted to fastq format for further processing. PU.1 ChIP-Seq data for HPC-7 cells and macrophages were obtained from previously published studies-(Wilson et al., 2010a, Heinz et al., 2010). Sequencing reads in fastq format were mapped to the mouse reference genome, mm9, using Bowtie. The output sam files from bowtie for replicate samples were merged and then converted to bed format of 200 bp width. Finally, coordinates in the reads bed file that extend beyond actual chromosome sizes were corrected. Visualization of mapped reads in the genome was done in UCSC Genome Browser with BigWig files. First, bed files were converted to wig files. BigWig density profiles were then generated from the wig files using wigToBigWig from UCSC.

The peak identification parameters were: 1)The peak identification threshold: peak height >=10; 2) Genomic regions relative to genes: promoter region (500bp to TSS); proximal promoter region (5kb to TSS) 3) IgG background – height for IgG peak < 10; 4) IgG

background – Fold change of specific pulldown vs IgG >= 2. Numbers of cell cycle gene sets: 1) 52 in DEGs and 121 in non-DEGs for Pu.1 bounded genes; 2) 163 in DEGs and 836 in non-DEGs for all genes.

Read Density Visualization

Visualization of genome-wide promoter read densities were carried out using the seqMINER software (Ye et al., 2011). First, transcription start sites for the entire genome were obtained from UCSC refGene table and were used as reference coordinates in seqMINER. Second, processed bed files were used as input aligned reads. Finally, clustering and heatmap of the promoter region were generated for +/-5kb region around the transcription start site. In Figure 4c the Integrative Genomics Viewer (www.broadinstitute.org/igv/) was used for visualization of ChIP seq reads.

3.11 Viral vectors and transduction

Specific shRNA and a NSC shRNA were cloned into the lentiviral vector pGhU6 (Radomska et al., 2012) containing a eGFP sequence via Hpa1 and Xho1 restriction sites. Knockdown efficacy of constructs at protein level was tested in HEK293T cells that have been cotransfected with murine CDK1 (CDK1 Mm p3xflag-CMV, kindly provided by Peter Sicinski, Dana Faber) or murine CDC25A (CDC25A-pCMV-Sport6 obtained from Dana Faber/HCC DNA Resource Core [MmCD00320178]). Murine NIH3T3 cells have been transfected with shRNA constructs and knockdown of endogenous mRNA was tested in GFP sorted cells. For virus production, HEK293T cells were cotransfected using lipofectamine 2000 with selected shRNA constructs and lentiviral constructs (Gag-Pol and Env). Virus was harvested after 48 hours and concentrated using a Centricon Plus-70 100000 MWCO column (Millipore). Lentiviral transduction was performed in culture dishes (Falcon 1008; Becton Dickinson, Lincoln Park, NJ) in the presence of polybrene (8µg/ml) (Sigma). Various dilutions for each virus were tested in cultured LSK cells (2000 cells per well in a 96-well dish) of wild type mice to achieve a transduction efficacy of > 20% (GFP+). For all experiments, LSKs were cultured in CellGenix SCGM medium + 100ng/ml SCF, 50ng/ml TPO, 10ng/ml flt3.

3.12 Chromatin Immunoprecipitation

Chromatin immunoprecipitation (ChIP) assays were done on total bone marrow cells (2 X 10^6 cells/one ChIP) DNA using a EZ ChIP (Upstate Biotechnology) and followed the manufacturer's protocols with some modifications. Formaldehyde was added to the cells in a culture dish to a final concentration of 1% and incubated at 37°C for 10 min. The cells were washed in 1 mL of ice-cold PBS with proteinase inhibitors, and resuspended in 400 µL of SDS lysis buffer. Lysates were sonicated for nine 10 second pulses on wet ice and centrifuged at 15,000 rpm for 10 min at 4°C. Supernatants were loaded on 1% agarose gels and determined to have reduced DNA lengths between 200 and 1,000 bp. The sonicated samples were pre-cleaned with salmon sperm DNA/protein A agarose beads (Upstate Biotechnology). The soluble chromatin fraction was collected, and 8 µL of polyclonal rabbit antibody to PU.1 (Spi-1, Santa Cruz sc-352), polyclonal rabbit antibody to RunxL1 (CST #4334), IgG control antibody or no antibody, was added and incubated overnight with rotation. After rotation, chromatin-antibody complexes were collected using salmon sperm DNA/protein A agarose beads and washed according to the manufacturer's protocol. Immunoprecipitated DNA was recovered using a QIAquick PCR Purification Kit (Qiagen) and analyzed by q-PCR (primer sequence information in Supplementary table S3). One additional primer set was used to amplify the glyceraldehyde-3-phosphate dehydrogenase (GAPDH) gene as an internal control. Relative enrichments for PU.1 and Runx1 antibodies were calculated by taking the ratio between the net intensity of the PU.1 PCR product from each primer set and the net intensity of the bound sample of the IgG control and dividing this by the same ratio calculated for the input sample. The value of each point was calculated as the average from two independent ChIP experiments and a total of four independent PCR analyses.

3.13 Reporter assays

For transient reporter assays, distinct sequences as shown in Table S2 of the indicated cell cycle regulators were cloned into either pXP2 or pGL4 firefly luciferase reporter vectors. The reporter vectors used in this study (pXP2, pGL2, pGL4) lack eukaryotic promoter or enhancer sequences. For pXP2, the regulatory sequences of interest were cloned into the Xho1 site of the multiple cloning region, 33 bp upstream of the start site of the luciferase reporter gene. The Cdc25a promoter sequence was cloned into the EcoRV site of the multiple cloning region

55 bp upstream of the start site of the luciferase reporter gene of the pGL4 plasmid. Generation of the Gfi1 minimal promoter reporter constructs in pGL2 was described previously (Wilson et al., 2010b). PU.1 core motives were mutated from GGAA to TCGC, using a QuikChange® Site-Directed Mutagenesis Kit and following manufacturer's instructions (Stratagene, La Jolla, CA). Sequences for mutagenesis primers are listed in Table S3. For luciferase experiments, 1.5 x 10^5 HEK293T cells were cotransfected with reporter constructs (100 ng) and increasing amounts of PU.1-pCDNA3 plasmids (0, 50, 100, 200, 400 ng). DNA input was equalized by addition of pDNA3 plasmid. Transfections were normalized with the 20 ng of renilla luciferase vector as an internal control.

3.14 Statistical Analysis

CRU frequencies were calculated with L-Calc software (StemCell Technologies). The statistical differences in frequencies between sets of limiting dilution analyses were assessed on basis of the asymptotic normality of the maximum likelihood estimates and calculated using Chi-square test. Log-rank non-parametric test (Mantel-Cox) was used for survival studies upon 5'-FU treatment. For Laser Scanning Cytometry analysis, or data, which did not meet criteria of a normal distribution, the non-parametric Mann Whitney *U*-test was used (Realtime PCR for Ccna2). In all other experiments, statistical significances were assessed by Student's unpaired t test. Statistical significance was indicated as * for $p<0.05$ and ** for $p<0.01$. For normalized data, Gaussian error propagation was applied.

4 Results

4.1 Chromatin structure, positive forward regulation and PU.1 transcription in normal Hematopoietic Stem Cells

To provide lifelong supply of blood cells, hematopoietic stem cells (HSCs) need to carefully balance both, self-renewing cell divisions and quiescence. While several regulators have been identified which control this mechanism, we here demonstrate that transcription factor PU.1 acts upstream of these regulators. So far, attempts to uncover PU.1's role in HSC biology have failed due to technical limitations of complete loss of function models. Using hypomorphic mice with decreased PU.1 levels specifically in phenotypic HSCs we found reduced HSC long-term repopulation potential that could be rescued completely by restoring PU.1 levels. PU.1 prevented excessive HSC cell divisions and exhaustion by controlling transcription of multiple cell cycle regulators. Levels of PU.1 were sustained through autoregulatory PU.1 binding to an upstream enhancer which formed an active looped chromosome architecture in HSCs. These results establish that PU.1 mediates chromosome looping and functions as master regulator of HSC proliferation.

4.1.1 Mice with a selective mutation of a distal PU.1 binding site express decreased levels of PU.1 in HSC

We previously identified a potential autoregulatory site within the -14kb URE of murine PU.1, which we characterized *in vitro* (Okuno et al., 2005). To genetically dissect a functional role for autoregulation of PU.1 *in vivo,* we generated knock-in mice ($PU.1^{ki/ki}$) with targeted disruption of this particular binding site by homologous recombination (**Figure 2**).

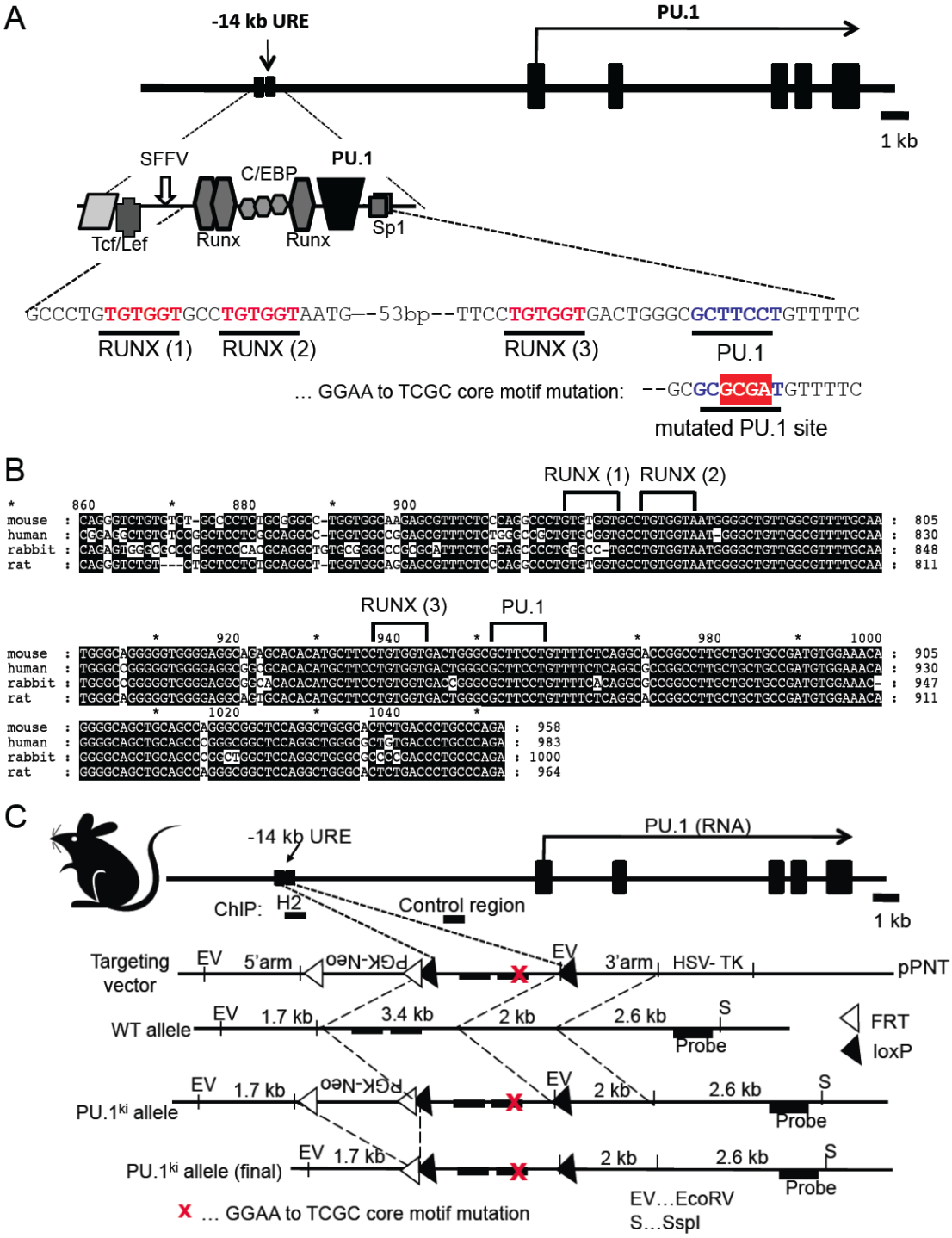

Figure 2. **A,** Cartoon illustrating the PU.1 locus (modified from (Hoogenkamp et al., 2007)). **B,** shown are location, species homology and sequences of RUNX and PU.1 sites in the -14kb URE, as well as the sequence of the mutated allele. **C**, Diagram of the PU.1 locus indicating the targeting strategy of knock-in mice (PU.1$^{ki/ki}$) with a mutated autoregulatory site at homology region H2 of the -14kb URE. In the "final" PU.1$^{ki/ki}$ allele, FRT recombinase was used to remove the PGK-Neo cassette.

Chromatin immunoprecipitation (ChIP) analyses of total bone marrow cells confirmed successful abolishment of PU.1 binding to the -14kb URE in PU.1ki/ki mice, whereas URE binding of Runx1 to binding sites in close proximity to the PU.1 site remained largely preserved (Figure 3).

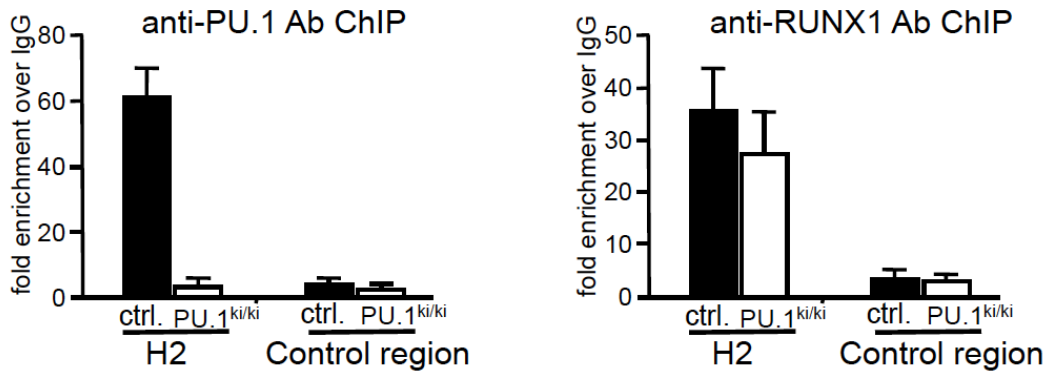

Figure 3. Quantitative chromatin immunoprecipitation (ChIP) of total bone marrow cell lysates using normal rabbit IgG and antibodies against PU.1 and Runx1. Black bars in Fig. 1a indicate RQ-PCR primer locations at H2 and a control region located 5 kb upstream of the PU.1 transcriptional start site. One additional primer set was used to amplify the glyceraldehyde-3-phosphate dehydrogenase (GAPDH) gene as an internal control. Relative enrichments for PU.1 and Runx1 antibodies were calculated as fold enrichment over IgG control. "ctrl" indicates bone marrow of mice after homologous recombination with a similar targeting vector as for autoregulatory site mutants but with unmutated URE. Shown are values as avg. + s.d. of two independent ChIP experiments and a total of four independent RQ-PCR analyses.

PU.1 levels of PU.1$^{ki/ki}$ mice were not changed in unselected total bone marrow cells (data not shown). However, in phenotypic HSCs (defined in this study as Lin^{-}Sca1^{+}c-kit^{+}CD150^{+}CD48- (Kiel et al., 2005)), PU.1 mRNA levels of PU.1$^{ki/ki}$ mice were reduced by 66% compared to controls, similar to levels of PU.1 heterozygous knockout (PU.1+/-) mice in which exons 4 and 5 were deleted (Iwasaki et al., 2005) (Figure 4A). Interestingly, both PU.1ki/ki and PU.1+/- mice displayed increased numbers of total bone marrow cells (Figure 4B) and phenotypic HSCs (Figure 4C) compared to controls.

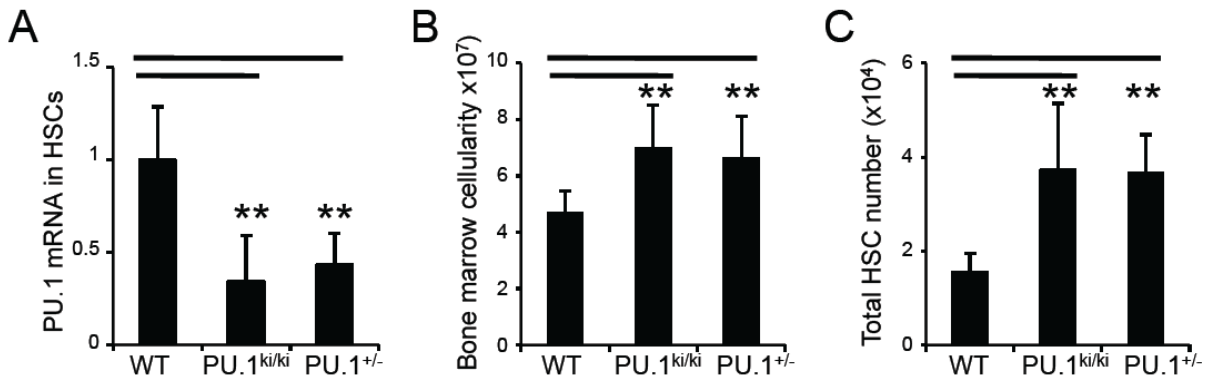

Figure 4. PU.1ki/ki hypomorphs show increased numbers of phenotypic HSCs. **A,** PU.1 mRNA levels in Lin-Sca1+c-kit+CD150+CD48- cells (HSCs) of wild type (WT), PU.1 autoregulatory site mutants (PU.1ki/ki), and PU.1 heterozygous (PU.1+/-) mice (Iwasaki et al., 2005) (Realtime PCR; average values [avg.] + standard deviation [s.d.] as fold change to WT; n=7-8; **P<0.01). **B, C,** Total number of mononuclear cells and HSCs in bone marrow at age of 3 months (avg. + s.d. of two femurs, tibias, fibulas; n=5-9; *P<0.05, **P<0.01).

4.1.2 Bone Marrow Homing of HSCs from adult PU.1ki/ki mice is preserved

Previous reports, including one from our group, indicated that complete loss of PU.1 resulted in decreased numbers of HSCs due to defective homing (Fisher et al., 1999, Kim et al., 2004, Iwasaki et al., 2005). In spite of this, using laser-scan cytometry on femur sections of wild type and PU.1ki/ki mice we established that HSCs of PU.1ki/ki localized normally within the bone marrow niche (Figure 5A). PU.1ki/ki hypomorphs with decreased but not absent PU.1 levels demonstrated normal HSC homing in short term bone marrow transplantation assays (Figure 5B). In addition, microarray gene expression analysis of adult HSCs of PU.1ki/ki and wild type mice were compared with data of fetal liver PU.1 knockout mice, which have been reported to have severe homing defects (Fisher et al., 1999, Kim et al., 2004). In contrast to PU.1ki/ki, PU.1 knockout HSCs showed profound changes in the expression of genes involved in mediating interactions with the microenvironment (Figure 5C, D), thus supporting that homing defects described for PU.1 fetal liver knockouts are not present in HSCs of adult PU.1$^{ki/ki}$ mice.

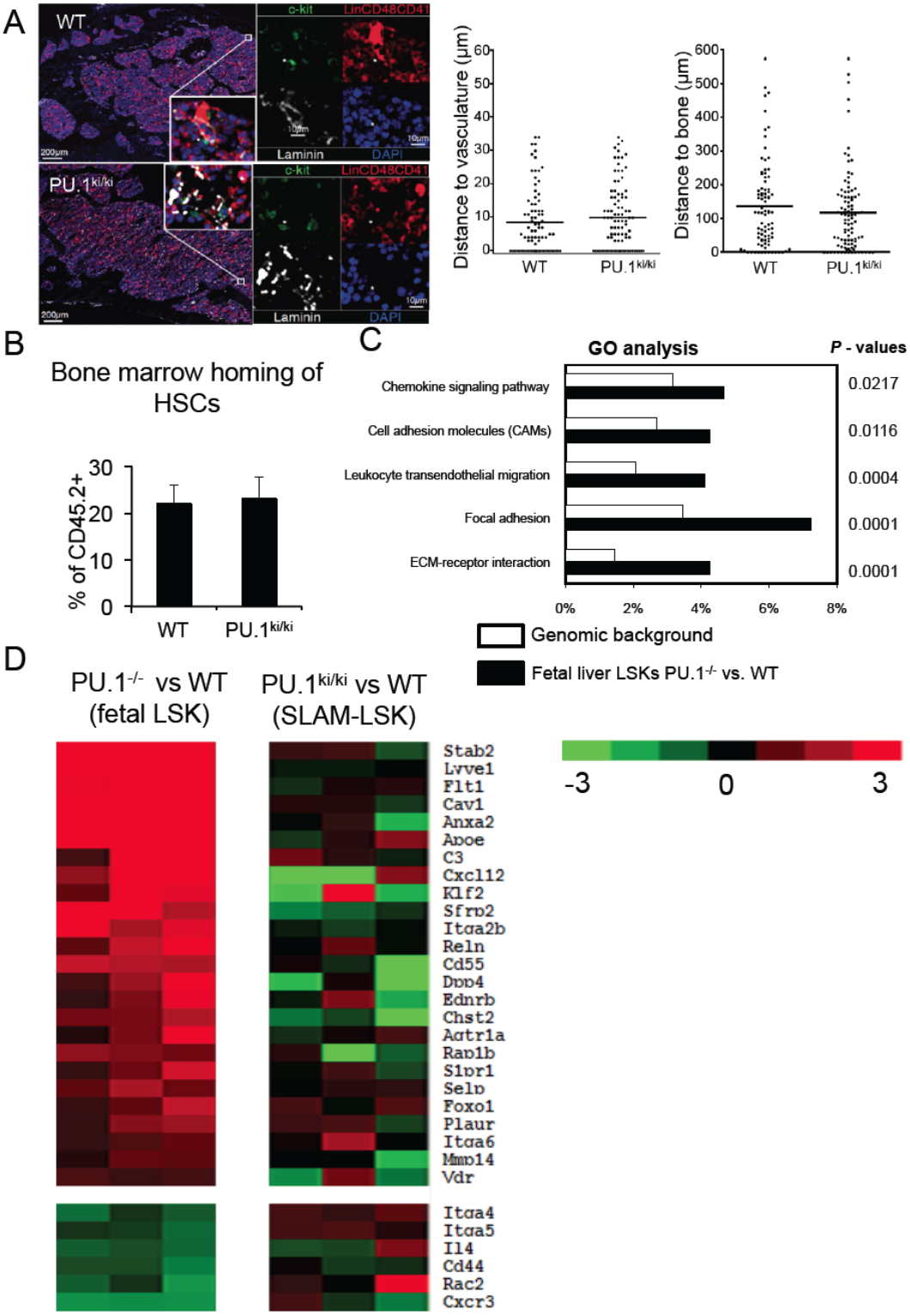

Figure 5. Bone Marrow Homing of HSCs from adult PU.1ki/ki mice is preserved in contrast to PU.1-/-. **A,** Representative images of HSC-enriched Lin-CD41-CD48-c-kit+ cells within BM cavities (left). Distance to bone marrow vasculature (laminin) and to bone (endosteal surfaces) in femoral sections as analyzed by Laser Scanning Cytometry (n=3; numbers of cells analyzed: 86 [WT], 95 [PU.1ki/ki]). **B,** Homing of PU.1ki/ki HSCs is unaltered. 2 x 10^6 bone marrow cells of 3-4 month old wild type (WT) or PU.1ki/ki mice (C57BL/6J, CD45.2+) were transplanted into irradiated (900 rads) C57BL/6J, CD45.1+ recipients. After 16 hours bone marrow was analyzed for CD45.2+ percentage of Lin-Sca1+CD150+CD48- cells (HSCs) (average values [avg.] + standard deviation [s.d.], n=5). **C, D,**

Microarray gene expression analysis (Affymetrix Mouse 430_2) of E14 fetal liver LSK from PU.1 knockout mice (PU.1-/-) (Iwasaki et al., 2005) vs. corresponding wild type, and of 3-4 month old PU.1ki/ki vs. wild type HSCs. **C**, Gene Ontology analysis indicated significant changes in pathways mediating interactions with the microenvironment in PU.1-/- vs wild type (WT) fetal liver LSKs. Black bars show % of relative enrichment of changed genes per group compared to background (white bars = expected share): Pathways of significantly changed gene expression between PU.1-/- and WT. **D**, Heat map of genes involved in homing: Fold changes as log2 expression (red [+], green [-]) of three PU.1-/- or PU.1ki/ki replicates compared to the mean of three corresponding controls are depicted. The mean expression intensities for PU.1-/- LSK are significantly larger or smaller than the mean of the controls ($P<0.05$), whereas there is no significant change between PU.1ki/ki HSCs and controls.

4.1.3 PU.1$^{ki/ki}$ hypomorphs are defective in HSC function

To test if the observed increase of phenotypic HSC numbers in PU.1$^{ki/ki}$ mice reflected quantitative differences of functional long-term (LT)-HSCs we performed competitive repopulation transplantations with limiting dilutions of purified phenotypic HSCs. After 6 months, long-term lymphomyeloid reconstitution in peripheral blood and HSCs in bone marrow of donor cells were assessed and plotted as percent non-responding mice (**Figure 6**). Intriguingly, phenotypic HSCs of PU.1$^{ki/ki}$ mice demonstrated a dramatic (13.6 fold) decrease of functional LT-HSCs.

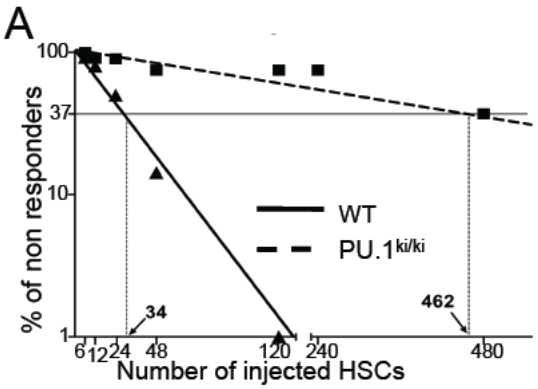

Quantification of CRUs

Injected No of SLAM+ KSL cells	WT	PU.1$^{ki/ki}$
6	1/13	0/15
12	2/10	1/11
24	4/8	1/10
48	6/7	1/4
120	8/8	2/8
240	7/7	2/8
480	9/9	5/8
HSC frequency	1 in 34	1 in 462
(95% confidence interval)	(27 - 44)	(388 - 728)

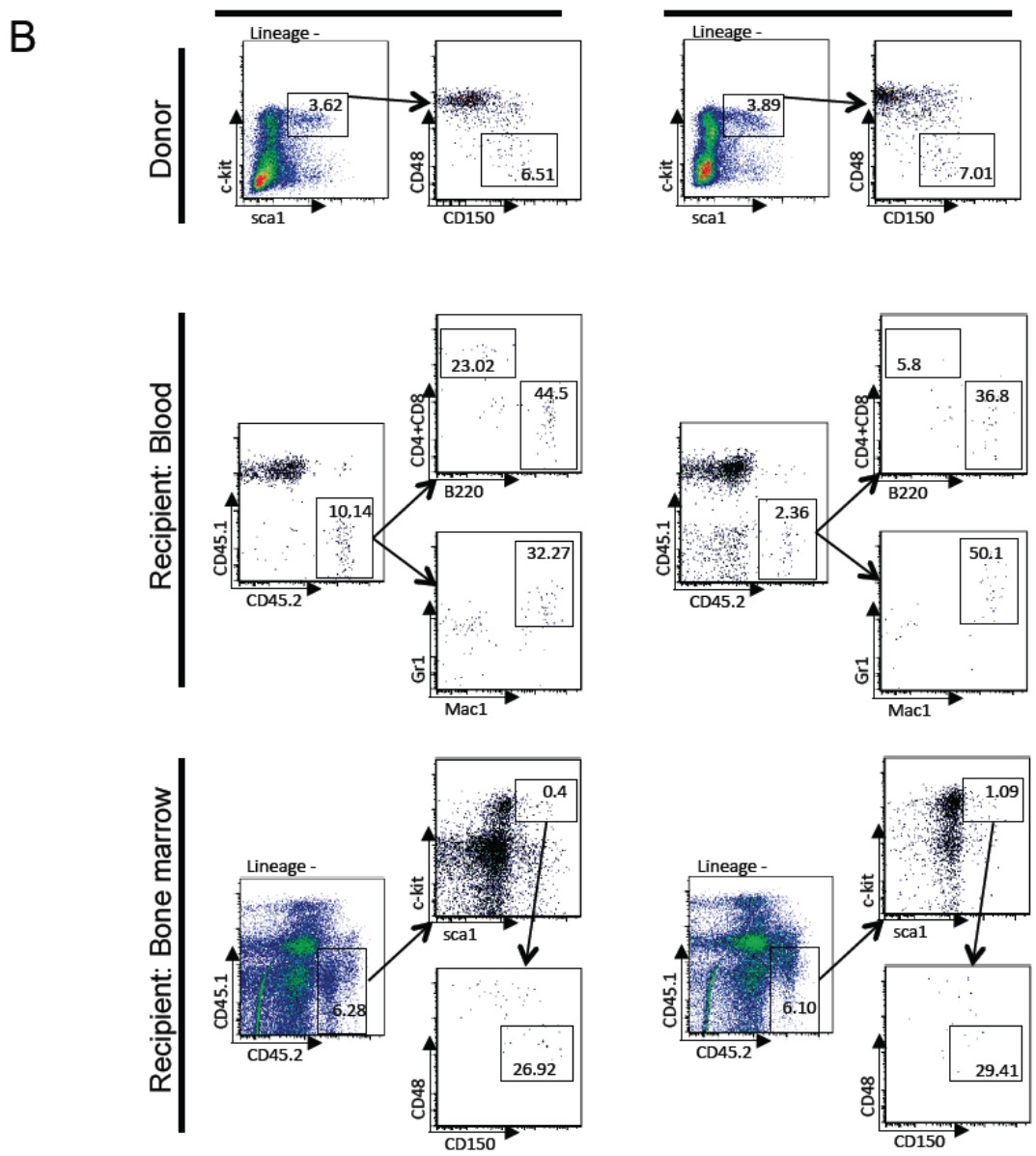

Figure 6. PU.1$^{ki/ki}$ hypomorphs are defective in HSC function. **A**, Limiting dilution CRU assay: Indicated HSC numbers of wild type or PU.1$^{ki/ki}$ mice (CD45.2^{+}) were cotransplanted with 2x10^{5} bone marrow cells of a competitor (CD45.1^{+}) into lethally irradiated (1300rads) recipients (CD45.1^{+}). Reconstitution was evaluated in blood and bone marrow 6 months after transplantation. Mice with CD45.2^{+} chimerism <0.3% were considered as non-responders (*P*=0.0001).
B, Representative FACS analyses of limiting dilution transplantation experiments using phenotypic HSCs of either wild type ("control") (left) or PU.1$^{ki/ki}$ (right) donors (CD45.2+) into CD45.1+ recipient mice. 24 weeks after transplantation blood and bone marrow) were assessed for positive long-term reconstitution. One positive example of recipients from each group (wild type = Control, PU.1$^{ki/ki}$) is shown.

To evaluate the potential of PU.1$^{ki/ki}$ HSCs to regenerate bone marrow after repetitive injury, we analyzed mice after weekly administration of the antimetabolite 5'-fluorouracil (5-FU) (**Figure 7**A). We observed decreased survival in PU.1$^{ki/ki}$ mice indicating that HSCs of PU.1$^{ki/ki}$ either exhaust prematurely, have increased cell cycle activity, or both. To test for HSC exhaustion, we further analyzed long-term reconstitution capacity in serial transplantation assays. Interestingly, after three rounds of transplantation HSCs of PU.1$^{ki/ki}$ mice failed to repopulate the bone marrow of lethally irradiated recipients, thus showing that HSC of PU.1$^{ki/ki}$ hypomorphs exhausted prematurely (**Figure 7**B). Moreover, competitive long-term reconstitution transplantation assays utilizing total bone marrow cells also revealed reduced HSC function of PU.1+/- similar to what was observed with PU.1ki/ki (**Figure 7**C). Restoration of PU.1 levels by crossing to a human PU.1 transgenic (Leddin et al., 2011) (**Figure 7**D) rescued HSC function of both PU.1ki/ki and PU.1+/- bone marrow cells (**Figure 7**C), demonstrating that HSC function was strictly related to PU.1 levels.

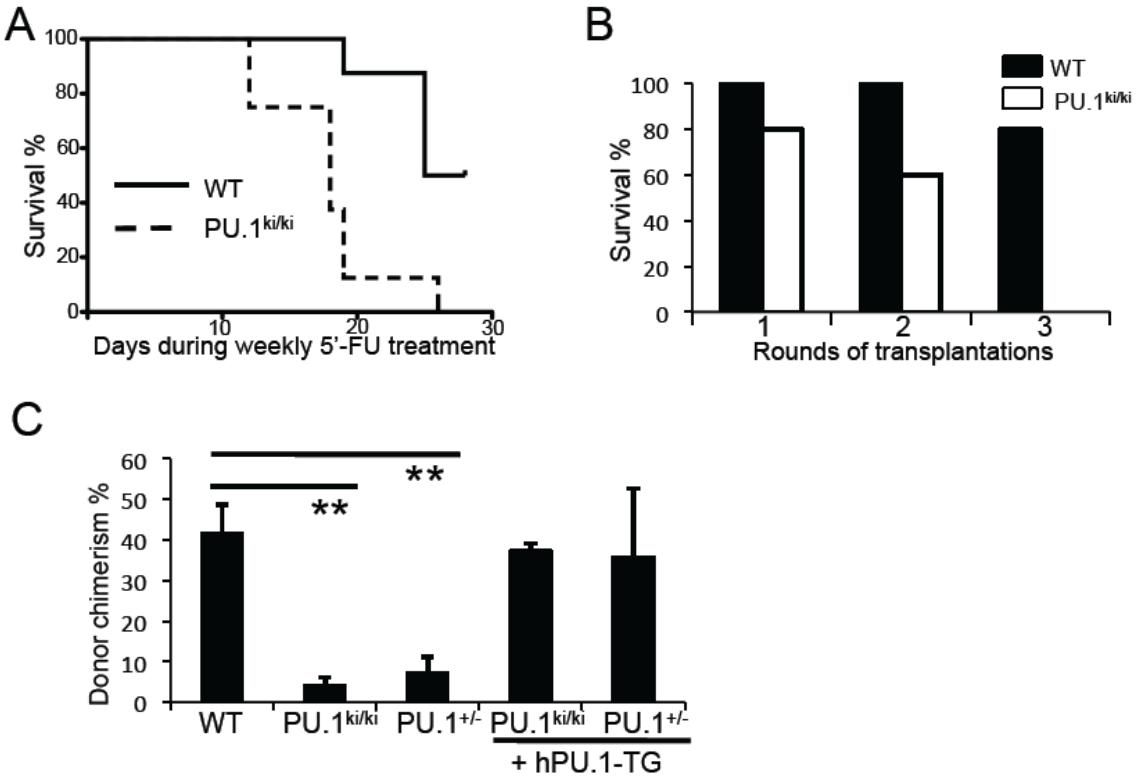

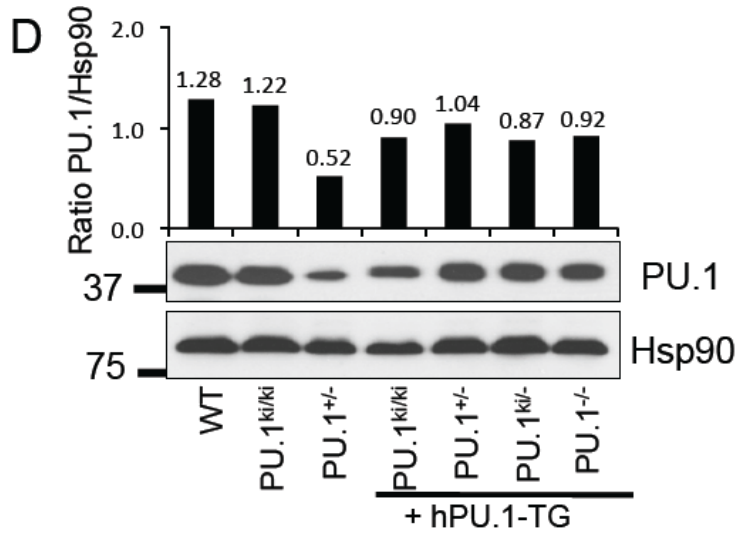

Figure 7. A, Reduced capability of PU.1$^{ki/ki}$ mice to regenerate bone marrow after repetitive injuries by weekly 5'-FU administration (i.p. 150mg/kg). Results are shown as Kaplan-Meier survival curves (n=8, P=0.002 [Mantel-Cox]). **B**, Serial transplantation assays: Rounds of transplantations with 2x10^6 bone marrow cells were performed in 16-week intervals. Bar graphs indicate survival after each round of transplantation (n=5). **C**, 2x10^6 bone marrow cells of indicated donor mice (CD45.2$^+$) were cotransplanted with 2x10^6 CD45.1$^+$ bone marrow cells into lethally irradiated CD45.1+ recipients. Bar graphs show donor chimerism in blood after 6 months (avg. + s.d., n=5-8; **P<0.01). In the two graphs on the right, PU.1$^{ki/ki}$ and PU.1$^{+/-}$ mice were "rescued" by breeding to a strain harboring a human transgene expressing PU.1 ("+ hPU.1-TG") (Leddin et al., 2011). **D,** A human PU.1 transgene normalizes PU.1 levels in PU.1ki/ki and PU.1+/- mice. Immunoblot and densitometric quantification using total bone marrow cell extracts of bone marrow of indicated mice. Human and murine PU.1 were detected using a cross-reactive antibody. The antibody does not react with the truncated PU.1 (lane 3). Endogenous murine Hsp90 served as a loading control. PU.1 levels in total bone marrow are decreased in PU.1$^{+/-}$ but not in PU.1$^{ki/ki}$ in which decreased levels are restricted to the HSC compartment. Importantly, human PU.1 transgene expression (+hPU.1-TG) (Leddin et al., 2011) restores PU.1 protein expression to a level that is comparable to wild type (WT) and which does not result in PU.1 overexpression (e.g. in the PU.1$^{ki/ki}$ x hPU.1-TG mice).

4.1.4 Increased Cell Cycle Activation in HSCs of PU.1 Hypomorphs

To directly assess the role of PU.1 in HSC proliferation, we measured 5-bromodeoxyuridine (BrdU) incorporation *in vivo*. Indeed, the proliferative fraction of both PU.1$^{ki/ki}$ and PU.1$^{+/-}$ (Back et al., 2004) HSCs was doubled compared to wild type (Figure 8A). In concordance with BrdU incorporation assays, cell cycle analysis using PyroninY/Hoechst staining revealed that purified HSCs of PU.1$^{+/-}$ (Iwasaki et al., 2005) and PU.1$^{ki/ki}$ mice had a significant increase in dividing cells, as evidenced by an increased fraction of the S/G2/M cell cycle phase. Restoration of PU.1 levels by crossing PU.1$^{ki/ki}$ mice to a human PU.1 transgenic (Leddin et al., 2011) (**Figure 7**D) reversed the increased S/G2/M fraction to normal (Figure

8B). These results demonstrate that PU.1 regulates proliferation in HSC, and this effect was directly related to levels of PU.1.

To reveal potential mechanisms through which PU.1 levels might control HSC proliferation we performed microarray gene expression analysis of purified HSCs of PU.1$^{ki/ki}$ and wild type mice. Differentially expressed genes were mapped to known pathways using Gene Ontology (GO) pathway analysis. Strikingly, cell cycle genes and genes of pathways directly affecting proliferation (such as canonical Wnt-, MAPK-, and p53 signaling) were significantly overrepresented (Figure 8C). Similarly, gene set enrichment analysis (GSEA) (Mootha et al., 2003) revealed significant enrichment of genes representing activated G2 cell cycle phase in PU.1$^{ki/ki}$ HSCs (Figure 8D). From the list of cell cycle genes differentially expressed in microarray analysis (Table 1) we selected eight to validate differences in mRNA expression by quantitative real time PCR (RQ-PCR) (Figure 8E). Low PU.1 levels resulted in decreased expression of cell cycle inhibitors, such as Gfi1, Cdkn1a (p21), and Cdkn1c (p57), and increased levels of cell cycle activators such as Cdk1, Cyclin D1, E2f1, and Cdc25a.

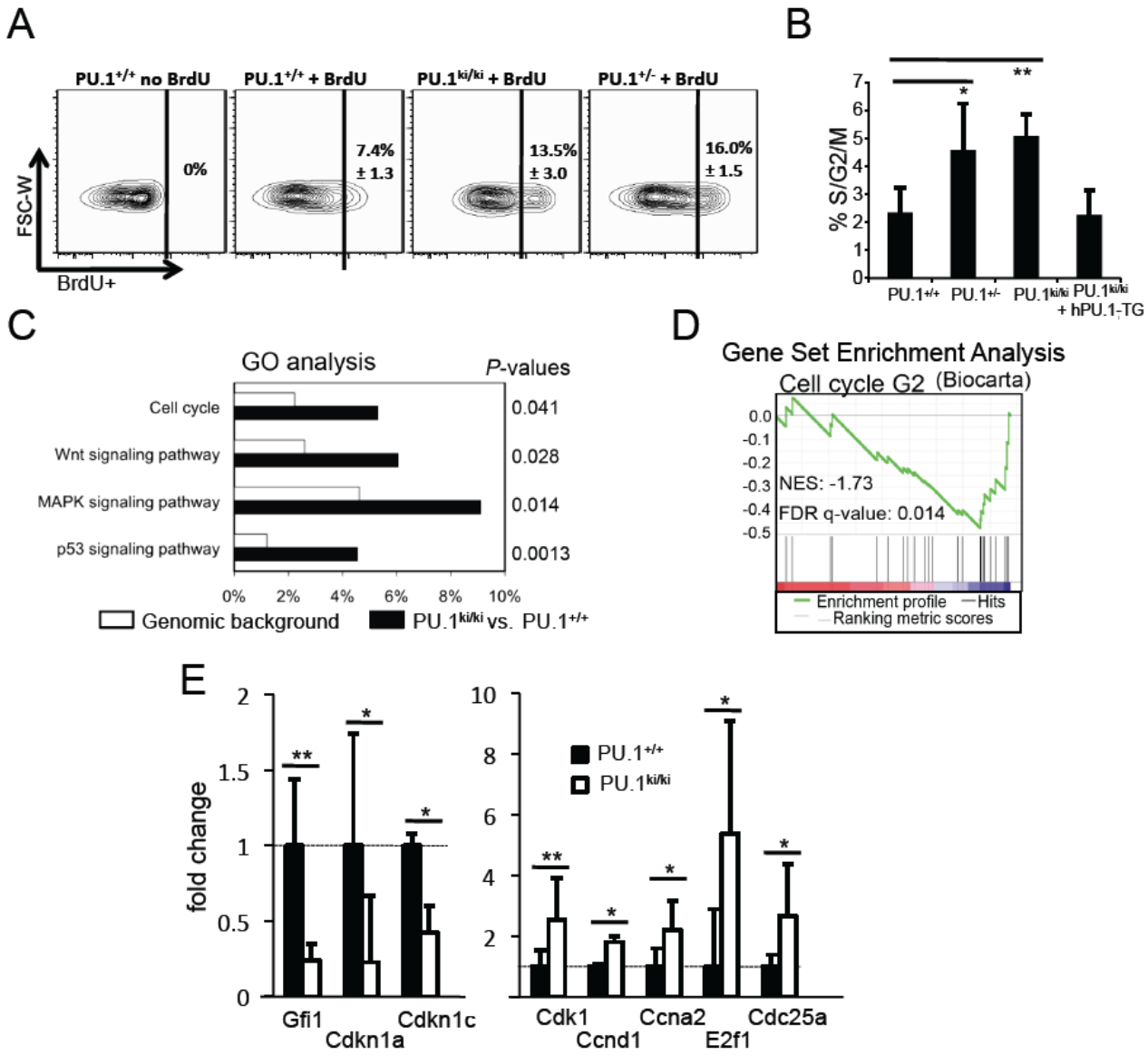

Figure 8. PU.1 restricts HSC cell divisions. **A,** HSC proliferation assay: BrdU (one bolus i.p. 100mg/kg, followed by 16h p.o. 0.8mg/ml) was administered before bone marrow harvest. BrdU incorporation was measured by flow cytometry on gated Lin$^-$Sca1$^+$c-kit$^+$CD150$^+$CD48$^-$ cells (avg. % ± s.d.; n=4; difference PU.1$^{ki/ki}$ and PU.1$^{+/-}$ to WT P<0.05, respectively). **B,** Quantification of S/G2/M cell cycle phase: Purified Lin$^-$Sca1$^+$ckit$^+$CD150$^+$CD48$^-$ cells (HSCs) were stained with PyroninY and Hoechst33342 and analyzed by flow cytometry (avg. % + s.d.; n=4; *P<0.05, **P<0.01). In the graph on the right, PU.1$^{ki/ki}$ mice were "rescued" by breeding to a strain harboring a human transgene expressing PU.1 ("+ hPU.1-TG") (Leddin et al., 2011). See also Figure S3B. **C,** Gene Ontology (GO) analysis indicating significant changes between PU.1$^{ki/ki}$ and wild type (PU.1$^{+/+}$) in cell cycle and indicated proliferation associated pathways. Black bars show % of relative enrichment of changed genes per group compared to background (white bars = expected share). **D,** Gene Set Enrichment Analysis (GSEA) (Mootha et al., 2003) showed significant differences between PU.1$^{ki/ki}$ and wild type using an a priori defined set of genes ("Biocarta_G2_Pathway" – signatures [MSigDB]). Shown are Normalized Enrichment Score (NES) and False Discovery Rate (FDR) with q-value < 0.05 to indicate statistical significance. **E,** Altered expression of cell cycle regulator genes in sorted Lin$^-$ Sca1$^+$ckit$^+$CD150$^+$CD48$^-$ cells (HSCs) of PU.1$^{ki/ki}$ mice. RealTime-PCR of selected genes in HSCs (avg. + s.d. as fold change to wild type (PU.1$^{+/+}$); n=3-4; *P<0.05, **P<0.01**).**

Table 1. Expression level changes of Cell Cycle Regulators in HSCs of PU.1 Hypomorphs.

PU.1 Occupancy	fold change $PU.1^{ki/ki}$ vs. WT (2-log)	Gene symbol	Gene Title
Yes	-1.65789862	Gfi1	growth factor independent 1
Yes	-1.348691838	Cdkn1a	cyclin-dependent kinase inhibitor 1A (P21)
no	-1.035584535	Cdkn1c	cyclin-dependent kinase inhibitor 1C (P57)
Yes	-1.027207285	Gadd45b	growth arrest and DNA-damage-inducible 45 beta
Yes	0.620985623	Smc3	structural maintenace of chromosomes 3
Yes	0.88673181	Cdc25b	cell division cycle 25 homolog B (S. pombe)
no	0.970119669	Ccnd1	cyclin D1
no	0.994218509	Espl1	extra spindle poles-like 1 (S. cerevisiae)
no	1.048708046	Cdc25c	cell division cycle 25 homolog C (S. pombe)
no	1.170287378	Ccna2	cyclin A2
Yes	1.204059067	Mcm5	minichromosome maintenance deficient 5, cell division cycle 46 (S. cerevisiae)
Yes	1.275318348	Cdk1	cyclin-dependent kinase 1
Yes	1.310911787	E2f1	E2F transcription factor 1
no	1.63048556	Anapc1	anaphase promoting complex subunit 1
Yes	1.681368695	Mad2l1	MAD2 mitotic arrest deficient-like 1 (yeast)
no	1.710971404	Orc5l	origin recognition complex, subunit 5-like (S. cerevisiae)
Yes	1.989962006	Cdc25a	cell division cycle 25 homolog A (S. pombe)
no	2.041443757	Anapc2	anaphase promoting complex subunit 2
Yes	2.058000672	Mcm2	minichromosome maintenance deficient 2 mitotin (S. cerevisiae)
Yes	2.585261603	Hdac1	histone deacetylase 1
Yes	2.732744911	Dbf4	DBF4 homolog (S. cerevisiae)

To functionally study whether Cdk1, E2f1, and Cdc25a mediate the hyperproliferation of $PU.1^{ki/ki}$ HSCs we designed five shRNA constructs for each gene and cloned them into the lentiviral vector pGhU6 (containing eGFP). We analyzed the knockdown efficiency of individual shRNA constructs at both, protein and RNA levels and selected the most efficient ones for subsequent experiments (Figure 9A). HSC-enriched LSK cells of individual wild type and $PU.1^{ki/ki}$ mice (n = 4) were transduced with lentivirus expressing either a shRNA against specific cell cycle activators (shCdk1, shE2f1, shCdc25a) or a non-silencing control shRNA (NSC). Knockdown efficacy of all three genes was analyzed in GFP+ sorted LSKs, respectively (Figure 9B).

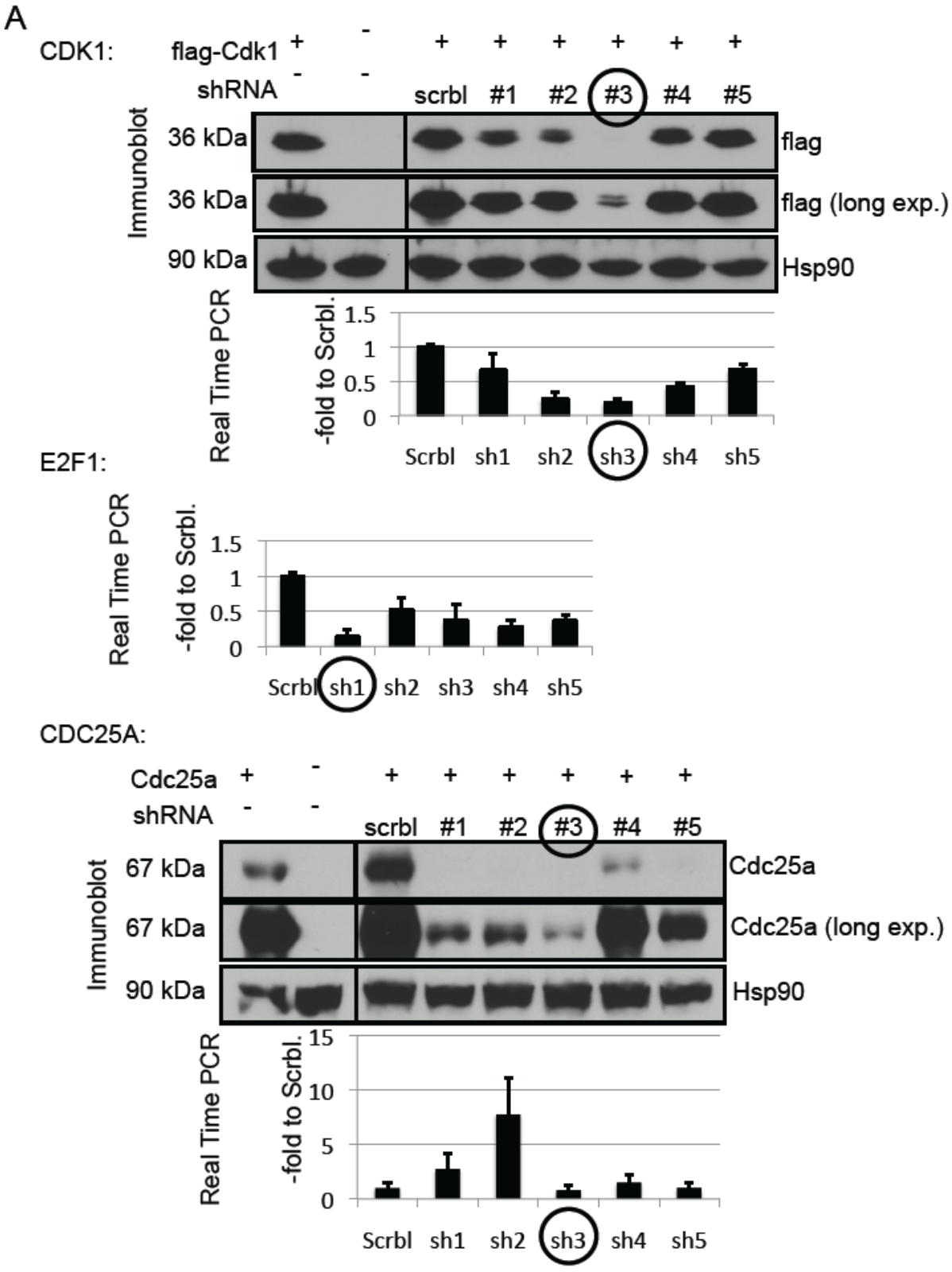
A
CDK1:
flag-Cdk1
shRNA
scrbl
#1
#2
#3
#4
#5
Immunoblot
36 kDa
flag
36 kDa
flag (long exp.)
90 kDa
Hsp90
Real Time PCR
-fold to Scrbl.
Scrbl
sh1
sh2
sh3
sh4
sh5
E2F1:
CDC25A:
Cdc25a
67 kDa
Cdc25a (long exp.)

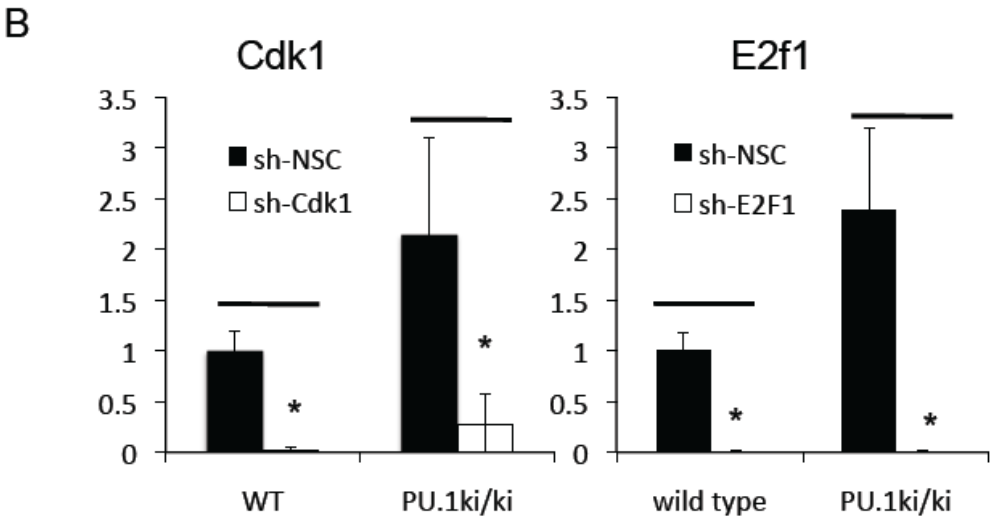

Figure 9. Test for knockdown efficacy of shRNA constructs, **A,** Indicated specific shRNAs were cloned into the lentiviral vector pGhU6 (Radomska et al., 2012). Knockdown efficacy of constructs targeting Cdk1 and Cdc25a at the protein level was evaluated in human HEK293T cells after cotransfection (48 hours) with either flag-tagged murine Cdk1 or untagged murine Cdc25a. Shown are immunoblots with indicated antibodies using whole cell lysates. Real-time PCR evaluation of endogenous target gene knockdown was performed on GFP-sorted murine NIH3T3 cells that prior to harvest had been transfected with indicated constructs for 48 hours (average values [avg.] + standard deviation [s.d.]. Circles highlight the individual construct that was selected for consecutive experiments. **B.** Evaluation of target gene knockdown efficacy in GFP-sorted LSK of mice with indicated genotype using real-time PCR (average values [avg.] + standard deviation [s.d.], n = 3, **P*<0.05). Note that due to the low number of cells available for analysis, levels of E2f1 after knockdown were undetectable. Since knockdown of Cdc25a was restricted to protein levels (a), and since the amount of GFP+ LSK cells was limited to ~5000 cells per mouse, immunoblotting was not possible to confirm knockdown of Cdc25a protein in the LSK population.

BrdU incorporation assays were performed to assess the proliferation of transduced GFP+ LSKs 12 hours after BrdU application (Figure 10). Similar to our previous results with SLAM+LSKs, the proliferative (BrdU+) fraction of PU.1$^{ki/ki}$ LSKs was doubled compare to wild type. Surprisingly, knockdown of either E2f1 or Cdc25a alone was sufficient to restore normal proliferation. This highlighted the critical role of either factor for the hyperproliferative phenotype induced by lower PU.1 levels. Interestingly, knockdown of either factor in wild type cells did not perturb LSK proliferation, indicating that they might not be essential to maintain basic proliferation in healthy conditions and that their reduction could be compensated. Knockdown of Cdk1 alone in either wild type or PU.1$^{ki/ki}$ LSKs was not sufficient to change proliferation, pointing to a compensatory mechanism by other factors in play. However, since many cell cycle regulators are changed in PU.1$^{ki/ki}$ mice, it is still possible that CDK1 might contribute to the hyperproliferative phenotype as part of a composite effect.

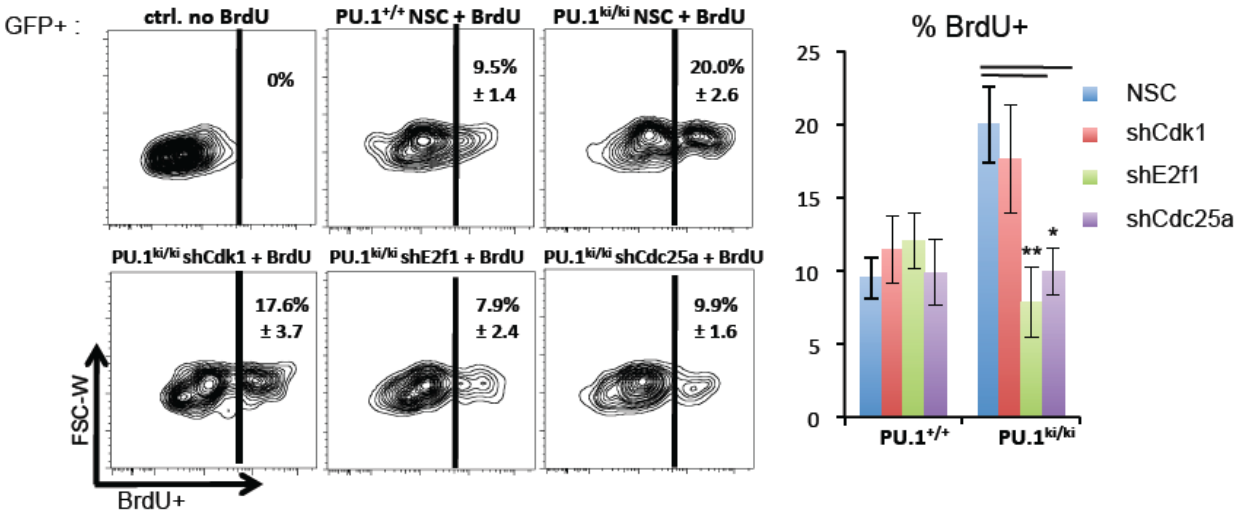

Figure 10. BrdU proliferation assay on HSC-enriched LSK cells of wild type and PU.1$^{ki/ki}$ mice (n=4) upon lentiviral shRNA knockdown of specific cell cycle activators (shCdk1, shE2f1, shCdc25a) or a non-silencing control shRNA (NSC). BrdU incorporation was measured after 12 hours by flow cytometry on gated GFP+ cells (avg.% + s.d.; n=4; *P<0.05, **P<0.01).

4.1.5 PU.1 transcriptionally induces Cell Cycle Inhibitors and represses Cell Cycle Activators

To test if binding of PU.1 to promoters of putative target genes might be correlated to "active" or "repressed" histone marks, we chose a whole-genome approach. By obtaining H3K4me3 and H3K27me3 ChIP-Seq data for LSK cells and PU.1 ChIP-Seq data for HPC-7 cells from (Adli et al., 2010, Wilson et al., 2010a) respectively, we mapped sequencing reads to the mouse reference genome. Figure 11A shows the patterns of PU.1 binding to +/- 5kb either side of all annotated mouse promoters in relation to the histone marks H3K4me3 ("active") and H3K27me3 ("repressed") as stacked heatmaps. Three types of promoters with either the "active", "repressed" or "no" histone marks at all, could be distinguished. Interestingly, PU.1 binding was largely restricted to promoters with the "active" H3K4me3 mark. As shown on the right panel a substantial proportion of H3K4me3 bound promoters were also bound by PU.1 (Figure 11A).

We next combined PU.1 ChIP-Seq data (Wilson et al., 2010a) with the differentially expressed genes in SLAM+LSK cells of PU.1$^{ki/ki}$ and wild type mice. Among all genes that were dysregulated in PU.1$^{ki/ki}$ mice, binding of PU.1 to promoters of cell cycle genes was significantly enriched pointing to the predominant role for PU.1 in regulating cell cycle in HSCs (Figure 11B).

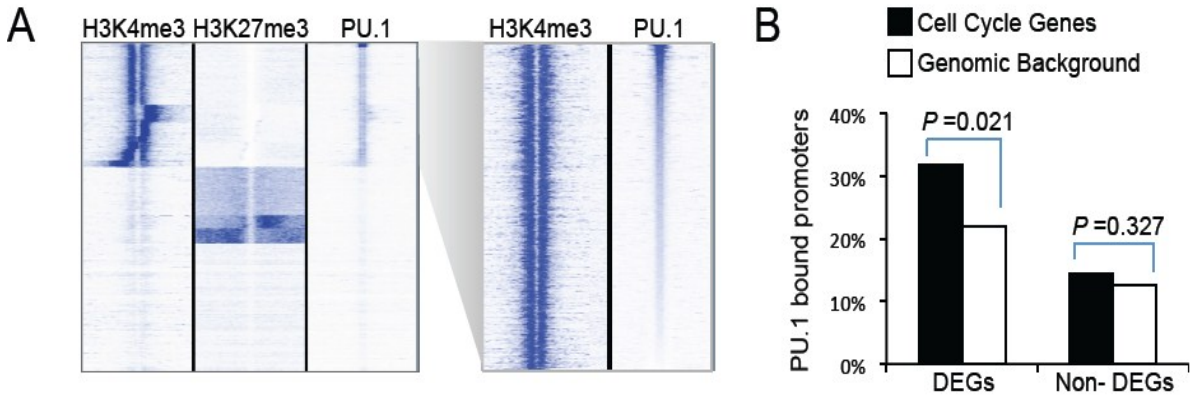

Figure 11. A. PU.1 binding was largely restricted to promoters with the "active" H3K4me3 mark. H3K4me3 and H3K27me3 ChIP-Seq data for LSK cells (Adli et al., 2010) and PU.1 ChIP-Seq data for HPC-7 cells (Adli et al., 2010, Wilson et al., 2010a), were mapped to the mouse reference genome, mm9 and shown as stacked heatmaps. **B.** Fraction of PU.1-bound genes to all genes in the categories differentially expressed genes (DEGs) or non-DEGs comparing the GO-group of cell cycle genes with the whole genome.

In line with differential expression of cell cycle genes and concurrence of PU.1 association with the active histone mark H3K4me3 at promoters genome-wide we expected PU.1 binding to promoters of genes that were downregulated in HSCs of $PU.1^{ki/ki}$ mice. Indeed, PU.1 bound promoters and enhancers of cell cycle inhibitors such as Gfi1 and Cdkn1a (Figure 12). Surprisingly, we also observed distinct PU.1 binding to promoters and enhancers of cell cycle activators such as Cdk1, E2f1, and Cdc25a (Figure 12, Table 2).

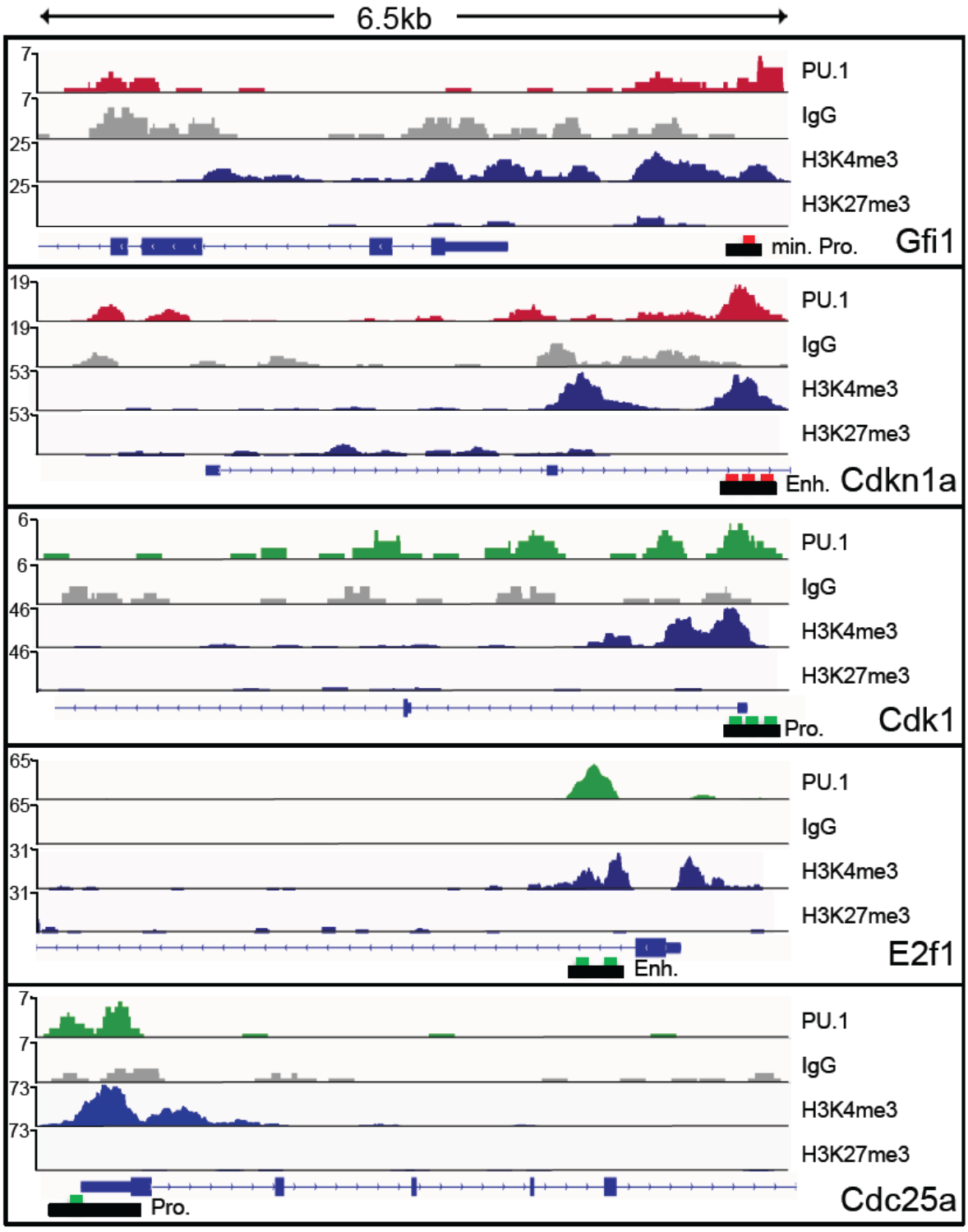

Figure 12. PU.1, H3K4me3 and H3K27me3 binding profiles for promoter and enhancer regions of PU.1 target genes. PU.1 ChIP-Seq data (red and green tracks) of the hematopoietic stem cell line HPC-7 (Wilson et al., 2010a) are shown in comparison to IgG control (grey tracks). A 6.5kb stretch of Gfi1, Cdkn1a (p21), Cdk1, E2f1, and Cdc25a loci are shown. Black bars indicate the sequences that were used in reporter assays. Red and greed marks at black bars stand for putative PU.1 binding sites.

To evaluate the transcriptional regulation through PU.1 on a subset of promoters and enhancers of its putative target genes we applied functional transcriptional reporter assays. Based on ChIP-seq data, we selected promoter and enhancer regions of Gfi1, Cdkn1a, Cdk1, E2f1, and Cdc25a and cloned them into pXP2, pGL2, and pGL4 reporter vectors respectively (Table 2 for detailed sequence information). Each sequence contained between 1 and 3 putative PU.1 binding sites according to calculated transcription factor binding using MatBase software (genomatix©) (indicated with red or green marks on promoter/enhancer indicating black bar in Figure 12).

Table 2. Sequences of indicated regions used for reporter assays

Gfi1 (min promoter): NCBI Reference Sequence: NT_109320.5: _5154
TGTCCCACTGGGGGATGGGGCTGGGGTTGAGAAGGCTAGTGAGCGCCTCTAACGCTCAGGAAGTGAAGTTTGTGGTTTTGGGGGCT
GAGCTCCGAAGGAGATTAAAAAAAAAAAAAAAAAAAAAAGTCAGAGAGACAGATCAGTCTCTCCCGAAAGCAAGATTCAGTTTGCACACTCTCA
GAGCTCGGTGCCCGCGCCCTGACCCCGAAGGTAGGTTTGCTGAACTGCTGTGCCT-5390

Cdkn1a (p21) enhancer (intron2): NCBI Reference Sequence: NT_039649.8: _7190
TCTGACTCATCGCGTGCTTTGGGCGTGGAGATCAAGGTGGAGGGGGCCAGAGCTAAGAGCACTTTCTTTGCTCTCGAGTGTCCGTG
CGTGCGTGTGTGCGTGCGTGCGTATGTGTGTGTGTGTGTGTCTGTGTACGTGCGTGTGTGTGTGTGTGTATGCGTGCGCGCGCGCGC
TCAGTCTGGTTTCCCAACATAGGCGGGAATTTAGGAAGCCTGGGCTCATCGTGACGTGTTTTGTGGCCCGGGGTCCCCCTCCTTTCCTCTCCT
CTCTCCACCCCAGGGTGACGCGCAGCTCCGGTGCCCAAGCAGTTTTGGCGGGCGGGCAGCGCCGGGCAGGAAACTGACTCACCACTCCTTGCT
CGGCCTACGCGCCGCCTACCGAGCGCCATTTCCTGAGTGCACAGCGCCCCCTACCGGCATCAGTGAGGACTGCAAGGCCGGCTAGGCGCGGGT
GGCACCACGGGCTTCTGCCACCCCCACCGCGGCTTAAAGGGAA-7691

Cdk1 promoter: NCBI Reference Sequence: NT_039500.8: _3726
CGCCCAGCTAATAACAAGCTCTTGATGTAGTGGTACTGTCACTTTGGTGGCTGGCTATCTAAATTCAATGCATTTGAATTGTGTTA
GTCTTGGAGGGAAATTACACACAGAAAGGTAGCTGGAGAAAAAAAGAGAATAGATTAGACTGTCCAGAAACAACAGGACGATATTGGAAGGAAA
ACAGAGCTCAAGAGTCAGTTGGCGCCCGCCCTCCTGCAATTCCTCTGGCCGCGGTTTCCGCTCCCTTTCGCGCTCTGCGCTCCCAGGCAGCCC
CGCCCAAGCGTAGCTCAGCTCTGATTGGCTCCTTTGAACGTCTACGTGCAATCGGATTGGCGGATCCCGGGAGCTTTACCGCGGCGAGTTTGA
AACTGCTGGCACTCGGCCTCTAAGCTCCTGGAGTTGCTGCGTCCGCGCAGTCCGGAACTGCGGTGTGGCCCCAGCCGGGACAGAGAGGTATGG
CGTGAGTCGGACTGGGTGCAGGCTGGGCCTGCGGGGGCTCCACGGGATCTGGGGGTTCCCCCGGGGAAGGGCAGGACATCCATGTGAGCCTGG
GGATCCCTTGTGGACGGGTAGGGCCTCCACGTGAGATCTTGGTCTCCTGTGGACGGGTAGGGCCTCACCTAAGTCCGGGATCCCTTATGG-
3867

E2F1:NCBI Reference Sequence: NT_039207.8: _31559
CTTGCCTGTCTGTTTGCTGAGCCTCGCTCCGGGCCTCGGCGTCTTCACCGGAGCGTCGGAACCATTAATGATTGTGTCTCACGT
GTATCCAGCTGGTGCTTGCTTAGTGCACGCTCAGGCTTTGGCACCAAATTCCCAATTCTGGTGTGAGCTGGGTGTTGTCACGTGCCCATCTGC
CAGAGGGAGGAACTGAGGCCCAGAGATGGGGAAGTGCTTCACGCAGCTGCAGATGGTGGGGCTGATATTTGAACTGATGTCTGCTGGCTTGCT
GCAGAACCTATGGCTAGGGAGTGCGCACAGTTGCTTGTTGGAGGTGAGAGAGGGTGACTGTTAGAGACATCTTCGGGAGATCCTCCTTAGTAG
CTCTGCCAGGTGCAGGCCTGGCCTTCCAGGCCTCTGGGGATAGGCCTCTTGATTGGGAGGCCTTCTCTG-31990

Cdc25a promoter: NCBI Reference Sequence: NT_039482.8: _12069
TTTCGGTAGGGACTAGCGCCCCCACAGAAAGTTTCATTGACTCCTTTCTCATTTCAGCCACCTCCCAACTCTTCAGGCTTCGCCCC
CACCGAGAGAGGGCGTGACCTCGAGGAGGCCCACGAGACGCTTCCTCCTTTCCTTCTCATTGGTCCGGCTCAGCTGTCATTCGGGAGCGAGGA
GAAGTTTGCTTCCTGATTGGTGAATTCCGTTTGGCGCCAACTAGGAAAGGGGCGGGGCGGCGGCTATCCTGAGTGTGCAGCAATTAACGCTAA
GGCCACTTTGGTGGTGAGGGAAGTGAAGGTTCCTTCTCTGCGAGCCGGCTACGGAGCAAGGAGGGAGAAAAAAAGTGAGGCGAGTTAGTCGGA
GCGGTGGTCTCAAGACTCTTCCTCCACGGAGTTTGTTTGGATTTAATCTTGAGGTTGCAGGCGCCCGCCCGCCTGCGGGCCTCGCGGGACAGA
GAGGGAAGCACCGGTGCTTGTGCCTGGCGCCTGCCGAGTCCCCTACGCTCGCCGGTCCGCGCCGCTGCCCGTGGCGGCCGCGTCTCTGAACCG
CGGGGTCGTGTTTGTGTTTGACCCGCGGGCGCTGGTGGCGTGGCACGCGGCTGAAGCCGGTGCCAGCGGGGCGGGGCCCGGCGCAGCGGAGGC
GGAGGAAGACGGAGCGGGAGTCCGGGCAGGCCCGGCGGCGCCATGGAACTGGGCCCGGAGCCCCCCCACCGCCGCCGCCTGTTCTTCGCTTGC
AGCCCCACGCCTGCGCCGCAGCCCACGGGGAAGATGCTGTTTGGCGCGTCAGCTGCTGGCGGACTGTCCCCTGTCACCAACCTGACGGTCACC
ATGGACCAGCTGGAAGGACT-12919

Cotransfection of the indicated reporter constructs with increasing amounts of PU.1 expression plasmid resulted in a dose dependent increase of reporter activity for the Gfi1

promoter and a Cdkn1a (p21) intron 2 enhancer (Figure 13 red bars). In contrast, reporter activity of a E2f1 intron 1 enhancer (Figure 13A), and of the Cdk1 and Cdc25a promoters demonstrated a PU.1 dose-dependent decrease (Figure 13B, green bars). We went on to mutate the putative PU.1 binding sites of the Gfi1 promoter, the Cdk1 promoter and the Cdc25a promoter. Mutation of PU.1 binding sites in either promoter significantly reduced the PU.1's activating function on Gfi1 and its repressive function on Cdk1 and Cdc25a transcriptional activity (Figure 13B). In summary, these reporter assays demonstrated that PU.1 positively regulated transcription of cell cycle inhibitors Gfi1 and Cdkn1a (p21) and negatively regulated transcription of the cell cycle activators Cdk1, E2f1, and Cdc25a through direct binding to their promoters/ enhancers. These results demonstrate that PU.1 directly controls multiple regulators of cell division in HSCs.

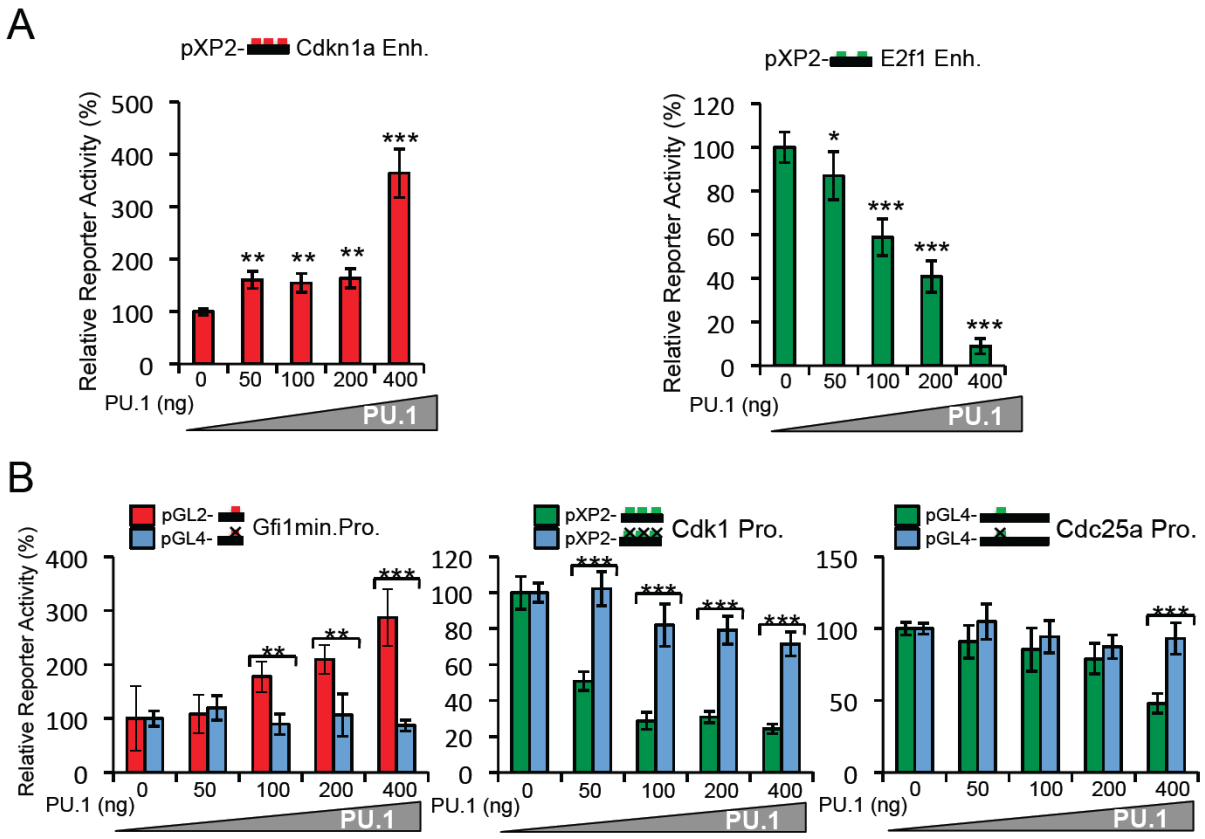

Figure 13. Reporter assays in either pXP2, pGL2, or pGL4 luciferase vectors of indicated promoters and enhancers cotransfected with increasing amounts of PU.1 expression plasmid. Shown are mean values ± standard deviation; *P*-values: * <0.05, **<0.01, ***<0.001 compared to reporter levels with 0ng PU.1 set as 100%, n=4; **B**. Reporter assays for Gfi1, Cdk1, and Cdc25a either with or without targeted PU.1 binding site mutations. P-values are demonstrated in comparison of mutated versus unmutated reporter activity of the corresponding PU.1 dose.

4.1.6 Testing for Positive Autoregulation of PU.1 in HSCs *In Vivo*

To confirm positive PU.1 autoregulation in HSCs in a different *in vivo* model, we utilized conditional PU.1 knockout mice. In these mice, excision of PU.1 exons 4 and 5 could be induced by poly-inosinic–polycytidylic acid (pIpC) administration. Resulting truncated transcripts ($PU.1^{Ex1-3}$) demonstrated the expected loss of the RNA corresponding to the DNA binding ETS domain. Truncated transcripts were equally stable compared to wild-type (full length) PU.1 mRNA (Figure 14A, B) (Iwasaki et al., 2005). We quantified murine truncated PU.1 transcripts with a murine-specific TaqMan RQ-PCR (Exon1-2, Figure 15A), and found an average reduction of 61% after excision in phenotypic HSCs (Figure 14C). Importantly, introduction of a human PU.1 transgene into the $PU.1^{Ex1-3}$ background (Leddin et al., 2011) rescued repression of $PU.1^{Ex1-3}$ transcripts, demonstrating that PU.1 indeed is autoregulated (Figure 14C).

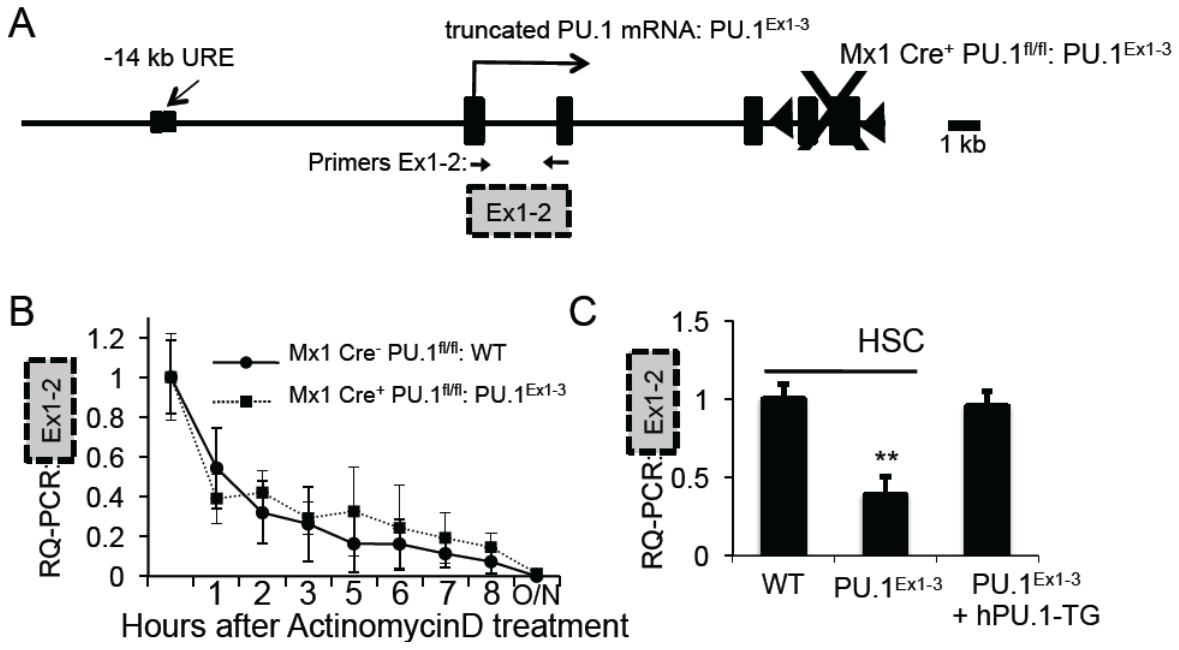

Figure 14. Positive PU.1 autoregulation in HSCs. **A,** Mouse model with induced truncation of PU.1 transcripts ($PU.1^{Ex1-3}$) which lack the DNA binding domain (black boxes: -14kb URE and Exons, black triangles: loxPsites). **B,** Stability of truncated $PU.1^{Ex1-3}$ transcripts is comparable to that of wild type. After ActinomycinD (5µg/ml) treatment of cultured $Lin^-Sca1^+ckit^+$ cells, $1x10^4$ cells were harvested at indicated timepoints and TaqManPCR was performed (Ex1-2 and 18S, avg. ± s.d. relative to starting point; n=3). **C**, Positive autoregulatory loop: Transgenic expression of human PU.1 protein restored $PU.1^{Ex1-3}$ transcript levels in HSCs. TaqManPCR (Ex1-2 and 18S) of purified $Lin^-Sca1^+ckit^+CD150^+CD48^-$ cells (HSCs) of $MX1Cre^-PU.1^{fl/fl}$ (WT), $MX1Cre^+PU.1^{fl/fl}$ ($PU.1^{Ex1-3}$) and $PU.1^{Ex1-3}$ crossed to a human PU.1 transgene ($PU.1^{Ex1-3}$+hPU.1-TG), (avg. + s.d. as fold change to WT; n=3-4; $^{**}P<0.01$).

However, this autoregulatory loop may also involve other transcription factors, especially other Ets factors. TaqMan RQ-PCR analysis of the Ets factors Fli1, Elf1, Erg, and Etv6 in HSCs and LSKs revealed that at least Erg and Etv6 were expressed at detectable levels in HSCs (Figure 15B).

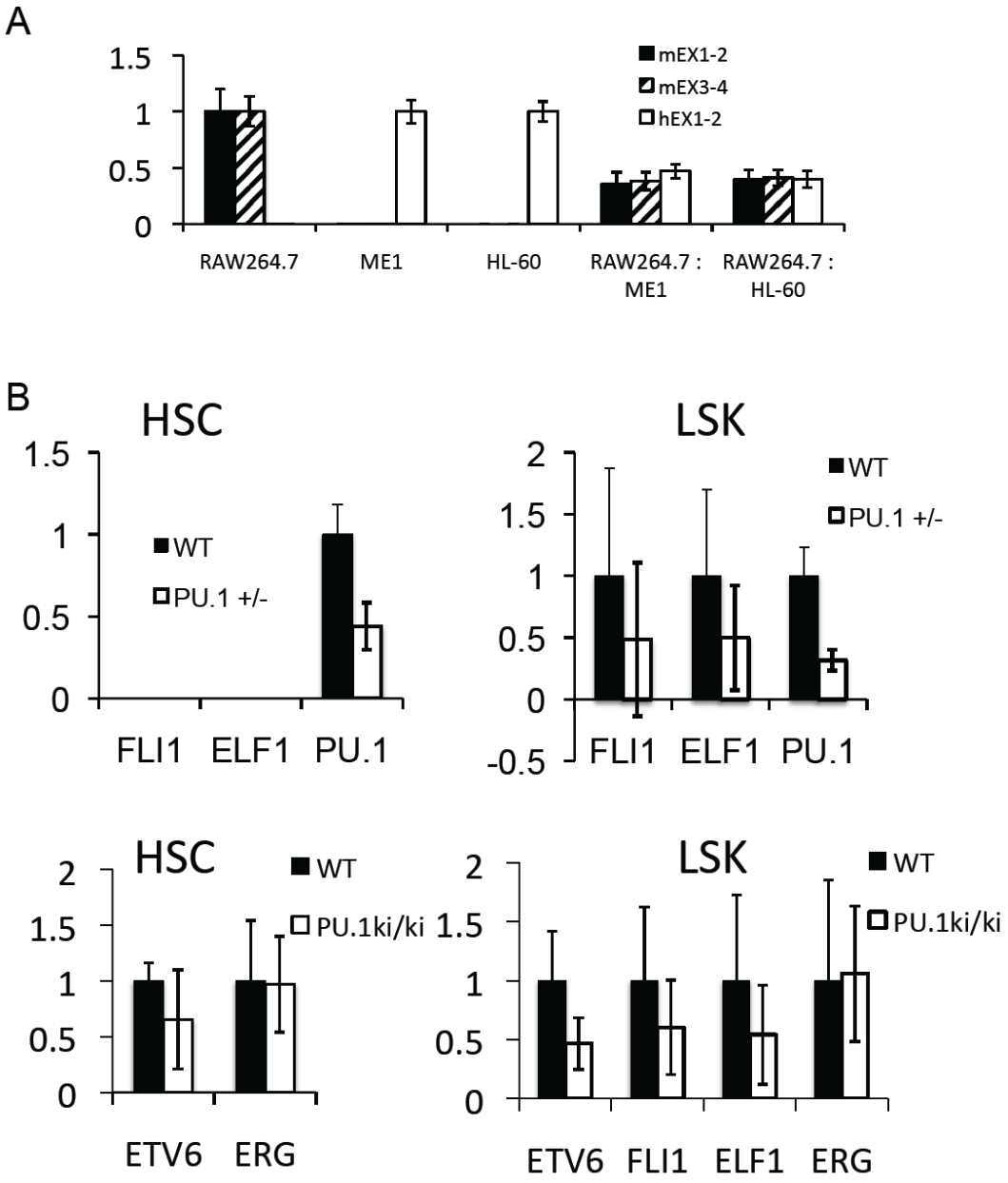

Figure 15. A, Species specificity of indicated TaqMan RQ-PCR assays using murine (RAW264.7) or human (ME1 and HL-60) PU.1 expressing cell lines, or a mixture of the indicated murine and human lines (average values [avg.] + standard deviation [s.d.], n=2). **B,** Fli1, Elf1, PU.1, Etv6, and Erg mRNA levels in $Lin^{-}Sca1^{+}c\text{-}kit^{+}CD150^{+}CD48^{-}$ cells (HSCs) and $Lin^{-}Sca1^{+}c\text{-}kit^{+}$ (LSK) of wild-type (WT), PU.1 heterozygous ($PU.1^{+/-}$), and $PU.1^{ki/ki}$ mice as measured by TaqMan RQ-PCR (average values [avg.] + standard deviation [s.d.] as fold change to WT PU.1; n=4). There was no detectable expression of Fli1 and Elf1 in HSCs and no compensatory increase after PU.1 level reduction in HSCs and LSKs.

To provide direct experimental proof that PU.1 binding to the -14kb URE is essential for autoregulatory PU.1 transcription in HSCs and to rule out secondary effects related to the consequences of decreased transcription factor concentration we designed a new mouse model (Figure 16). In this model PU.1 levels were maintained through the balanced expression of a human PU.1 BAC (**Figure 7**D) (Leddin et al., 2011). Transcription of a murine allele with the mutated PU.1 binding site could be quantified using murine-specific PU.1 TaqManPCR (Ex3-4) that only detected full-length transcripts. The second murine allele was truncated (Ex1-3) and therefore undetectable with this assay. In macrophages, mutation of the PU.1 site at the -14kb URE had no impact on PU.1 transcription, even though PU.1 was bound at that site (Figure 16, **Figure 17**) (Wilson et al., 2010a, Heinz et al., 2010). However, in HSCs, we found that transcription levels of the mutated allele were decreased by 60%, which was similar to those observed in HSCs of PU.1$^{ki/ki}$ mice. These results proved 1) that direct PU.1 binding to the -14kb URE is essential for PU.1 transcription in HSCs; 2) that after excluding secondary effects of reduced PU.1 levels, the decrease of PU.1 transcription in HSCs was comparable to the one in PU.1$^{ki/ki}$ mice; 3) that secondary effects on PU.1 regulation in HSCs of the PU.1ki/ki model appeared to have no impact; and 4) that therefore the PU.1$^{ki/ki}$ model is an unbiased model to study direct involvement of the -14kb PU.1 binding site in gene regulation of HSCs.

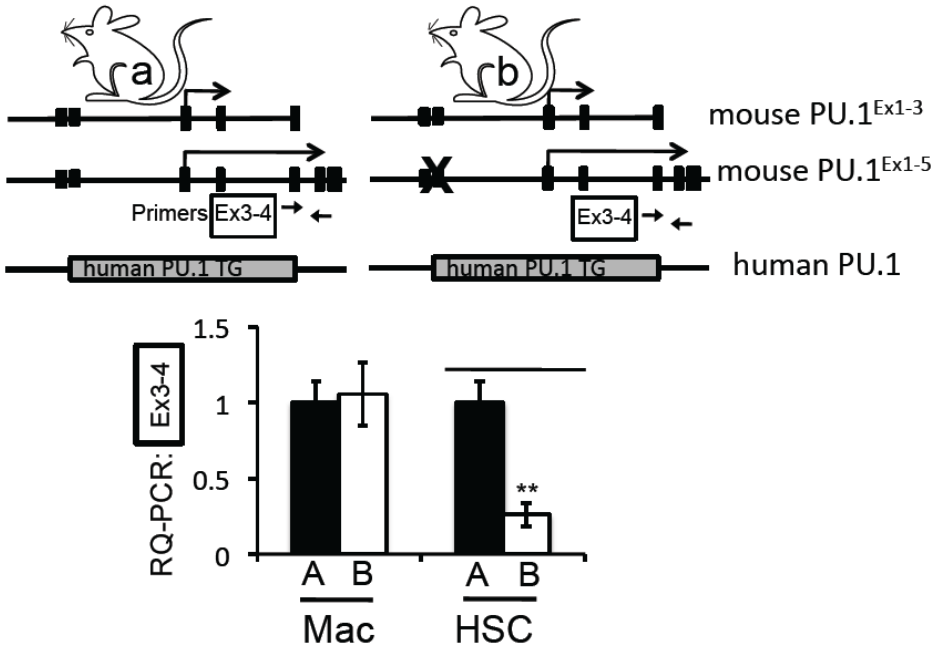

Figure 16. Mice with one PU.1^{Ex1-3} allele and one full-length allele either with (b) or without (a) a mutated PU.1 autoregulatory site at -14kb URE. Both (a and b) had one copy of a human PU.1 transgene (Leddin et al., 2011). Murine-specific PU.1 TaqManPCR Ex3-4 (full-length transcripts

only) was performed. For macrophages (Mac), and Lin$^-$Sca1$^+$ckit$^+$CD150$^+$CD48$^-$ cells (HSCs), the average values relative to wild type + s.d. are shown (n=5; $^{**}P<0.01$).

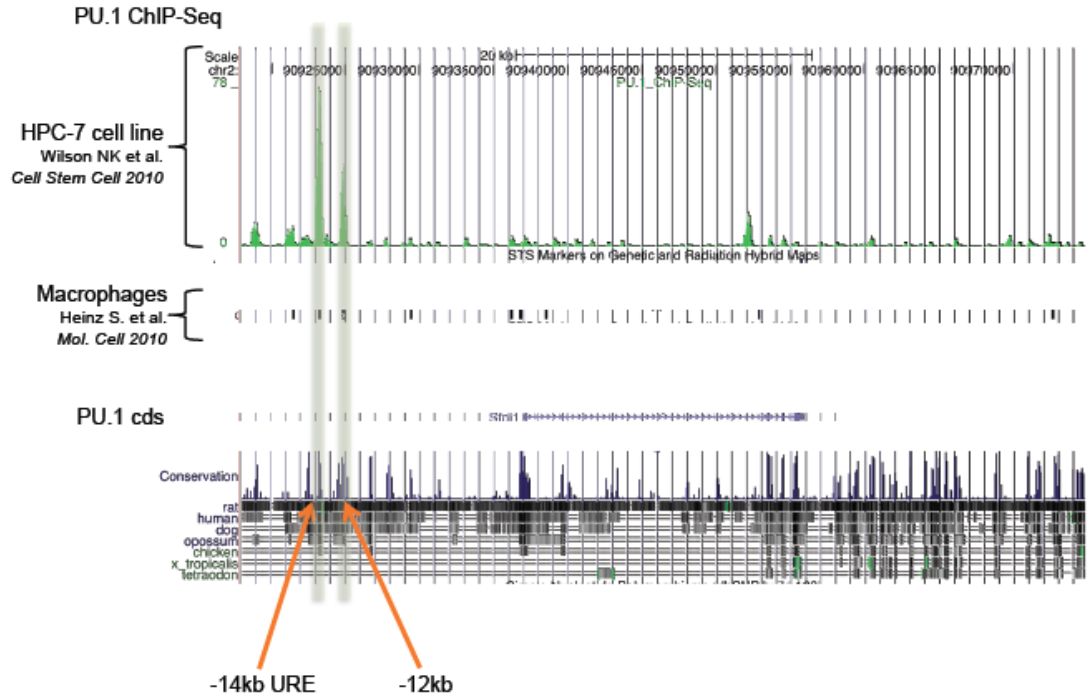

Figure 17. UCSC Genome Browser (http://genome.ucsc.edu/) illustration of PU.1 ChIP-Seq data of the hematopoietic stem cell line HPC-7 (Wilson et al., 2010a) and primary macrophages (Heinz et al., 2010) at the PU.1 locus. Both, HPC-7 cells and macrophages demonstrate PU.1 binding to the -14kb URE and a recently identified -12kb element (Leddin et al., 2011).

In conclusion, positive autoregulation of PU.1 could be demonstrated in three independent mouse models and accounted for more than 60% of PU.1 levels in HSCs.

4.1.7 Autoregulatory PU.1 Binding Mediates Chromosomal Loop Formation in HSCs

Recently, we reported that in cells with high expression of PU.1, the -14kb URE physically interacts with the proximal promoter (PrPr) thereby forming a chromosomal conformation poised for active transcription (Ebralidze et al., 2008). These studies employed chromosome conformation capturing (3C) and were performed on cell lines to obtain sufficient material (Dostie and Dekker, 2007, Ebralidze et al., 2008). We modified the 3C protocol to reduce the amount of cellular material needed and to quantify the degree of interaction between regulatory elements. We verified the linear (i.e. quantitative) range of this

assay from $1x10^6$ down to $5x10^4$ cells, which allowed us to assay the $Lin^-Sca1^+c\text{-}kit^+$ (LSK) population, which includes HSCs (Figure 18A,B).

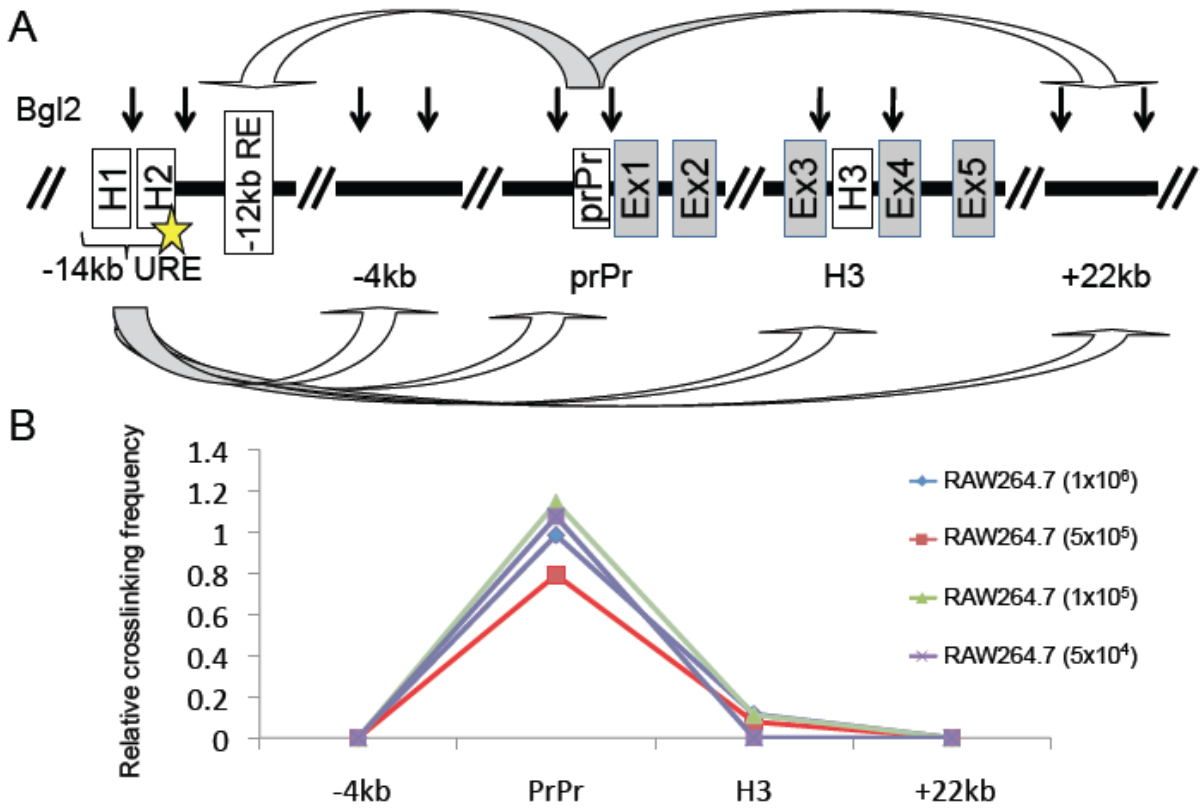

Figure 18. A, Diagram indicating genomic positions of homology regions (H1-H3), the -12kb regulatory element (-12kb RE), proximal promoter (prPr), Exons1-5 (Ex1-5) and Bgl2 restriction sites (vertical arrows) for Quantitative Chromosome Conformation Capturing (3C). Also shown is a genomic region at +22kb used as a control. **B,** Relative crosslinking frequency of H2 with indicated regions, measured by TaqMan PCR and calibrated with an intergenetic DNA amplicon (normalized to average interaction of H2-PrPr). Quantitative TaqManPCRs experiments were in a linear (i.e. quantitative) range from cell number $1x10^6$ down to $5x10^4$ (using dilutions of RAW264.7 cells). The PU.1 binding site in homology region 2 (H2) in the URE is indicated with an asterisk.

Using $2x10^5$ purified primary cells of pooled wild type and $PU.1^{ki/ki}$ animals, we found that mutation of the -14kb PU.1 site led to a loss of the physical interaction between -14kb URE and prPr (Figure 19) specifically in HSC/progenitors but not in macrophages.

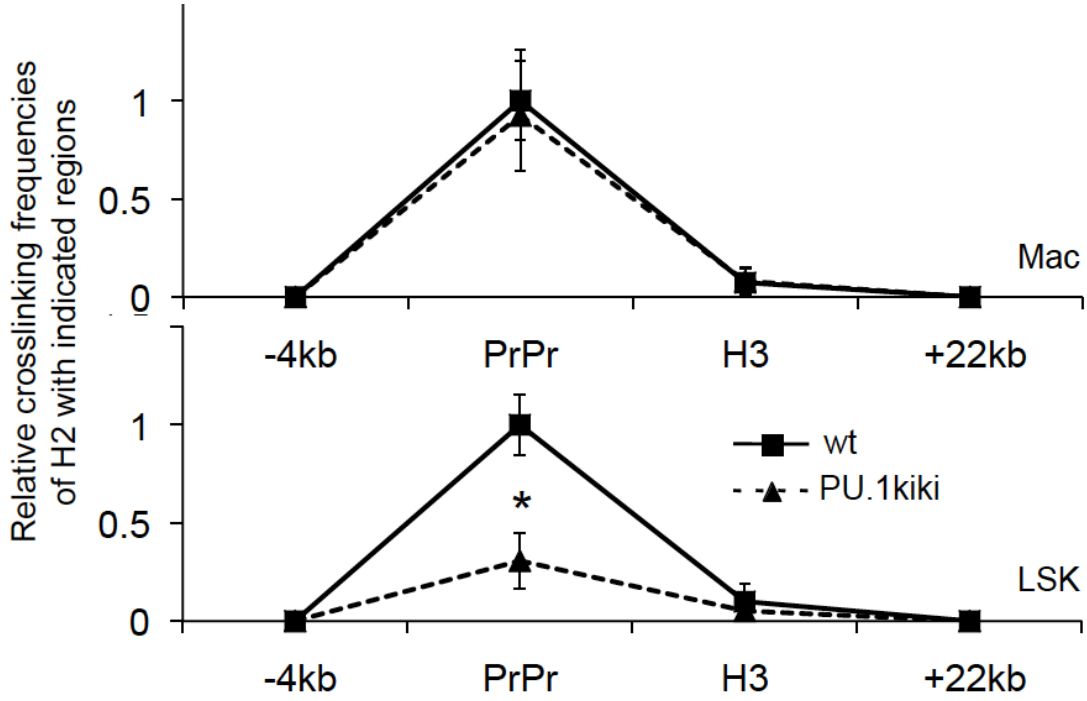

Figure 19. PU.1 binding to the -14kb URE site mediates a chromosomal loop formation in HSC/progenitors. 3C revealed a loss of physical interaction between the -14kb URE and PrPr specifically in $Lin^{-}Sca1^{+}ckit^{+}$ (LSKs) of $PU.1^{ki/ki}$. Bone marrow of 4 individual animals ($PU.1^{ki/ki}$ or wild type) was pooled and ~$2x10^{5}$ sorted cells were used (Macrophages [Mac], LSK for each biological duplicate). After crosslinking and Bgl2 digestion, ligated DNA was purified and interactions of the H2 region with indicated genetic locations was measured by TaqManPCR and calibrated with an intergenetic DNA amplicon. 3C experiments were performed as two independent biological and two technical replicates. Graphs represent results of three (Mac) or four (LSK) independent quantitative TaqManPCR experiments (avg. + s.d., *P<0.05). Crosslinking efficiencies are shown as relative values to H2-prPr interactions of wild type.

We have previously described an autoregulatory PU.1 site in a -12kb cis element and reported its activity exclusively in mature myeloid cells as compared to other cell types especially lymphoid cells (Leddin et al., 2011). To test if the -12kb element compensated for the -14kb URE, we quantified the strength of interaction of the -12kb element with the proximal promoter in macrophages of wild type compared to $mPU.1^{ki/ki}$ mice (Figure 20). Interestingly, we found that the crosslinking frequency was significantly higher in macrophages of mice with a PU.1 binding site mutation in the -14kb URE. This indicated that the -12kb cis regulatory element, which also harbors a PU.1 autoregulatory site, was more active in mature myeloid cells and might at least partially contribute to the observed normal PU.1 levels in macrophages.

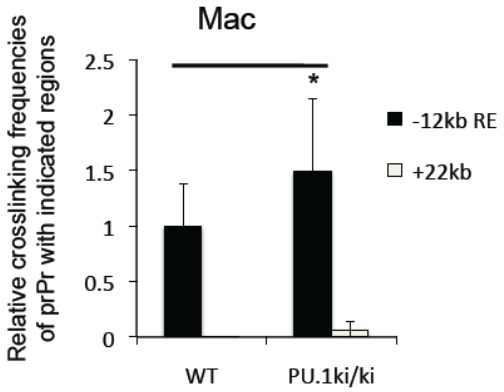

Figure 20. Relative crosslinking frequency of the -12kb element with the proximal promoter in macrophages (Mac) of wild type compared to PU.1$^{ki/ki}$ mice (average values [avg.] + standard deviation [s.d.], *P<0.05).

Taken together we propose a model in which PU.1 binding is necessary in HSCs to establish an active chromosomal conformation for proper PU.1 transcription to balance cell cycle activators and inhibitors (**Figure 21**).

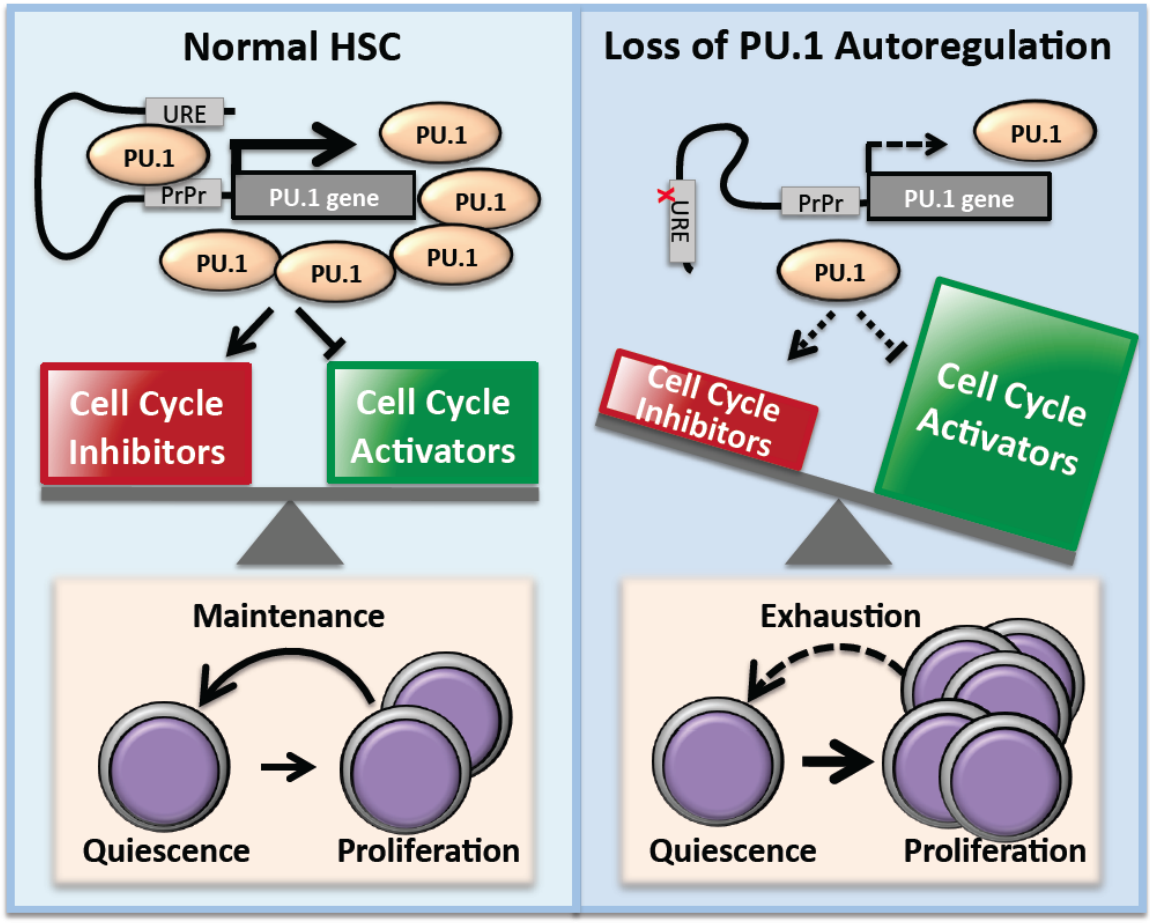

Figure 21. Cartoon: Positive autoregulation induces an active chromosome loop conformation resulting in sustained PU.1 levels which balance cell cycle inhibitors and activators to prevent exhaustion of adult hematopoietic stem cells.

4.2 Runx induced spatial chromatin organization of PU.1 pathway has a functional impact on normal and AML/ETO9a leukemic stem cells

Runx transcription factors contribute to hematopoiesis and are frequently implicated in hematologic malignancies. All three Runx isoforms are expressed at the earliest stages of hematopoiesis; however their function in hematopoietic stem cells (HSCs) is not fully elucidated. Here, we show that Runx factors are essential in HSCs by driving the expression of the hematopoietic transcription factor PU.1. Mechanistically, using a knock-in mouse model in which all three Runx binding sites in the -14kb enhancer of PU.1 are disrupted we observed failure to form chromosomal interactions between the PU.1 enhancer and its proximal promoter. Consequently, decreased PU.1 levels resulted in diminished long-term HSC function through HSC-exhaustion, which could be rescued by reintroducing a PU.1 transgene. Similarly, in a mouse model of AML/ETO9a leukemia, disrupting the Runx binding sites resulted in decreased PU.1 levels. Surprisingly, leukemia onset was delayed and limiting dilution transplantation experiments demonstrated functional loss of leukemia initiating cells. Our data demonstrate that Runx-dependent PU.1 chromatin interaction and transcription of PU.1 are essential for both normal and leukemia stem cells. Although low PU.1 levels have been considered as hallmark of leukemia, reducing PU.1 might also target the leukemic stem cell**.**

4.2.1 Runx binding sites in the PU.1 URE mediate PU.1 transcription in HSCs.

In order to understand the role of the three Runx factors in regulating PU.1 in hematopoietic stem cells, we first evaluated expression of the three Runx transcription factors in unselected bone marrow cells and HSCs ($SLAM^{+}LSK$, or Lineage-Sca1+cKit+CD150+CD48- (Kiel et al., 2005)). While expression of all Runx genes was clearly detectable in both populations, Runx1 was the most highly expressed factor in HSCs (Figure 22A). To test if loss of Runx1 would result in a compensatory upregulation of either Runx2 or Runx3 in HSCs, we utilized Mx1-Cre1 inducible Runx1 knockout mice (Growney et al., 2005) and tested changes of mRNA levels of individual Runx factors. Induced disruption of Runx1 resulted in non-detectable Runx1 mRNA levels in HSCs, indicating efficient excision. Interestingly, Runx3 levels were significantly increased, whereas Runx2 levels remained unchanged, suggesting that Runx3 might partially compensate for Runx1 loss

in HSCs (Figure 22B).

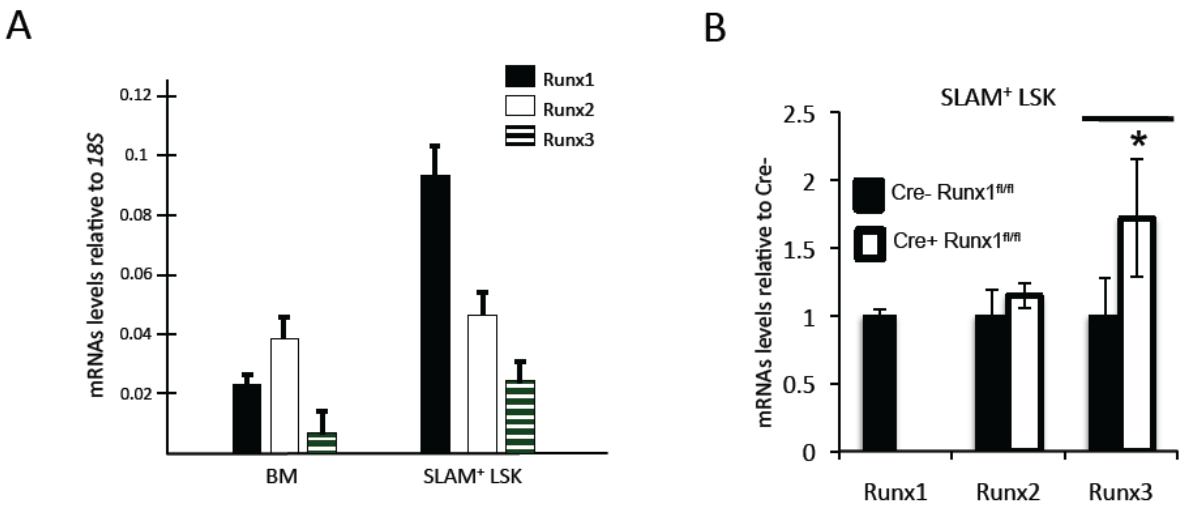

Figure 22. Runx factors mediate PU.1 transcription in HSCs through binding sites at the -14kb URE. **A.** mRNA levels of indicated Runx genes in unselected whole bone marrow cells (BM) and isolated SLAM+LSK cells (HSC enriched population). Shown are average (avg.) levels + standard deviation (sd.); n=7 (note that expression data for Runx1 have been presented in *Levantini et al. Supplementary Fig S1 (Levantini et al., 2011)*). **B.** mRNA levels of indicated Runx genes after CRE induced Runx1 deletion in SLAM+ LSK cells. Shown are avg. levels ± sd. (n=4), * indicates $p<0.05$.

The hematopoietic transcription factor PU.1 harbors three conserved Runx binding sites at its -14kb upstream regulatory element (URE) (**Figure 2**) (Huang et al., 2008). Reporter assays in stably transfected 416B cells demonstrated that the transcriptional activation potency of the URE depends highly on the intactness of all three Runx binding sites (Figure 23).

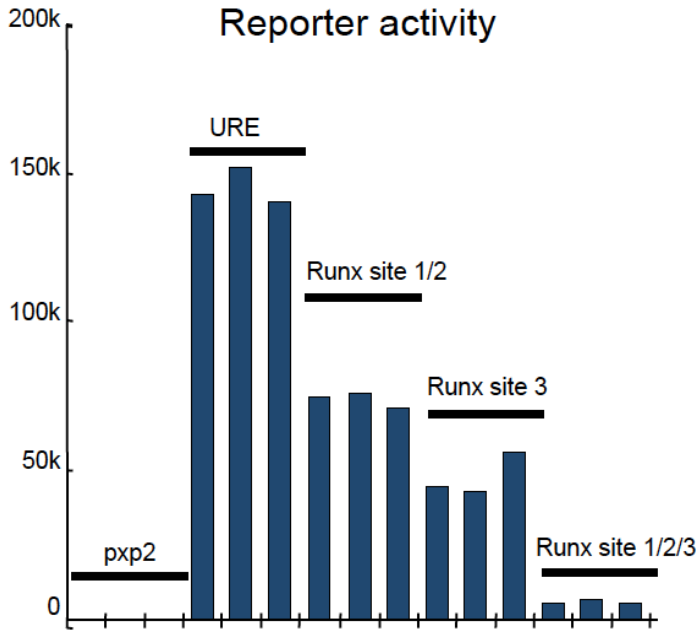

Figure 23. Mutation of the Runx binding sites (from TGTGGTA to TGACCTA) reduced URE reporter activity in individual clones of stably transfected 416B cells. Pxp2 luciferase vector plus PU.1 promoter were used as indicated with either a wild type URE, a URE in which Runx site 1 and 2 were mutated, a URE in which Runx site 3 was mutated, or a URE in which all three Runx sites were mutated. Bar graphs show the luciferase activity of independent cell clones relative to the activity of empty pxp2 vector. Activity values were normalized to the transgene copy number measured by Southern blot analysis.

We previously generated a knock-in mouse model (PU.1-URE-mRunx) in which binding of all Runx factors was abolished from the URE of PU.1 (Huang et al., 2008) (Figure 24A).

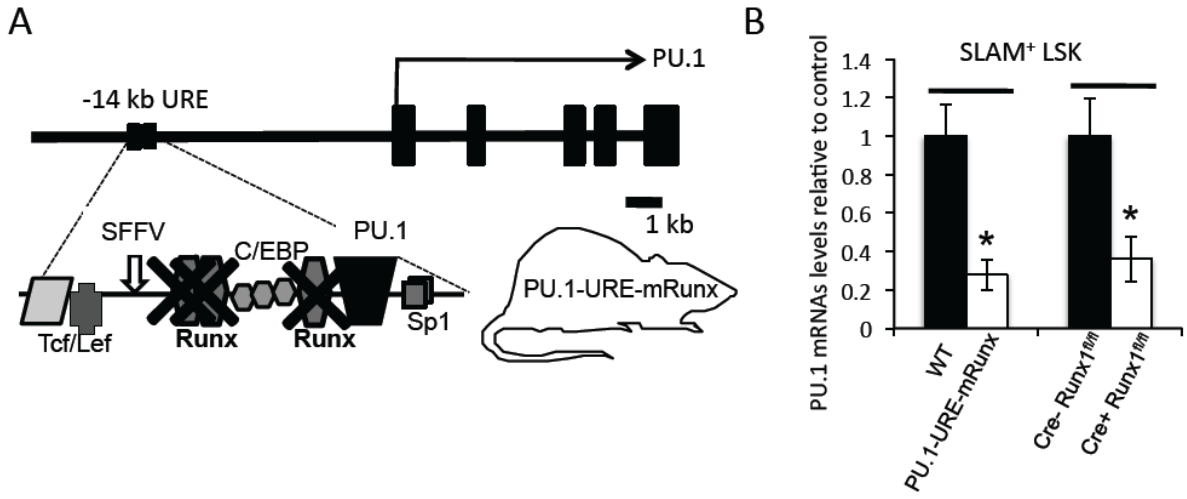

Figure 24. A. Simplified scheme of murine PU.1 locus indicating the three Runx binding sites, all of which have been selectively mutated from TGTGGTA to TGACCTA in the Knock-in mouse model "PU.1-URE-mRunx". **B**. PU.1 mRNA levels in SLAM+LSK cells of PU.1-URE-mRunx and Runx1 deleted mice compared to control. Shown are avg. levels ± sd. (n=4), * indicates $p<0.05$.

Electro-mobility shift assays demonstrated that in contrast to a loss of all three URE Runx binding sites, a loss of Runx1 alone led only to a minimal decrease of CBF binding due to the contribution of other Runx family members (Huang et al., 2008). Chromatin immunoprecipitation (ChIP) analyses of total bone marrow cells confirmed the loss of Runx binding to the -14kb URE in PU.1-URE-mRunx mice (Figure 25).

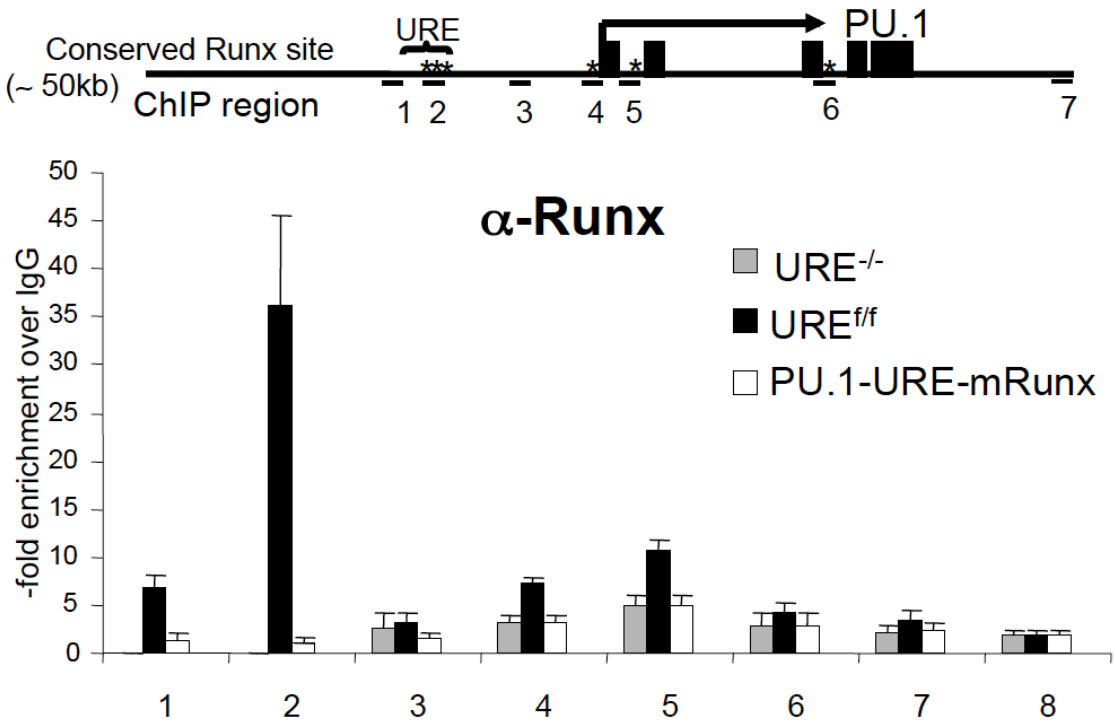

Figure 25. Quantitative chromatin immunoprecipitation (ChIP) of total bone marrow cell lysates using normal rabbit IgG and antibodies against Runx. Black bars in scheme indicate RQ-PCR primer locations of the PU.1 locus. One additional primer set was used to amplify the glyceraldehyde-3-phosphate dehydrogenase (GAPDH) gene as an internal control. Relative enrichments for Runx antibodies were calculated as fold enrichment over IgG. "URE fl/fl" indicates bone marrow of mice after homologous recombination with a similar targeting vector as for Runx site mutants but with unmutated URE serving as positive control, "URE -/-" (Rosenbauer et al., 2004) indicates bone marrow of mice with excised URE serving as negative control. Shown are values as avg. + sd. of four independent RQ-PCR analyses.

Importantly, PU.1 mRNA levels in HSCs of PU.1-URE-mRunx mice were reduced by 72% in comparison to controls (wild type), greater than the average reduction of 63% observed in Runx1 knockout mice (Figure 24B). These results revealed the major role of the URE Runx sites for PU.1 transcription in HSCs.

4.2.2 Disruption of Runx binding leads to a loss of URE-proximal promoter interaction

We recently reported that a stable interaction of the URE with the proximal promoter is required for efficient PU.1 transcription in hematopoietic progenitors/HSCs (Staber et al., 2013). To test if Runx binding is also necessary for loop formation in the PU.1 gene locus, we designed a chromosome conformation capturing (3C) experiment in which after DNA crosslinking and restriction enzyme digestion (with Bgl2), the frequency of interactions of the URE with other DNA fragments was quantified by TaqMan Real time PCR (Figure 26A).

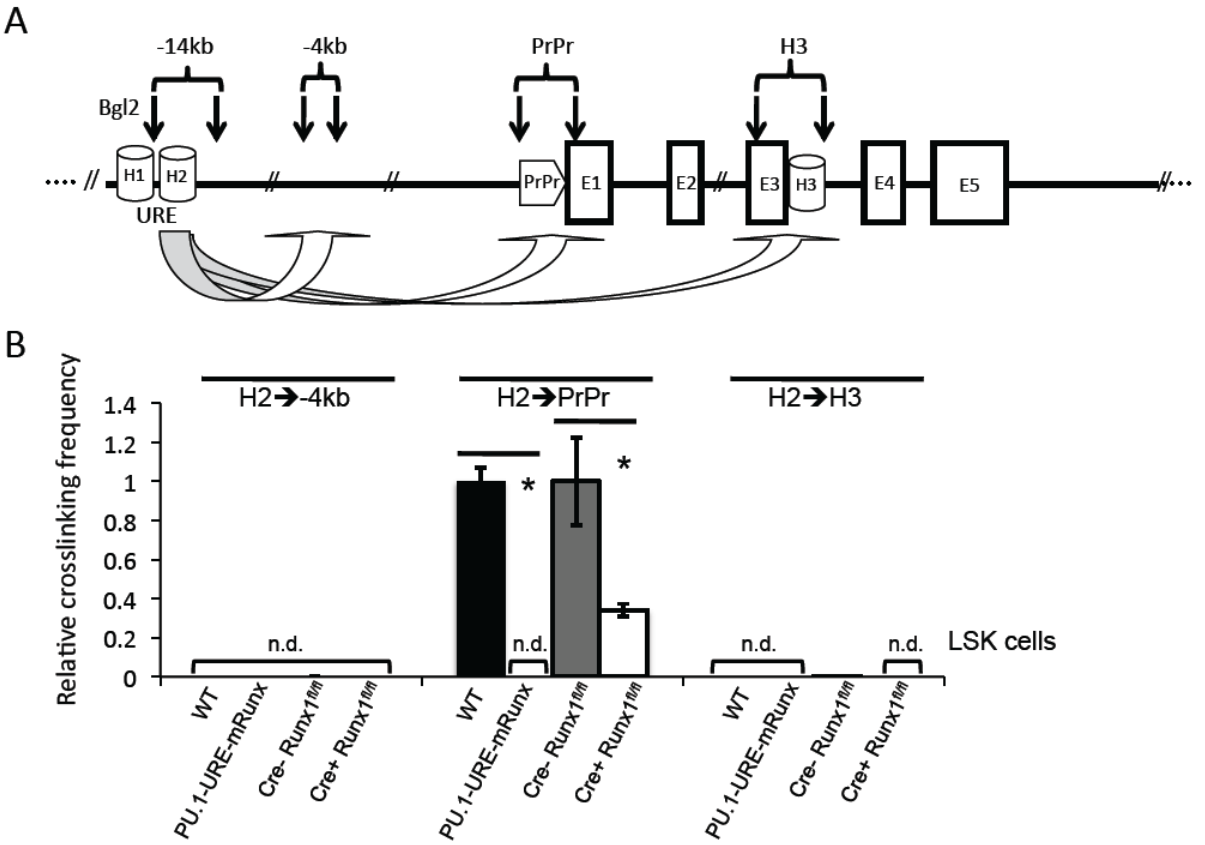

Figure 26. Runx site mutation leads to loss of URE-proximal promoter interaction in HSCs/progenitors. **A.** Simplified scheme of the PU.1 gene indicating the positions of homology regions (H1-H3), the -14kb upstream regulatory element (URE), proximal promoter (PrPr), Exon 1-5 (E1-E5), and Bgl2 restriction sites (vertical arrows) for quantitative chromosome conformation capturing (3C). The genomic region at -4kb was used as control. **B.** Quantitative 3C demonstrates a loss of URE-PrPr interaction in mice with disrupted Runx binding sites (PU.1-URE-mRunx) and a significant loss after induced Runx1 deletion in LSK cells. After crosslinking and Bgl2 digestion, ligated DNA was purified and interactions of the H2 region with indicated genetic locations was measured by TaqManPCR and calibrated with an intergenetic DNA amplicon. Graphs represent the results of four independent quantitative TaqManPCR experiments (avg. + sd; *, $p < 0.05$). Crosslinking efficiencies are shown as relative values to H2-PrPr interactions of WT and Cre-Runx1$^{fl/fl}$, respectively.

In LSK (lin-, sca+, cKit+) stem/progenitor cells, induced deletion of Runx1 resulted in a pronounced (66%) decrease in crosslinking frequency between the URE and proximal promoter. After disruption of Runx binding sites, however, crosslinking frequencies were not detectable (Figure 26B). To verify the dramatic effect of URE Runx site mutations on PU.1 folding, we also applied a semi-quantitative (PCR/Southern blot based) 3C approach investigating the interactions of the proximal promoter with other DNA segments in the PU.1 locus (**Figure 27**A). Using isolated cKit+ cells from bone marrows of PU.1-URE-mRunx and wild type mice, we could confirm the loss of interaction between URE and proximal promoter following Runx site mutation (**Figure 27**B).

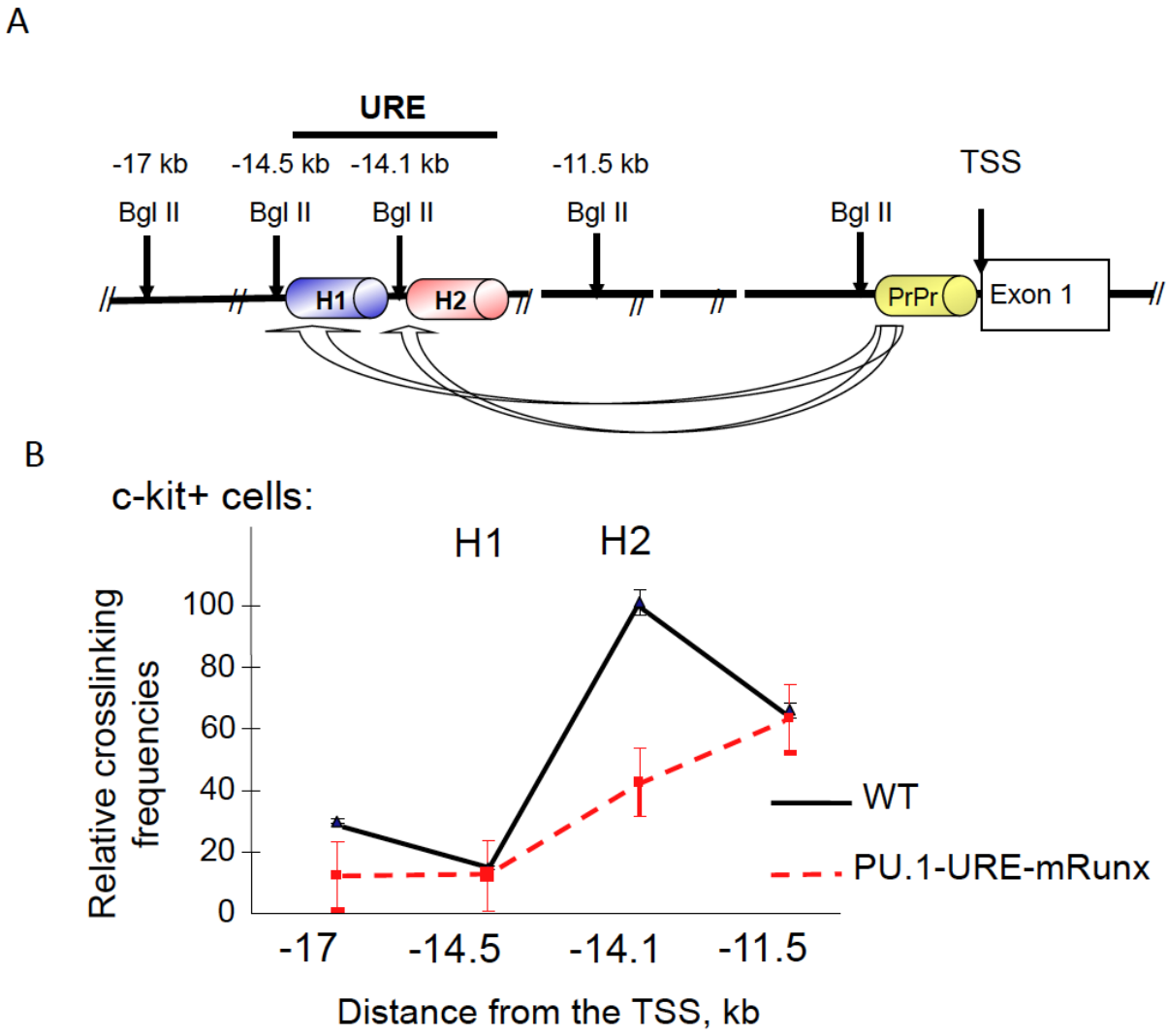

Figure 27. Runx site mutation leads to loss of interaction between H2 (in the URE) and the proximal promoter (PrPr). **A.** Diagram indicating: proximal promoter (PrPr); -14kb upstream regulatory element (URE); position of homology regions (H1-H2); Bgl II restriction sites used in 3C. B. Semi-quantitative 3C performed on paired (n=2) wild type (WT; black line) and Runx mutant (mRunx; red

line) c-kit+ bone marrow cells. The graphs represent results of two independent PCR/Southern blot experiments.

4.2.3 Mutation of the Runx binding sites results in loss of HSC function

Since PU.1-URE-mRunx mice expressed PU.1 at very low levels in HSCs, we next analyzed the HSC phenotype. The percentage of progenitors (LSK) and HSCs in PU.1-URE-mRunx mice was not different from wild type controls as determined at an age of 4 months (Figure 28A). Similarly, absolute cell numbers of LSKs and HSCs also appeared to be unchanged (Figure 28B).

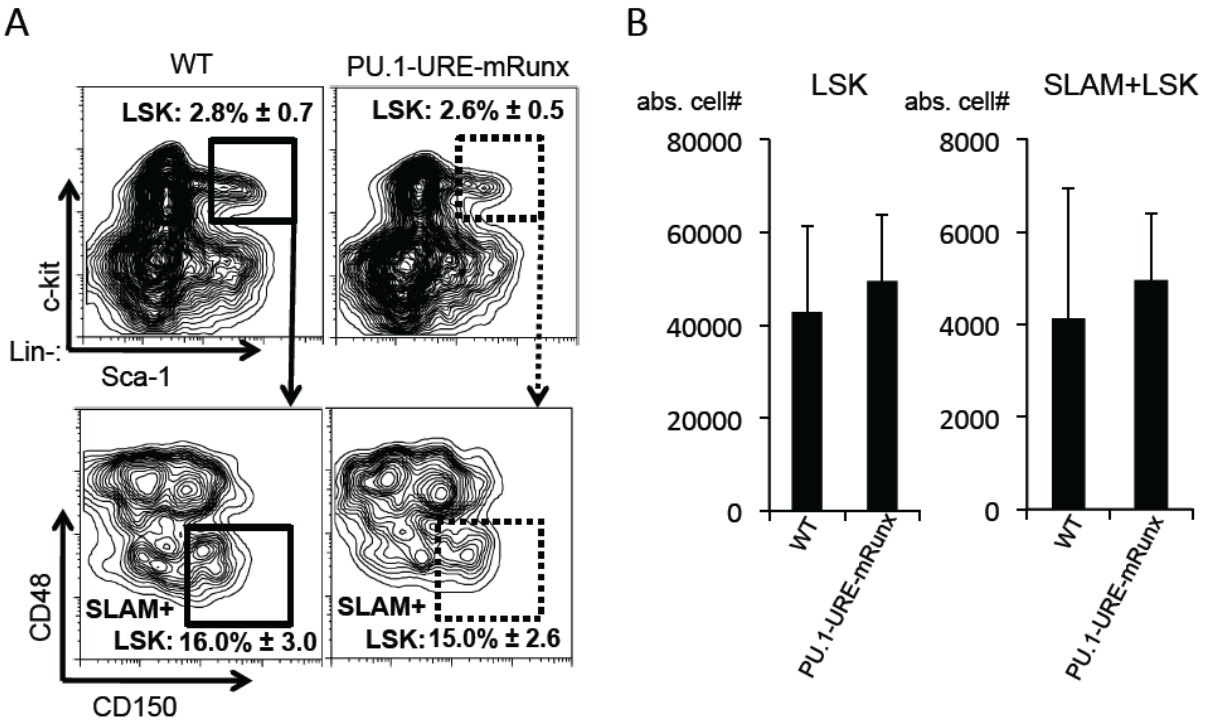

Figure 28. Runx binding site mutation leads to reduced numbers of functional HSCs. **A and B**. Phenotypic HSCs are unaltered in PU.1-URE-mRunx mice compared to WT (4 months). **A.** Flow cytometry of bone marrow samples demonstrating the avg. percentage ± sd. of LSK cells (from lineage negative population) and the avg. percentage ± sd. of SLAM+LSK cells (from LSK population). **B.** Total number of LSK and SLAM+LSK cells in bone marrow (avg. + sd. of 1 femur and 1 tibia; n=5).

HSCs of PU.1-URE-mRunx mice demonstrated normal bone marrow homing capabilities (**Figure 29**).

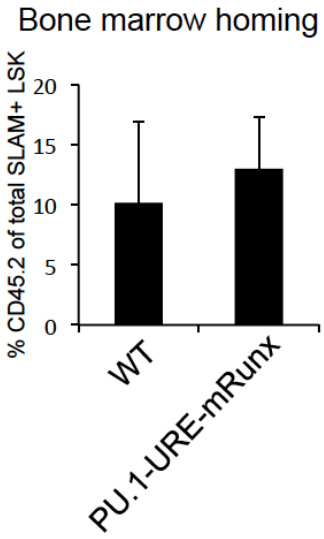

Figure 29. Homing of PU.1-URE-mRunx HSCs is unaltered. 5 x 10^5 bone marrow cells of 4 month old wild type (WT) or PU.1-URE-mRunx mice (C57BL/6J, $CD45.2^+$) were transplanted into irradiated (900 rads) C57BL/6J, $CD45.1^+$ recipients. After 16 hours bone marrow was analyzed. Shown is the avg. percentage + sd. of $CD45.2^+$ cells of $Lin^-Sca1^+CD150^+CD48^-$ cells (HSCs) (n=5).

To test if the Runx-PU.1 axis would impact the function of HSCs, we performed competitive repopulation transplantation with limiting dilution of phenotypic HSCs (Figure 30A). After 6 months, we evaluated hematopoietic reconstitution in blood and bone marrow considering mice with a CD45.2 chimerism of < 0.3% as negative responders. Quantification of competitive repopulating units showed a severe (24.5-fold) decrease indicating a dramatic loss of HSC long-term function (Figure 30B and C).

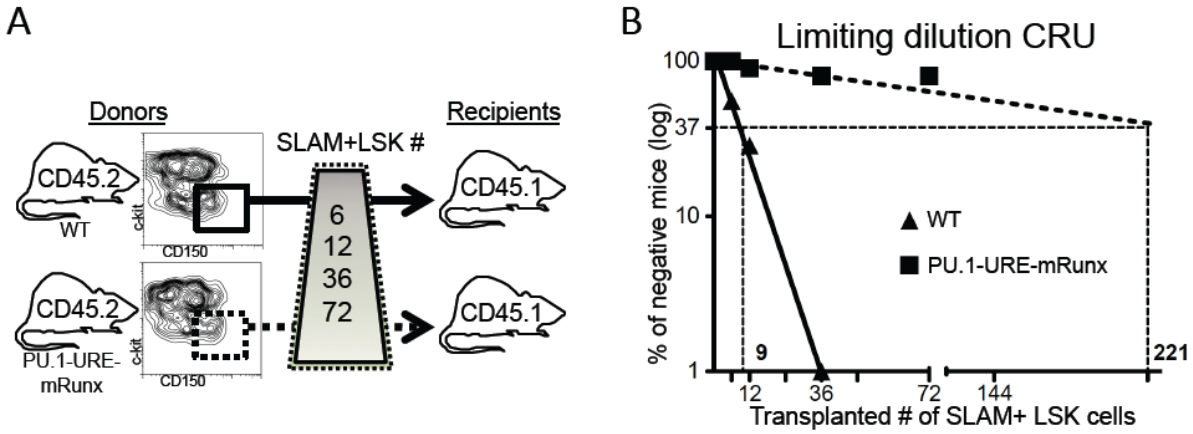

C

Quantification of CRUs (follow up >6 months)

Transplanted # of SLAM+ LSK cells	WT	PU.1-URE-mRunx
6	5/11	0/11
12	10/14	1/10
36	5/5	1/5
72	-	1/5
HSC frequency	1 in 9	1 in 221
(95% confidence interval)	(6 - 15)	(71 - 692)

Figure 30. **A.** Experimental scheme of the limiting dilution competitive repopulating units (CRU) assay. Indicted numbers of isolated SLAM+LSK cells of WT or PU.1-URE-mRunx mice (CD45.2) were transplanted together with $2x10^5$ unselected whole bone marrow cells of competitor mice (CD45.1) into lethally irradiated (1300 rads) recipients (CD45.1). **B** Semi-logarithmic plot showing the percentage of negative recipients as function of the number of transplanted SLAM+LSKs. CRUs are indicated as vertical dashed lines. **C.** Table showing the frequency of CRUs and the total number of transplantations per cell dose. Reconstitution was evaluated in blood and bone marrow 6 months after transplantation. Mice with CD45.2 chimerism < 0.3% were considered as non-responders.

To further analyze if the loss of functional HSCs of PU.1-URE-mRunx mice was related to premature HSC exhaustion we performed a series of analysis on HSCs after repetitive injuries and stress. We first evaluated their potential to regenerate bone marrow after repetitive injections with the antimetabolite 5'-fluorouracil (5-FU). Survival of PU.1-URE-mRunx mice was significantly decreased ($p < 0.0001$) upon weekly 5-FU injections demonstrating that HSCs of PU.1-URE-mRunx mice could not provide sufficient blood supply after injuries, a key physiologic task of HSCs (**Figure 31**).

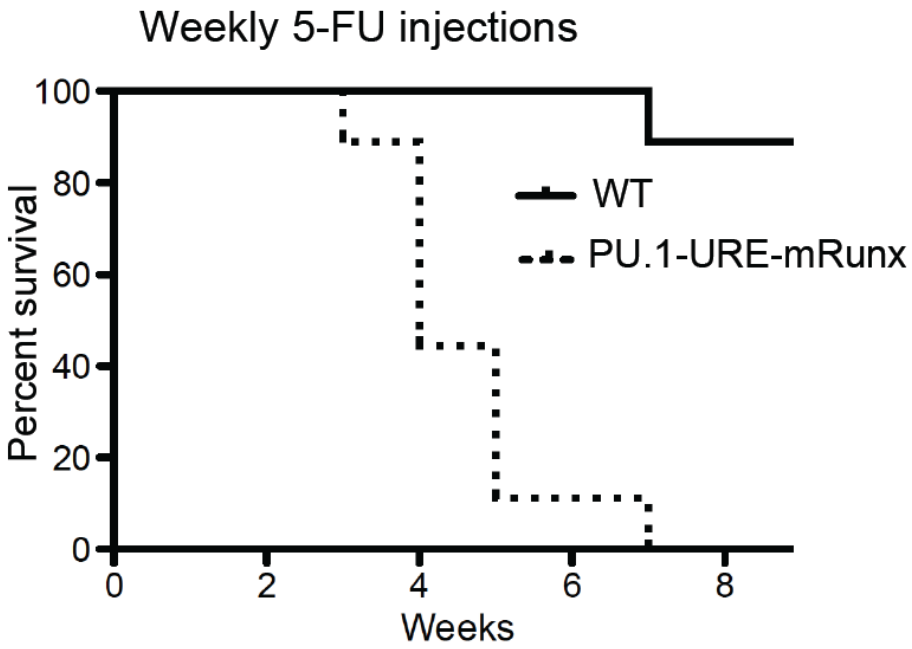

Figure 31. Reduced capability of PU.1-URE-mRunx mice to regenerate bone marrow after repetitive injuries by weekly 5-fluorouracil (5-FU) administration (intraperitoneally [i.p] injected 150 mg/kg). Results are shown as Kaplan-Meier survival curves (n = 9, $p<0.0001$ [Mantel-Cox]).

Using repetitive transplantation experiments we investigated if the potential to repopulate bone marrow exhausted with increasing rounds of transplantations. Indeed, HSCs of PU.1-URE-mRunx mice failed to repopulate bone marrows of lethally irradiated recipients after the third round of transplantations (**Figure 32**).

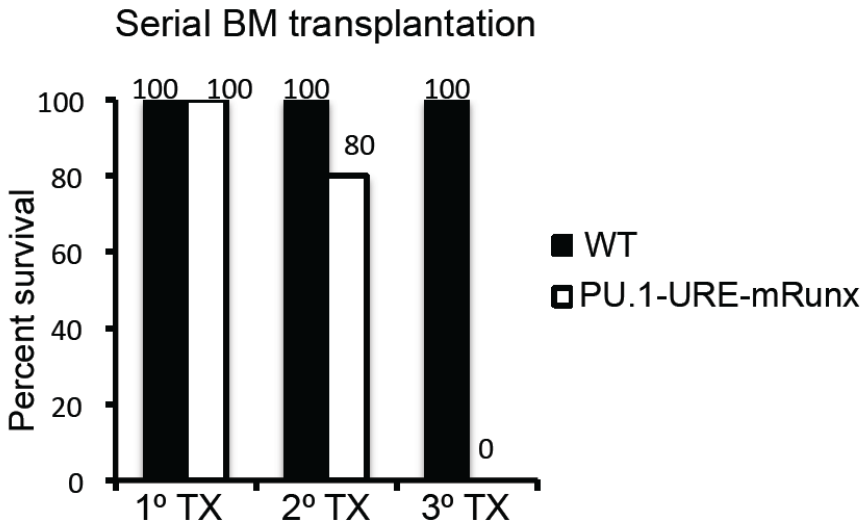

Figure 32. Serial transplantation assays. Rounds of transplantations with $5x10^5$ bone marrow cells were performed in 16-week intervals. Bar graphs indicate survival percentage after each round of

transplantation (n = 5).

Competitive long-term repopulation assays with total bone marrow cells also reflected the functional defects of HSCs of PU.1-URE-mRunx mice (**Figure 33**). We previously demonstrated in PU.1 knockout, PU.1 heterozygous, and PU.1 hypomorphic mice that by crossing to a human PU.1 transgenic strain, PU.1 protein levels were restored (Staber et al., 2013, Leddin et al., 2011). Importantly, we here show that HSC functions of PU.1-URE-mRunx mice could be rescued by the human PU.1 transgene (**Figure 33**), thus providing proof that the HSC phenotype of PU.1-URE-mRunx mice depended on PU.1.

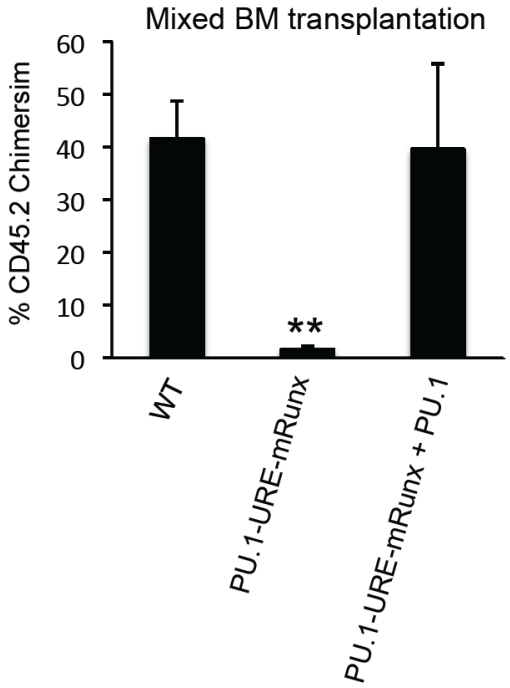

Figure 33. 1x10^6 whole bone marrow cells of indicated donor mice (CD45.2+) were co-transplanted with equal amounts of CD45.1+ wild type bone marrow cells into lethally irradiated CD45.1+ recipients. Bar graphs show donor chimerism in blood after 6 months (avg. + SD, n = 5; **, $p < 0.01$). Loss of chimerism of PU.1-URE-mRunx donors was restored by breeding to a strain harboring a human transgene expressing PU.1 (''+ hPU.1-TG'').

4.2.4 Delayed AML/ETO9a leukemia onset in cells of Runx binding site mutants

We next aimed to investigate if leukemic stem cells share the same dependence on the Runx-PU.1 pathway as normal HSCs. Given the role of Runx in regulation of PU.1 (Huang et al., 2008), and other studies suggesting that dysregulation of PU.1 is an important mechanism in AML (Vangala et al., 2003, Rosenbauer et al., 2004, Steidl et al., 2006, Aikawa et al., 2010), we chose to test this hypothesis using a model of AML/ETO transduced leukemia.

A truncated form of the AML/ETO fusion protein (AML/ETO9a) efficiently induces leukemia when expressed in a MigR1 retrovirus in fetal liver cells (Yan et al., 2006). We transplanted equal numbers of AML/ETO9a transduced E14.5 fetal liver cells of PU.1-URE-mRunx and wild type mice into CD45.2 recipients and analyzed leukemia development and survival (**Figure 34**).

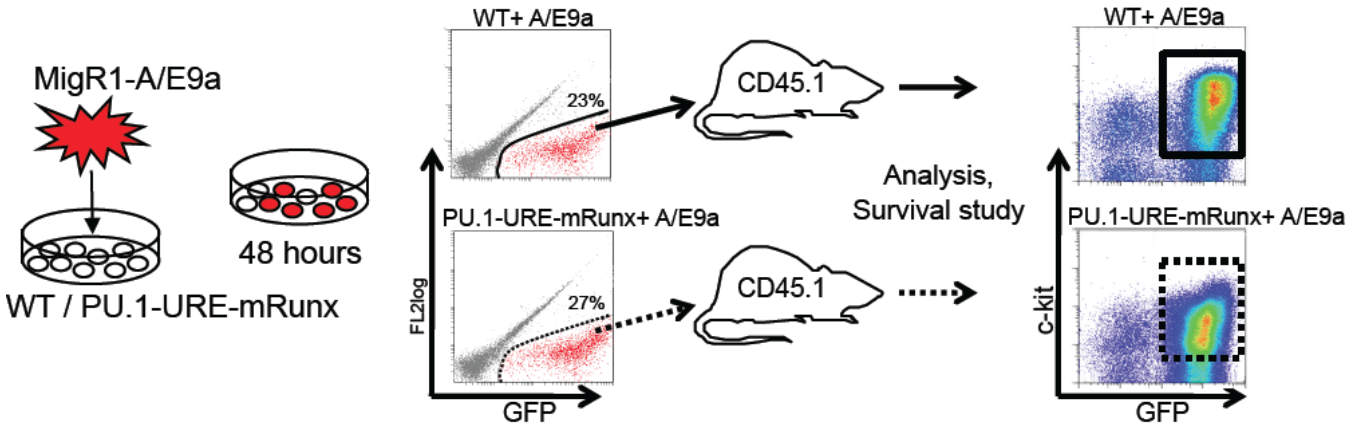

Figure 34. Experimental scheme: E14.5 fetal liver cells (lineage depleted) of PU.1-URE-mRunx and WT mice were retro-virally (MigR1) transduced with the fusion oncogene AML/ETO9a (A/E9a) harboring an eGFP signal. After 48 hours GFP positive cells were isolated and transplanted into CD45.2 recipient mice (n=7). Development of leukemia and survival was monitored. Moribund mice were taken for analysis.

AML/ETO9a protein was stably expressed in leukemic samples of recipients (**Figure 35**).

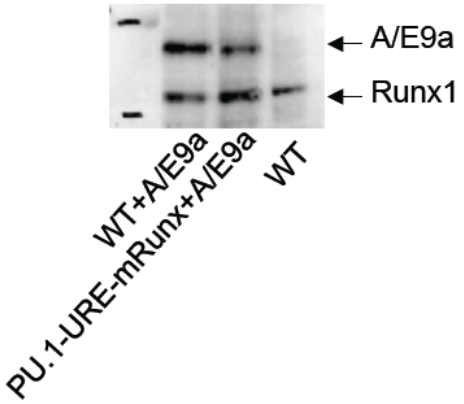

Figure 35. Representative Immunoblot demonstrating stable A/E9a protein expression in leukemic samples (spleen) of A/E9a recipients.

Leukemic cells derived from AML/ETO9a transduced PU.1-URE-mRunx cells showed significantly decreased PU.1 levels compared to those derived from AML/ETO9a transduced wild type leukemia cells (**Figure 36**).

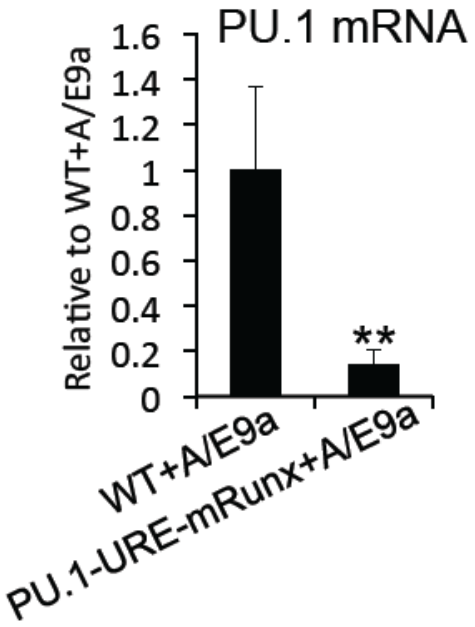

Figure 36. PU.1 mRNA levels of leukemic (c-kit+, GFP+) cells. Shown are avg. levels ± sd. relative to WT+A/E9a (n=4), ** indicates $p<0.01$.

All recipients eventually developed leukemia with similar patterns of multi-organ infiltration (Figure 37, Figure 38).

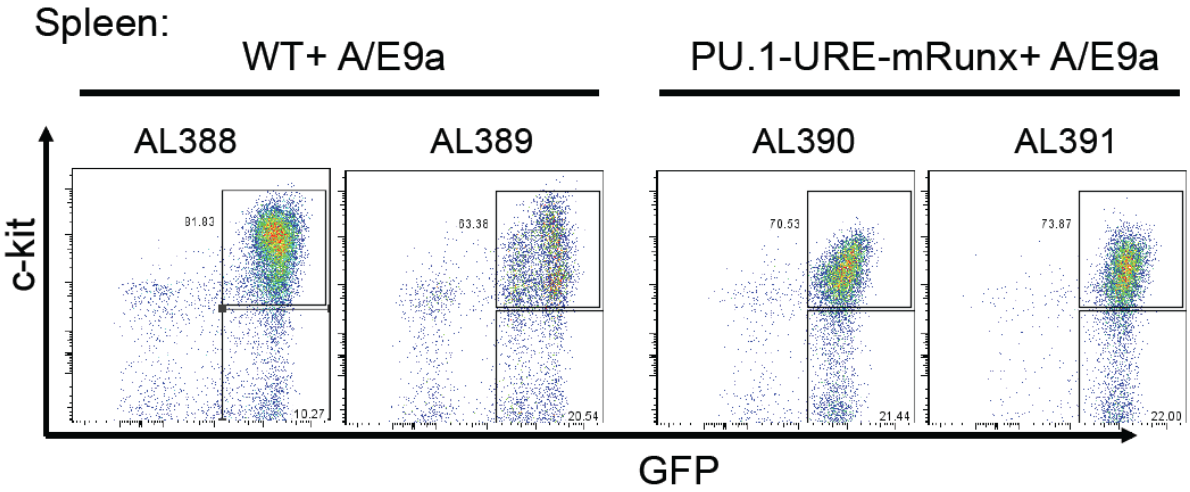

Figure 37. Representative flow cytometry analysis of spleens of moribund recipients of either WT+A/E9a or PU.1-URE-mRunx+A/E9a cells

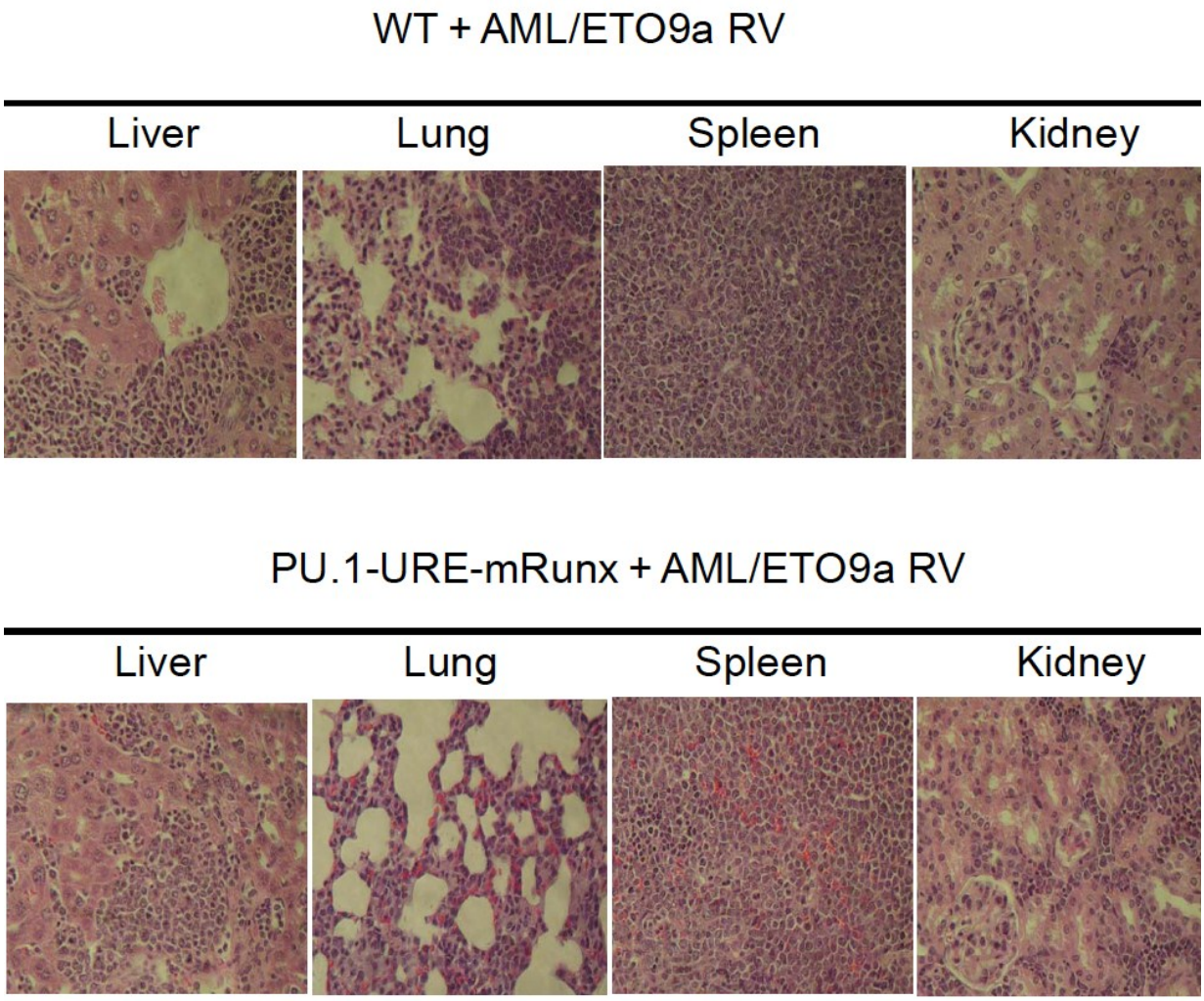

Figure 38. Histologic specimens of indicated organs showing diffuse infiltration of leukemic cells of moribund recipients of either WT+A/E9a or PU.1-URE-mRunx+A/E9a cells (HE staining).

However, disease onset of recipients of AML/ETO9a induced PU.1-URE-mRunx leukemic cells was delayed, and survival was significantly longer than of recipients of AML/ETO9a induced wild type cells (median 193 days versus 118 days, p=0.0013) (**Figure 39**).

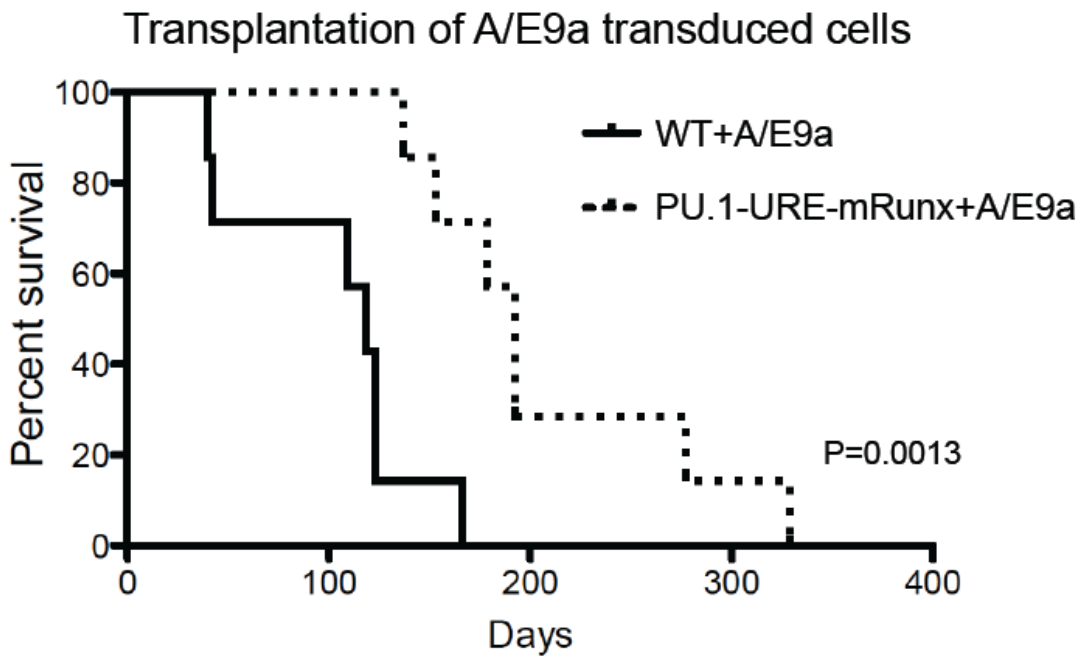

Figure 39. Kaplan Mayer survival analysis of recipients receiving either WT or PU.1-URE-mRunx cells transduced with A/E9a (n=7; p=0.0013).

4.2.5 Loss of AML/ETO9a leukemic stem cells in Runx site mutants

To investigate if the observed delay of leukemia onset was related to a decreased number of functional leukemic stem cells in AML/ETO9a PU.1-URE-mRunx recipients, we designed an experiment to quantify leukemia initiating cells (LICs) using limiting dilution transplantations (Figure 40).

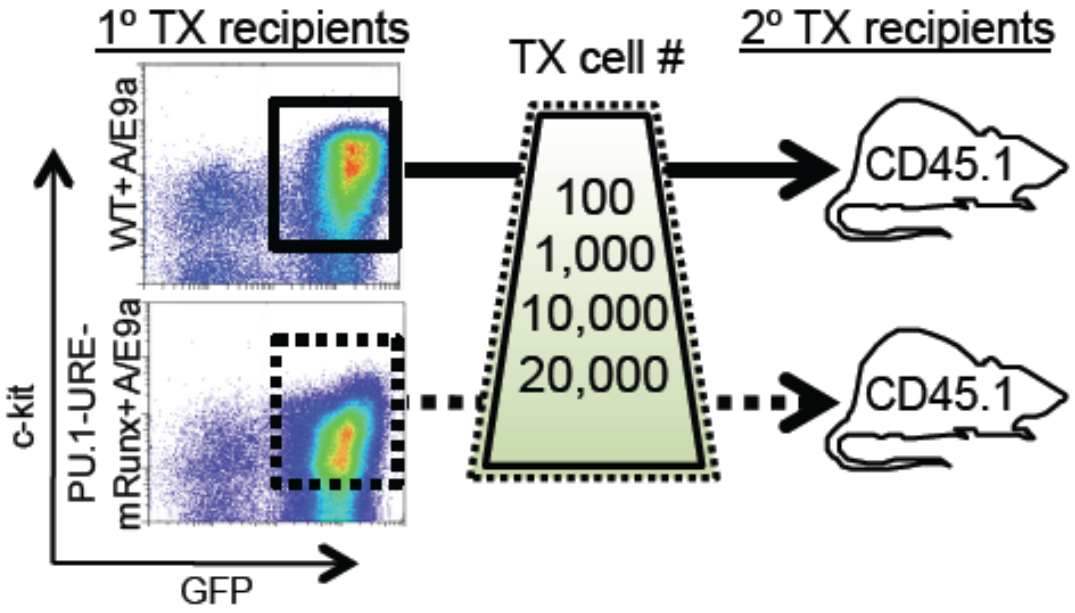

Figure 40. Experimental outline: WT+A/E9a and PU.1-URE-mRunx+A/E9a leukemic cells from moribund primary recipients (s. **Figure** 34, **Figure 37**, **Figure** 39) were isolated and transplanted in limiting dilutions to secondary recipients in which development of leukemia was monitored.

100, 1000, 10,000, or 20,0000 leukemic cells from primary recipients (AML/ETO9a transformed wild type and PU.1-URE-mRunx) were transplanted into secondary recipients (CD45.2+) respectively and development of leukemia was monitored with a follow-up of up to 4 months. LIC frequency of PU.1-URE-mRunx AML/ETO9a leukemias was dramatically decreased (1 in 32,741 compared to wild type AML/ETO9a; *** 1 in 184, $p < 0.0001$) (Figure 41, Table 3).

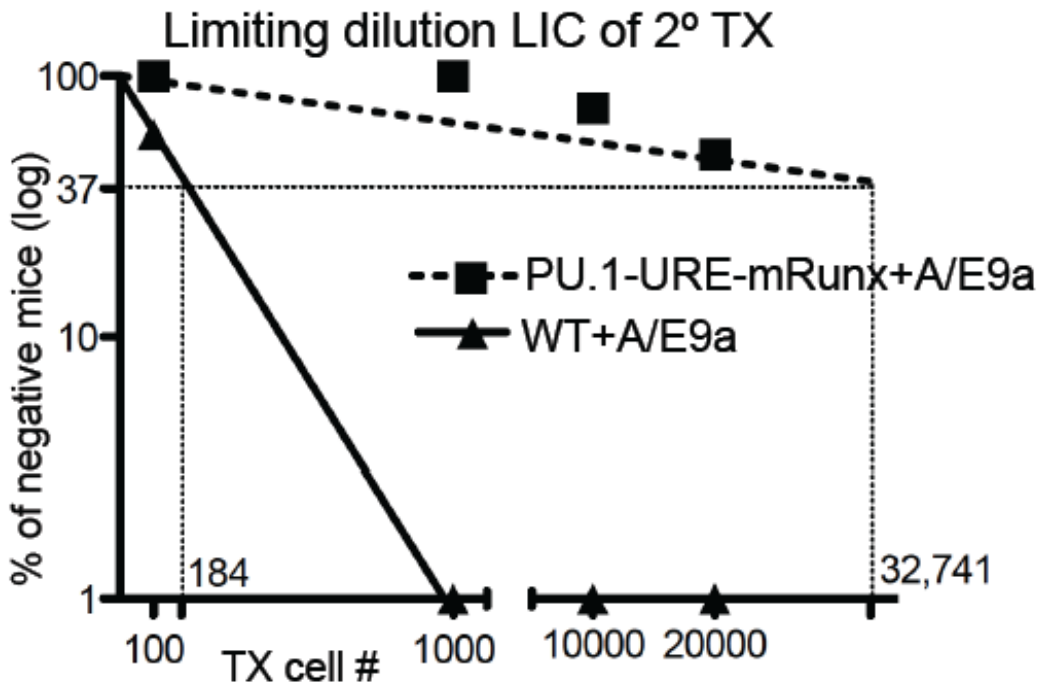

Figure 41. Logarithmic plot showing the percentage of negative recipients as function of the dose of transplanted A/E9a leukemia cells. Leukemia initiating cells (LICs) were calculated as for CRUs.

Table 3. Table showing the frequency of LIUs and the total number of transplantations per cell dose. Leukemia development was monitored by survival and evaluated in spleen and bone marrow. No GFP positive cells were detectable in bone marrow or spleen of surviving mice after 4 months, which were then considered as non-responders.

Quantification of leukemia initiation cells (LICs) (follow up 4 months)

Transplanted cell #	WT + A/E9	PU.1-URE-mRunx + A/E9a
100	2/5	0/5
1,000	5/5	0/5
10,000	5/5	1/4
20,000	5/5	2/4
LIC frequency	1 in 184	1 in 32,741
(95% confidence interval)	(56 - 609)	(10,525 - 101,846)

Leukemia was evident with splenomegaly (Figure 42), and leukemic cell (cKit+ and GFP+) infiltration of spleen (Figure 43) and bone marrow (Figure 44). Thus, as for normal HSCs, the Runx-PU.1 pathway is essential for leukemic stem cell function of AML/ETO9a leukemia.

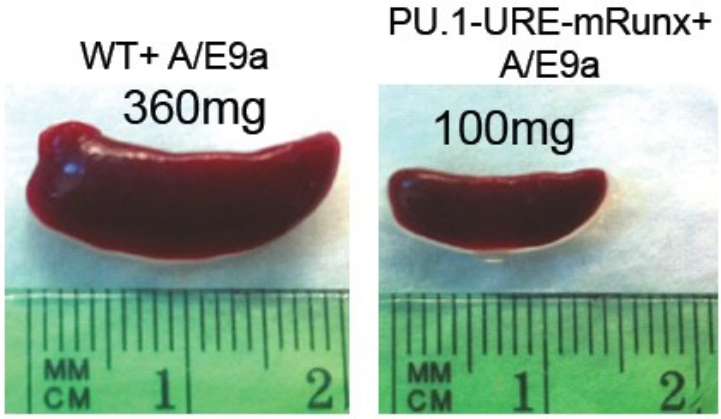

Figure 42. Representative picture of a leukemic (WT+A/E9a) and a non-leukemic (PU.1-URE-mRunx+A/E9a) spleen at 4weeks after transplantation.

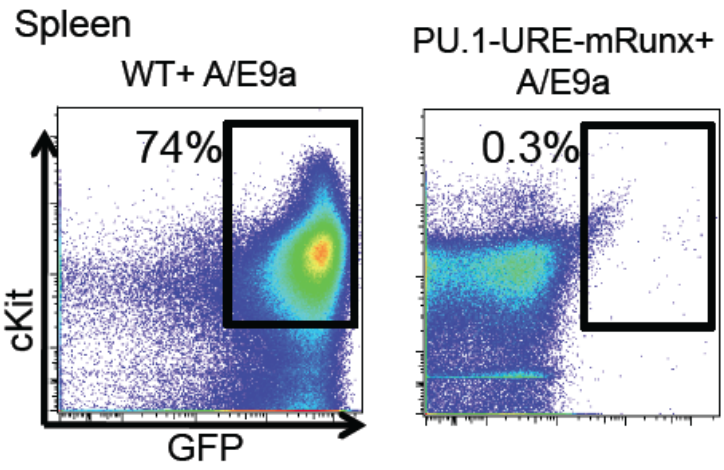

Figure 43. Flow cytometry analysis of spleens shown in **Figure 42**.

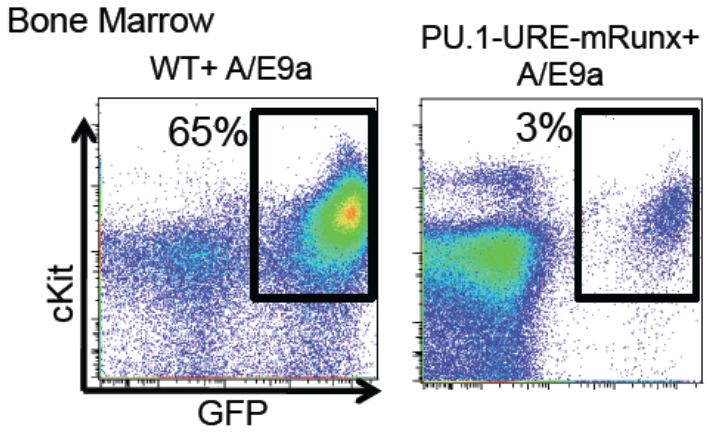

Figure 44. Flow cytometry analysis of bone marrows of mice of which spleens are shown in **Figure 42**.

4.3 Antisense transcription in normal blood development and core binding factor leukemia

During myeloid differentiation PU.1 levels need to increase to avoid a differentiation block, which would lead to leukemia. In contrast PU.1 expression needs to stop completely to develop T-cells (Figure 45). Here we demonstrate that expression of a long noncoding antisense RNA plays a central role in silencing the expression of PU.1. We provide evidence that specific 3-dimensional chromosome architectures facilitate expression of either PU.1 mRNA or PU.1 antisense transcription by locating distal enhancer- or modifier- segments either to the proximal or the antisense promoter. Our data suggest that Runx factors directly influences PU.1 antisense expression. We further show that fusion oncoproteins of CBF leukemias establish a specific higher-order chromatin structure leading to PU.1 antisense transcription and active PU.1 silencing. Thus, silencing transcription factor PU.1 is an active process that requires a specific chromosome formation and transcription of a non-coding antisense transcript

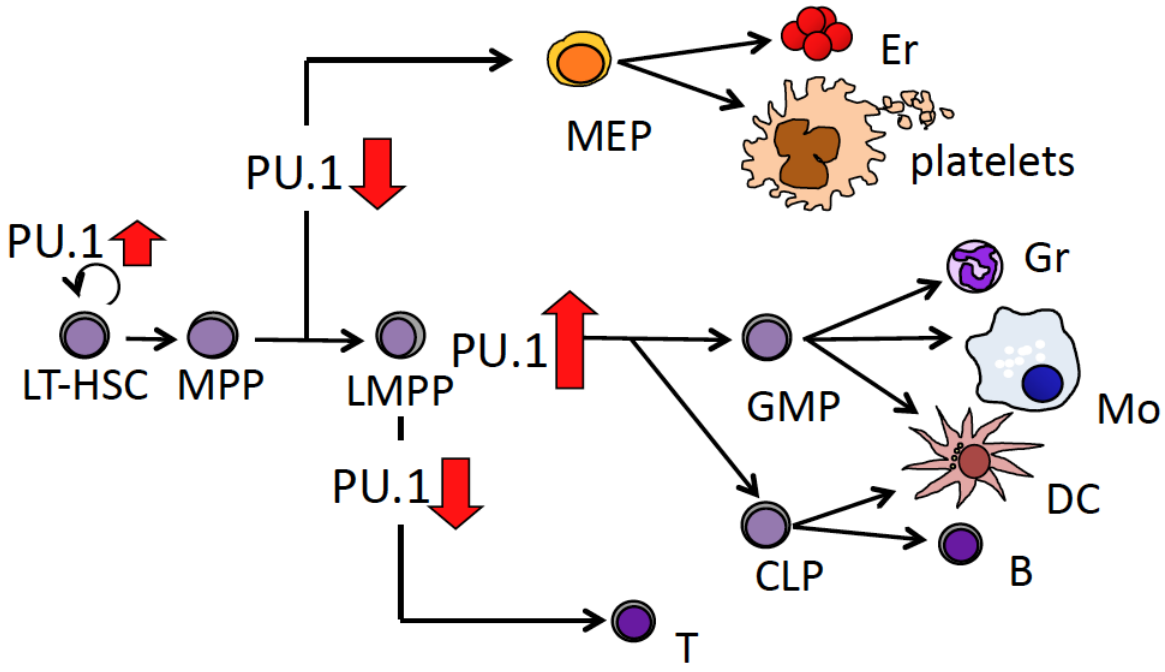

Figure 45. Scheme of PU.1 expression during normal hematopoiesis.

4.3.1 Mapping of noncoding transcripts of the PU.1 locus using tiling arrays

To sufficiently map the PU.1 antisense ncRNAs and to screen for additional potentially relevant ncRNAs, we designed, in collaboration with Roche Nimblegen, Madison, WI, USA, a high-resolution tiling array covering specific regions on human chromosome 11 (47313409 to 47563127) and murine chromosome 2 (90821954 to 91070913) (Figure 46). Both regions contain the PU.1 locus and span ~250kb in total. We designed 50mer probes overlapping 25bps to achieve high resolution coverage of the entire PU.1 locus with its up- and downstream regions. This will enable us to detect and map ncRNA expression within and around the PU.1 locus. **Figure 47** demonstrates proof-of-concept, showing strong expression of transcripts detected over the exons (Exon 1-5 in light blue boxes) of the PU.1 locus. The array is currently being validated and will be ready for use by the time this project starts. Samples to be hybridized to this array will include total RNA samples from various cell types with different spatial organization of the PU.1 locus, like granulocytes and T-cells (Ebralidze, 2008; Hoogenkamp, 2007, Hoogenkamp, 2009), to allow a comparative analysis of the expression of all detectable ncRNA transcripts. These data will help us to understand how PU.1 non-coding transcripts are associated with different chromatin and PU.1 expressions states.

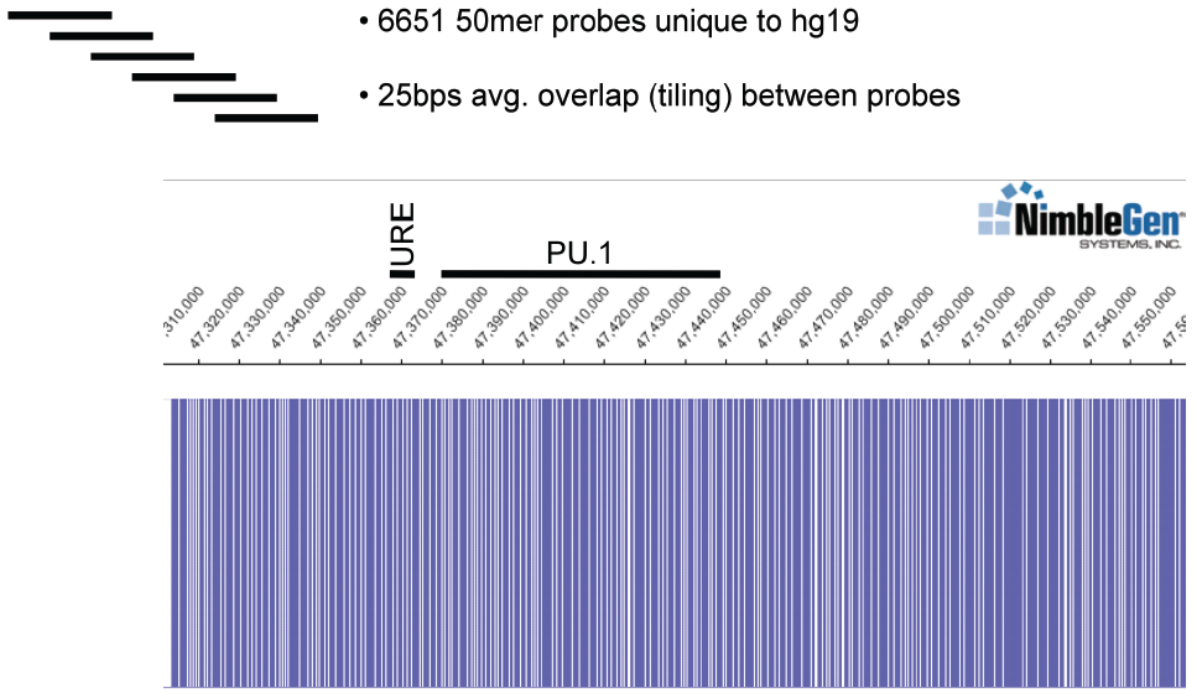

Figure 46. Design of tiling array (Roche Nimblegen).

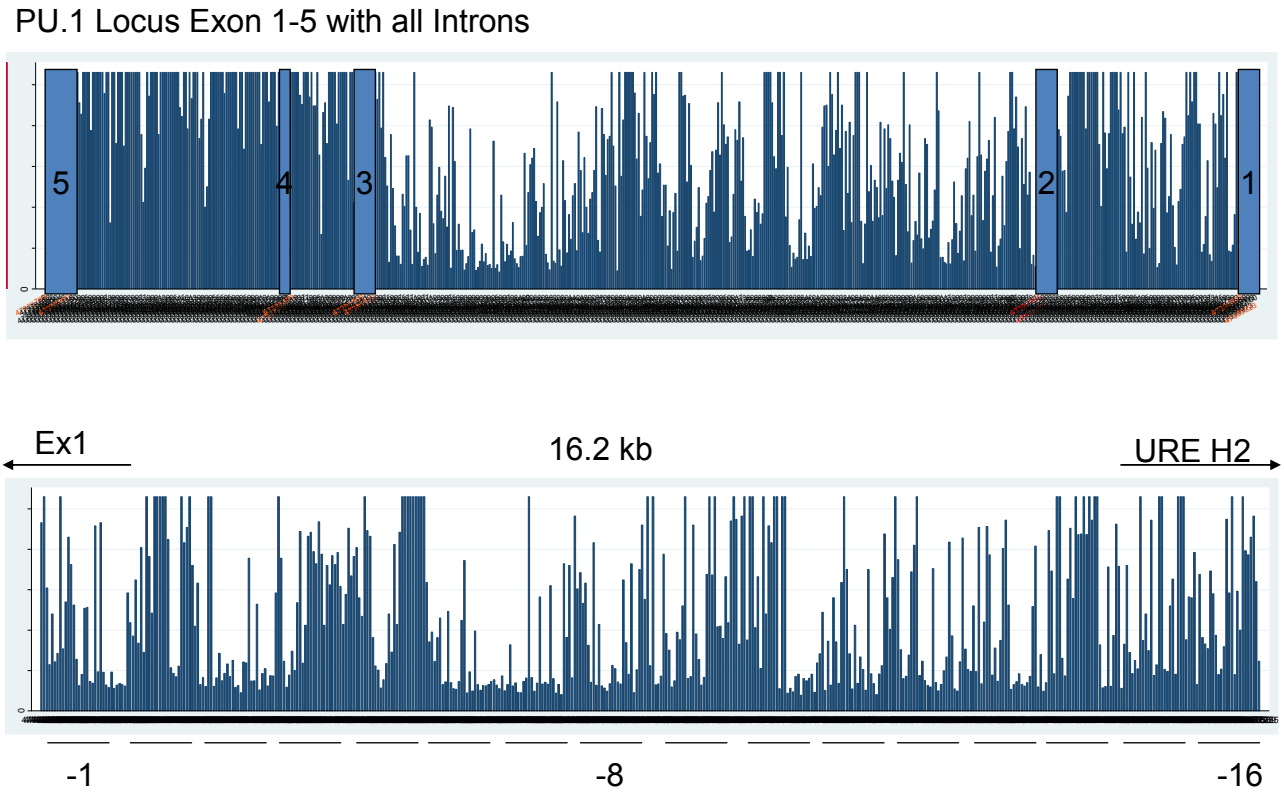

Figure 47. Expression values of hybridized oligonucleotides at indicated location of the PU.1 gene locus. High resolution tiling array analysis of the whole PU.1 gene locus. 1µg of ribosomal RNA depleted total RNA from U937 cells was hybridizid to the array. The PU.1 gene locus with Exons 1-5 (transparant and numbered for Ex1-5) shows the presence of transcripts along the exons and in various intronic regions.

For a better demonstration results of tailing array are illustrated in a scheme of the PU.1 AsPr region (Figure 48).

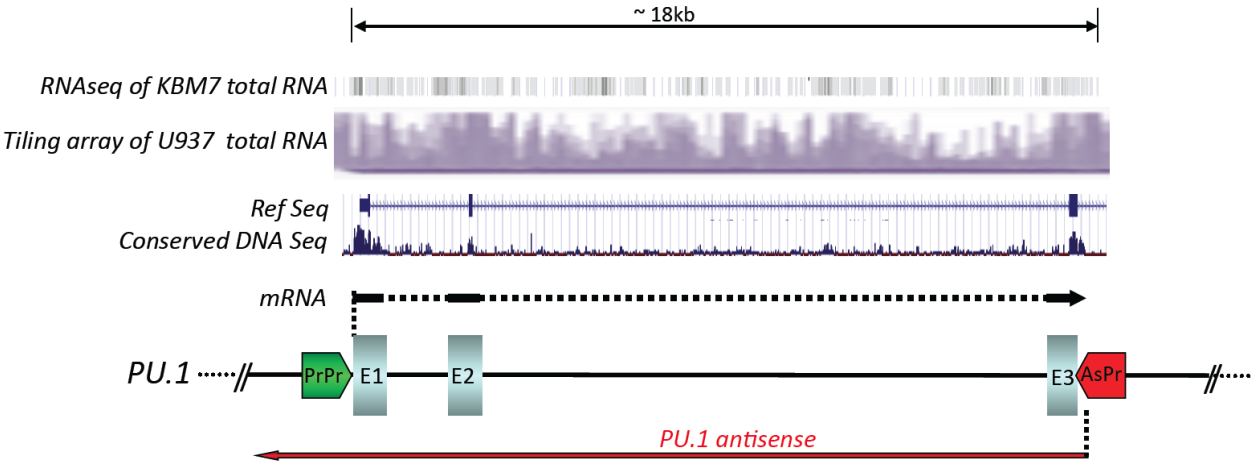

Figure 48. PU.1 mRNA and PU.1 antisense RNA expression. Scheme localizing transcripts at the PU.1 locus (PrPr-proximal promoter, AsPr-antisense promoter, E-exon). Expression is indicated by RNA-sequencing of the haploid cell line KBM7 (Burckstummer et al., 2013) and high resolution tiling array data of the myeloid cell lone U937 (Roche Nimblegen).

4.3.2 PU.1 mRNA and antisense expression during hematopoiesis

We have developed and validated highly-specific TaqMan-assays to quantify expression of PU.1 mRNA and antisense transcripts. Data from primary human bone marrow samples show an inverse expression pattern in mature cells (Figure 49). Lymphoid cells from peripheral blood (here not distinguishing B- and T-cells) demonstrate very high antisense but low or no PU.1 mRNA expression. In contrast, in monocytes PU.1 mRNA levels are high and PU.1 antisense levels are low.

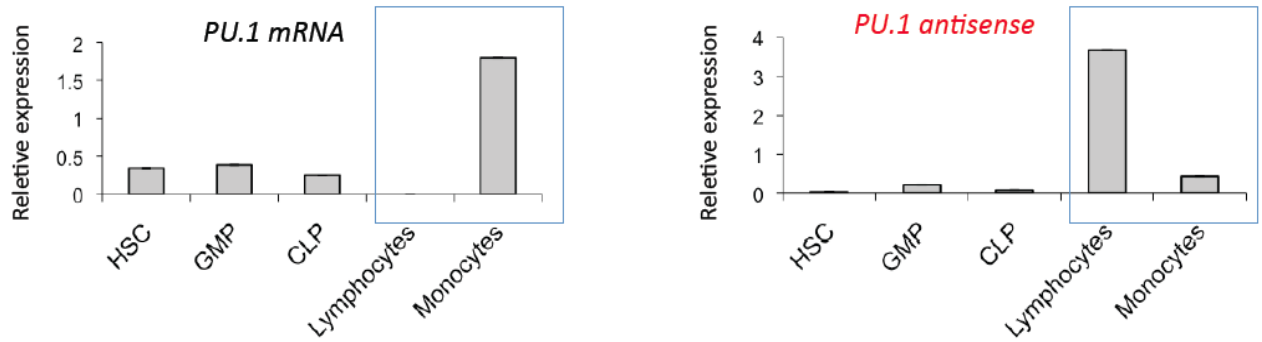

Figure 49. PU.1 mRNA and PU.1 antisense expression in human hematopoiesis. Hematopoietic stem cells, HSC: CD34+, CD38-, lin-; Granulocyte-macrophage progenitor, GMP: CD34+, CD38+, CD123+, CD45RA+, Common lymphoid progenitor, CLP: CD34+, CD38+, CD10+, CD45RA-. Lymphocytes and Monocytes were distinguished by size and granularity in the forward and sideward

scatter of flow cytometry. TaqManPCR was performed for PU.1 mRNA, PU.1 antisense RNA and 18S as house keeping gene; results are shown relative to mean.

4.3.3 PU.1 mRNA and antisense expression in leukemic subsets

Analysis of a few bone marrow samples obtained from patients with AML M0, and the two types of core-binging factor (CBF)-AML, t(8;21) and inv(16), demonstrated a relative increase of PU.1 antisense RNA levels in the CBF-AML samples (Figure 4), suggesting a putative functional role of antisense deregulation in leukemogenesis. This increase of PU.1 antisense expression can also be found in a murine model for inv(16) leukemia that has been published previously and is available to our lab through a collaboration with Lucio Castilla (not shown) (Kuo et al., 2006).

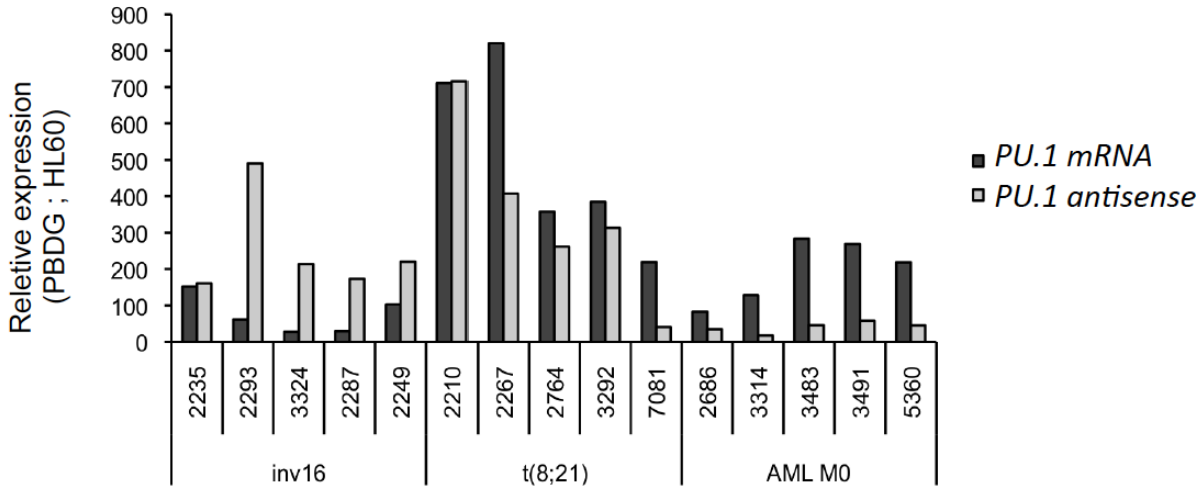

Figure 50. Human PU.1 mRNA and PU,1 antisense expression in leukemia samples. Patients with core-binging factor leukemias (inv16, t(8;21) show a relatively high PU.1 antisense expression compared to their respective PU.1 mRNA levels, suggesting a functional role of PU.1 antisense.

4.3.4 Runx1 and Runx3 bind and activate PU.1 AsPr

We identified a Runx site in the PU.1 antisense promoter region in intron3. We tested binding of Runx1 and Runx3 to this site by Electro-mobility shift assays (EMSA) gel and found that

both factors can physically bind to H3 and that specific antibodies for Runx1 and Runx3 super-shift the labeled probe (Figure 51).

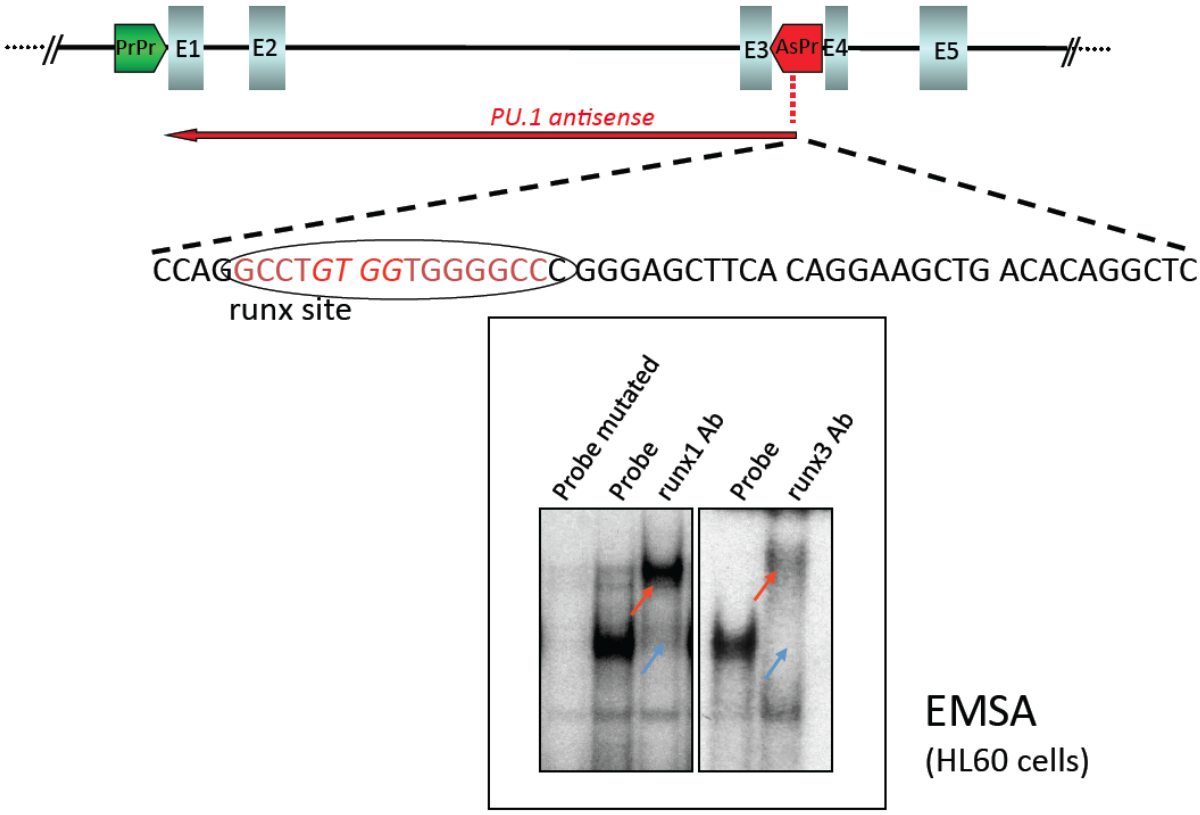

Figure 51. Electro mobility shift assay (EMSA) with supershift demonstrating binding of Runx1 and Runx3 at the antisense promoter region.

We also asked if Runx1 or Runx 3 can transactivate the antisense promoter in a similar fashion Runx1 does for the URE (Hoogenkamp, 2007, 2009). Therefore, we cloned a fragment of H3 i(ncluding the Runx site) in antisense direction into the pXP2-firefly-luciferase vector. Indeed, both Runx1 and Runx3, but not, lead to a strong dose-dependent increase in H3-ncRNA promoter activity, whereas Runx2, seems a less potent transactivator even when high concentrations of up to 200ng DNA (excess) were added to the pxp2-H3 promoter construct (Figure 52). Of note, Runx mediated transactivation capacity strictly relied on CBfb that was also added to the reaction.

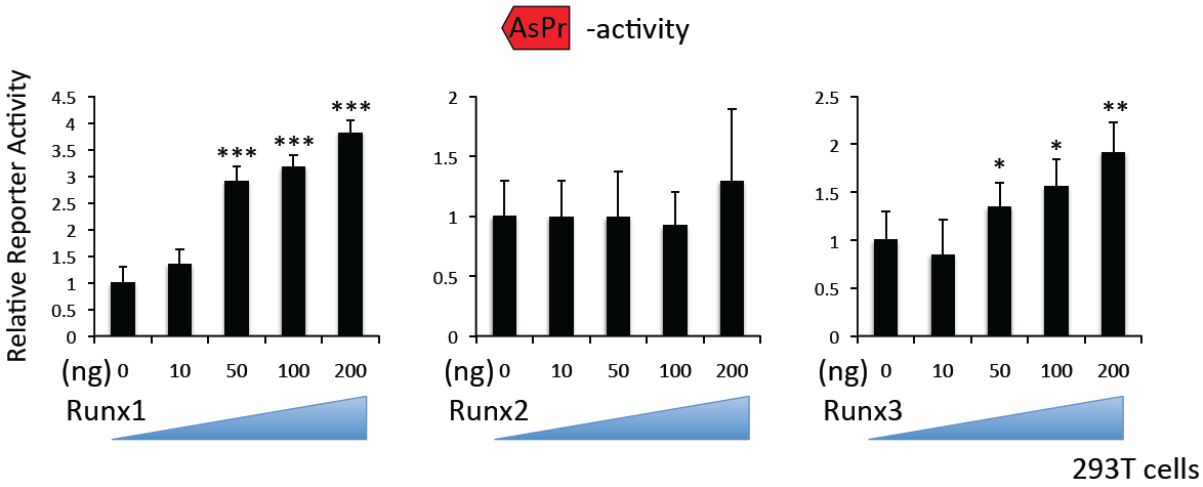

Figure 52. Reporter assays in pXP2 luciferase vectors of AsPr promoters cotransfected with increasing amounts of indicated Runx factors and 50ng of CBFb expression plasmids. Shown are mean values ± standard deviation; *P*-values: * <0.05, **<0.01, ***<0.001 compared to reporter levels with 0ng Runx set as 1; n=4.

4.3.5 *CBF-oncofusion proteins* bind and activate PU.1 AsPr

Public available ChIP-sequencing data of the AML1-ETO cell line Kasumi-1 (Ptasinska et al., 2012) show significant AML1-ETO binding at the region of the antisense promoter that decreased after siRNA mediated knockdown of AML1-ETO (Figure 53).

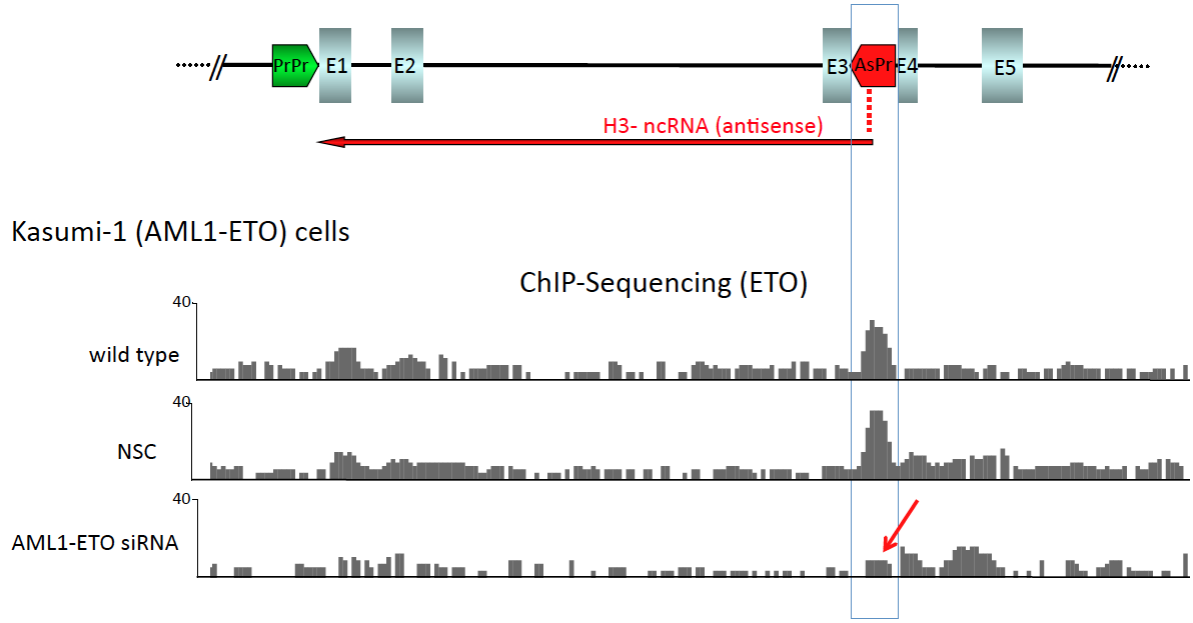

Figure 53. ChIP-sequencing data of AML1-ETO binding in Kasumi-1 cells. Note that Kasumi-1 cells do not express endogenous ETO, therefore detection of ETO stands for AML1-ETO, siRNA mediated

knockdown of AML1-ETO significantly decreases the (AML1)-ETO binding peak. Data were obtained from (Ptasinska et al., 2012).

We next asked if the fusion oncoproteins of t(8;21) and inv(16) leukemias might transactivate the AsPr similarly such as Runx1 and Runx3. Transient reporter assays in HEK293T cells indicated a dose dependent activation potential of the antisense reporter by the CBF fusion proteins AML1-ETO and CBFβ-MYH11 (inv16) (**Figure 54**).

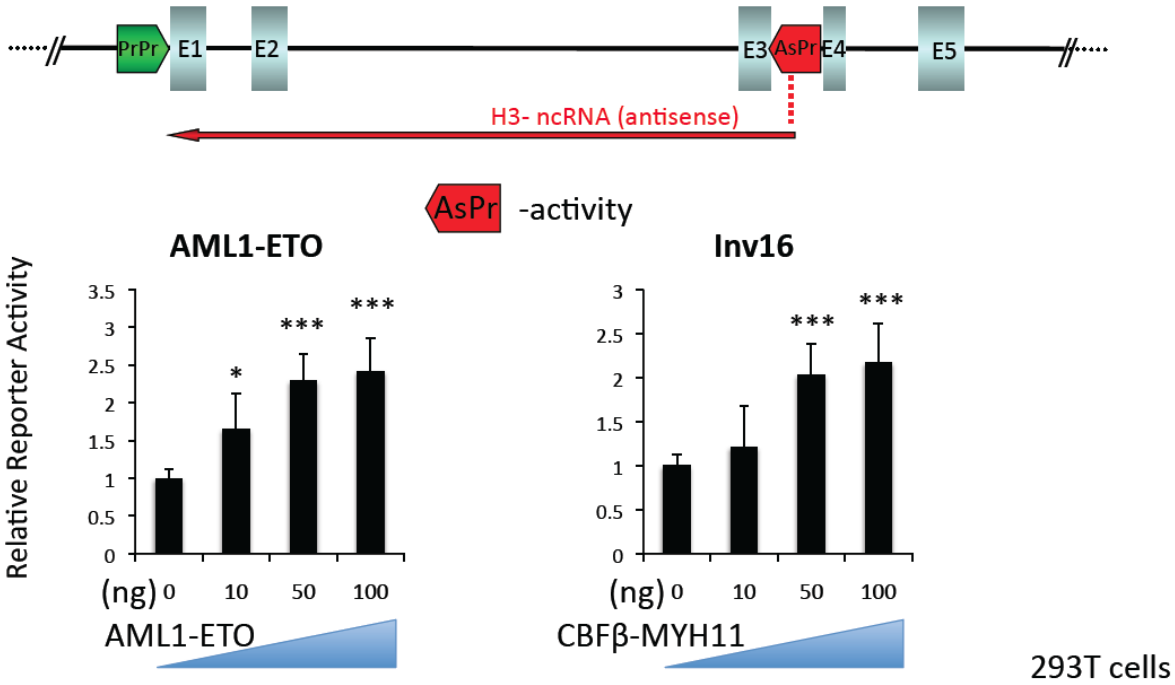

Figure 54. Similar to Runx1 and Runx3, reporter assays indicate a dose dependent antisense promoter activation by CBF fusion proteins (right) AML1-ETO and CBFβ-MYH11 in transient transfected HEK293T cells.

4.3.6 Block of *CBF-oncofusion proteins* reduces PU.1 As transcription

Dr. Bonifer's group provided us with material of the AML1-ETO siRNA knockdown experiment (Ptasinska et al., 2012). We found that after AML1-ETO knockdown PU.1 antisense was indeed decreased and PU.1 mRNA and protein levels were increased supporting our hypothesis of CBF induced PU.1 antisense expression (Figure 55, Figure 56).

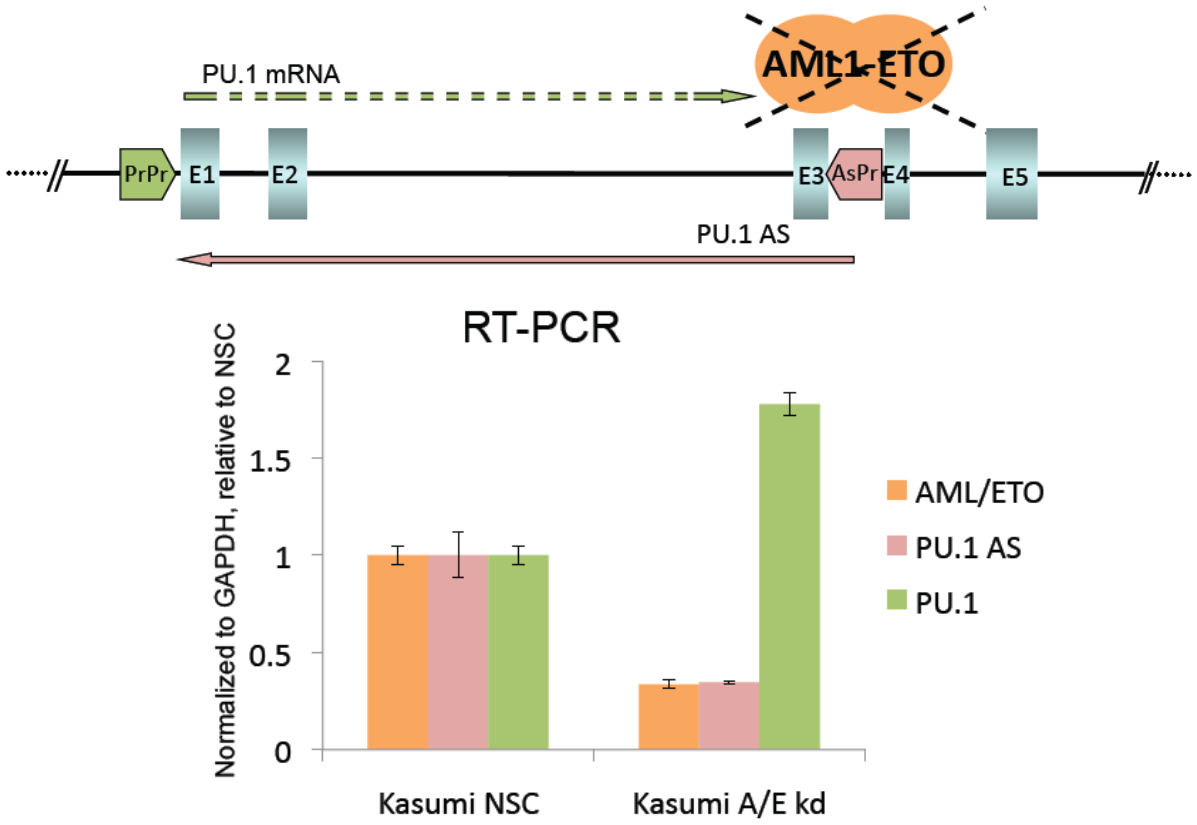

Figure 55. In AML1-ETO leukemic Kasumi-1 cells AML1-ETO knockdown decreases PU.1 antisense and increase PU.1 mRNA expression.

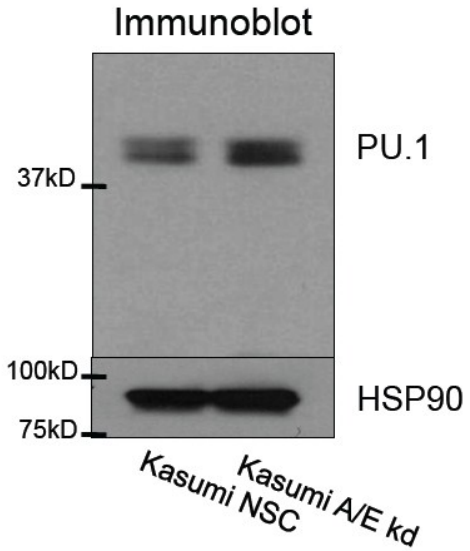

Figure 56. In AML1-ETO leukemic Kasumi-1 cells AML1-ETO knockdown increase PU.1 protein expression.

Another collaborator, Lucio Castilla, developed a small molecule inhibitor (AI-10-49) of CBFβ-MYH11 (inv16 fusion protein) (Illendula, Pulikkan et al. manuscript currently in revision in *Nature*). Treatment of ME-1 cells, a human inv16 leukemia cell line, decreased PU.1 antisense expression (Figure 57).

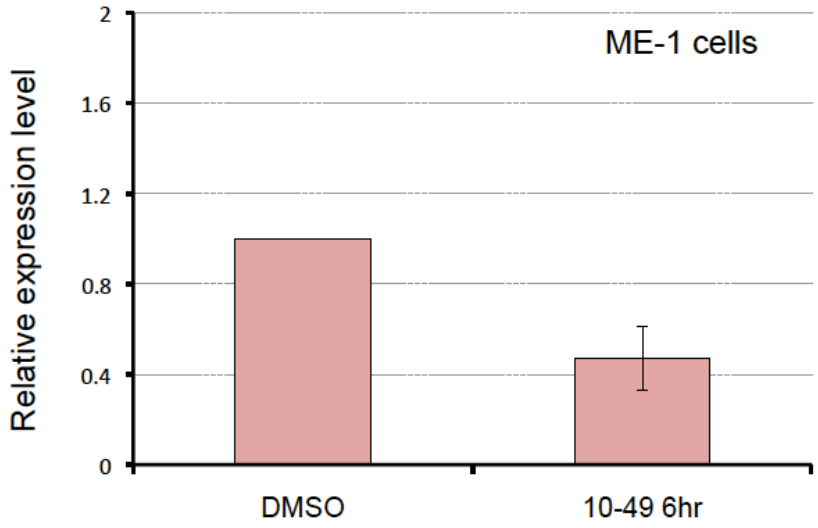

Figure 57. Treatment of ME-1 cells (inv16 leukemia cell line) with the small molecule inhibitor AL10-49 (targeting CBFb-MYH11) decreases PU.1 antisense levels.

4.3.7 Competitive promoter model

PU.1 expression relies on a proper function of its upstream regulatory element (URE) (Rosenbauer et al., 2004, Hoogenkamp et al., 2007, Huang et al., 2008, Staber et al., 2013), which contains three runx sites in its homology region 2 (H2) (Huang et al., 2008). Total bone marrow cells of mice in which the URE had been genetically deleted (Rosenbauer et al., 2004), demonstrated an almost identical reduction of PU.1 coding and non-coding antisense transcripts of ~ 80% indicating that the biogenesis of PU.1 mRNA as well as PU.1 antisense RNA rely on the URE (Ebralidze et al., 2008). Interaction of the URE with the proximal promoter is associated with sufficient PU.1 expression as revealed by quantitative chromosome conformation capture (3C) analysis (Staber et al., 2013). Importantly, our data show that in the non-PU.1-expressing T-cell line Jurkat the URE interacts with the PU.1

antisense promoter in intron 3 whereas in myeloid cells the URE interacts with the proximal promoter (Figure 58).

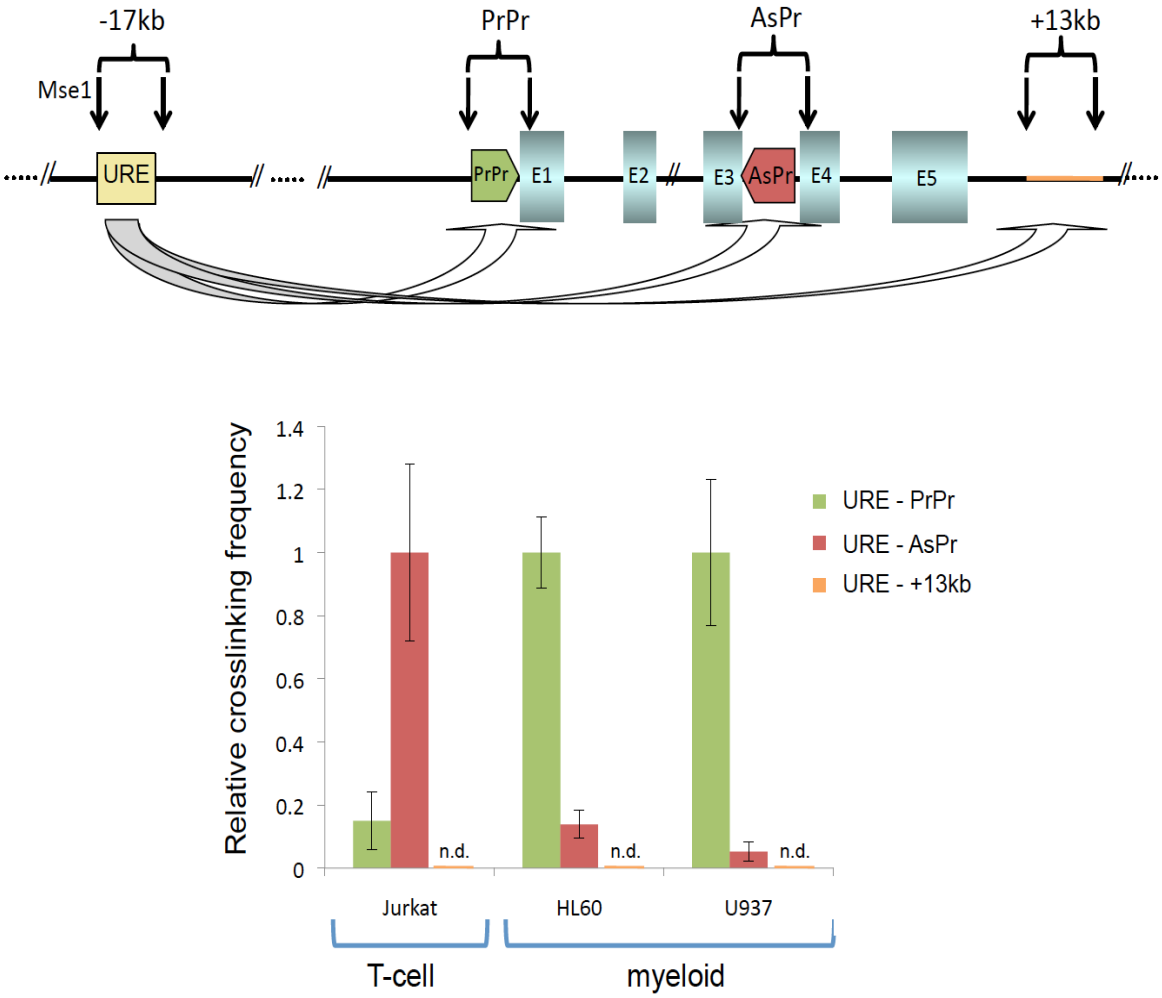

Figure 58. Chromosome conformation capturing of indicated cell lines demonstrating a strong interaction between the URE and the AsPr in Jurkat cells and strong URE PrPr interaction in the myeloid cell lines HL60 and U937. . Graphs represent the results of four independent quantitative TaqManPCR experiments (avg. + sd; *, $p < 0.05$). Crosslinking efficiencies are shown as relative values to either URE-AsPr (Jurkat) of URE-PrPr interactions (HL60, U937).

Of note, Jurkat cells have high antisense levels and strong antisense promoter activity (Ebralidze et al., 2008) and mice lacking the URE fail to suppress PU.1 levels during T-cell development (Rosenbauer et al., 2006) pointing to a crucial function of URE mediated antisense transcription involved in PU.1 silencing in T-cells. Based on these findings and our preliminary data we here propose a "competitive promoter model", in which the proximal promoter and the antisense promoter compete for interaction with the URE (Figure 59).

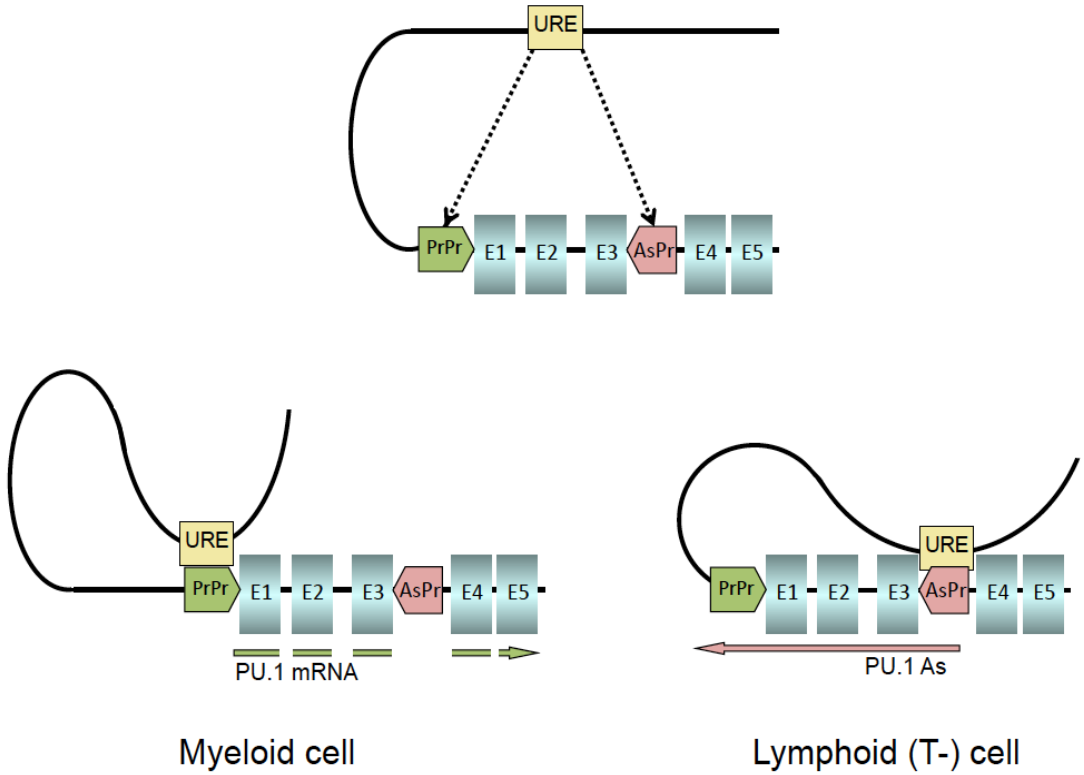

Figure 59. Competitive promoter model. Quantitiative 3C demonstrating strength of interactions of the URE with either the proximal or the antisense promoter.

Interestingly, preliminary 3C analysis of chromatin interactions of Kasumi-1 cells after AML1-ETO knockdown demonstrated that the interaction of the URE with the antisense promoter changed to an URE-proximal promoter interaction after AML1-ETO depletion (Figure 60).

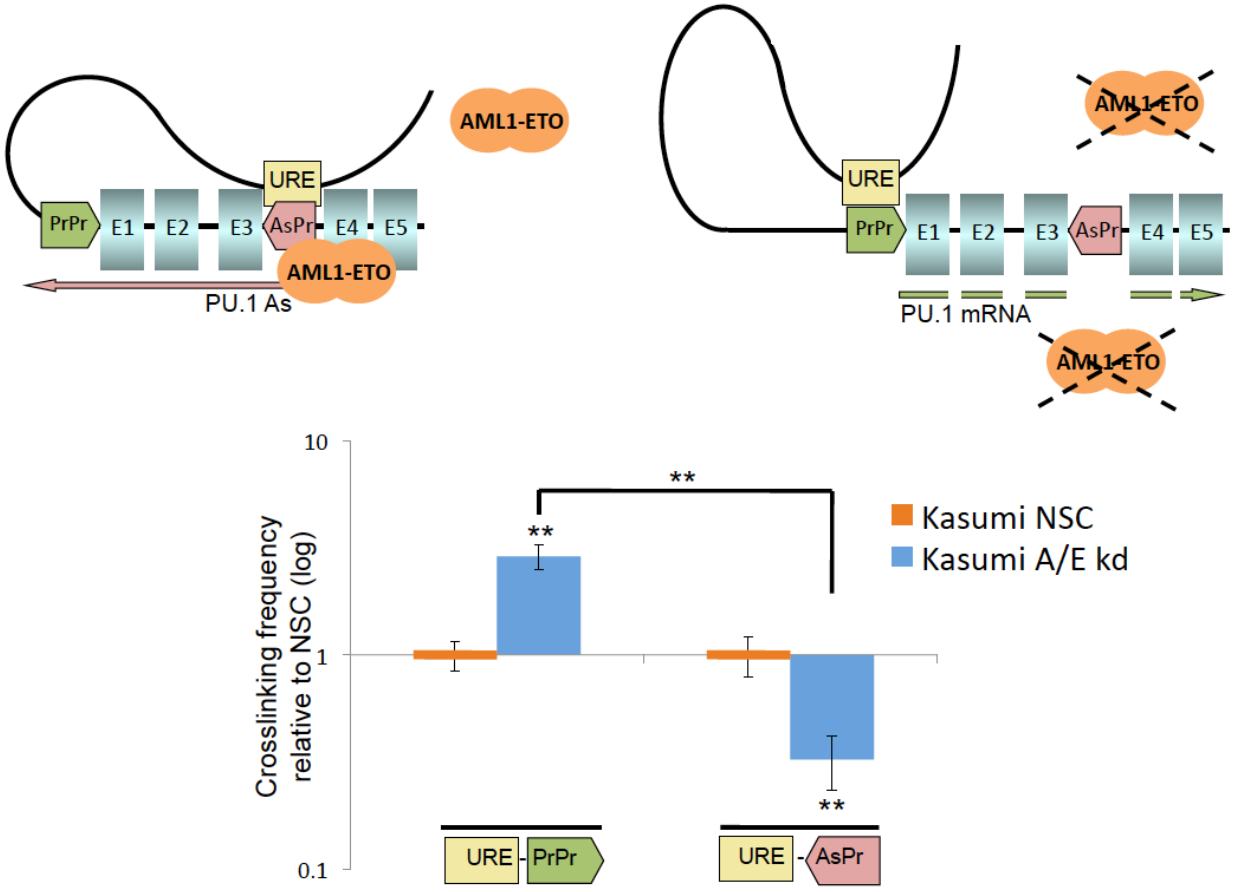

Figure 60. Changes of chromatin structure in Kasumi1 cells upon AML1-ETO knockdown.

These findings support the theory that CBF fusion proteins activate a PU.1 silencing process that is present during normal T-cell development and involves a specific chromatin configuration and transcription of the PU.1 noncoding antisense RNA.

4.3.8 Functional effect of PU.1 AS silencing *in vitro*

Given the high expression levels of PU.1 antisense transcripts in patients with (Figure 50) we asked for their functional contribution to the leukemic phenotype. We therefore utilized the lentiviral pGhU6 vector that allows for selection of successfully infected cells by flow cytometry through its eGFP cassette (Staber et al., 2013). Overexpression of PU.1 induces monocytic/macrophage differentiation of Kasumi-1 (Vangala et al., 2003). We infected Kasumi-1 cells with shRNAs targeting PU.1 antisense transcripts (shPU.1 AS) and found a

significant, 60% knockdown of PU.1 antisense transcripts and an approximately 4 fold increase of PU.1 mRNA compared to non-silencing control (shNSC) (Figure 61).

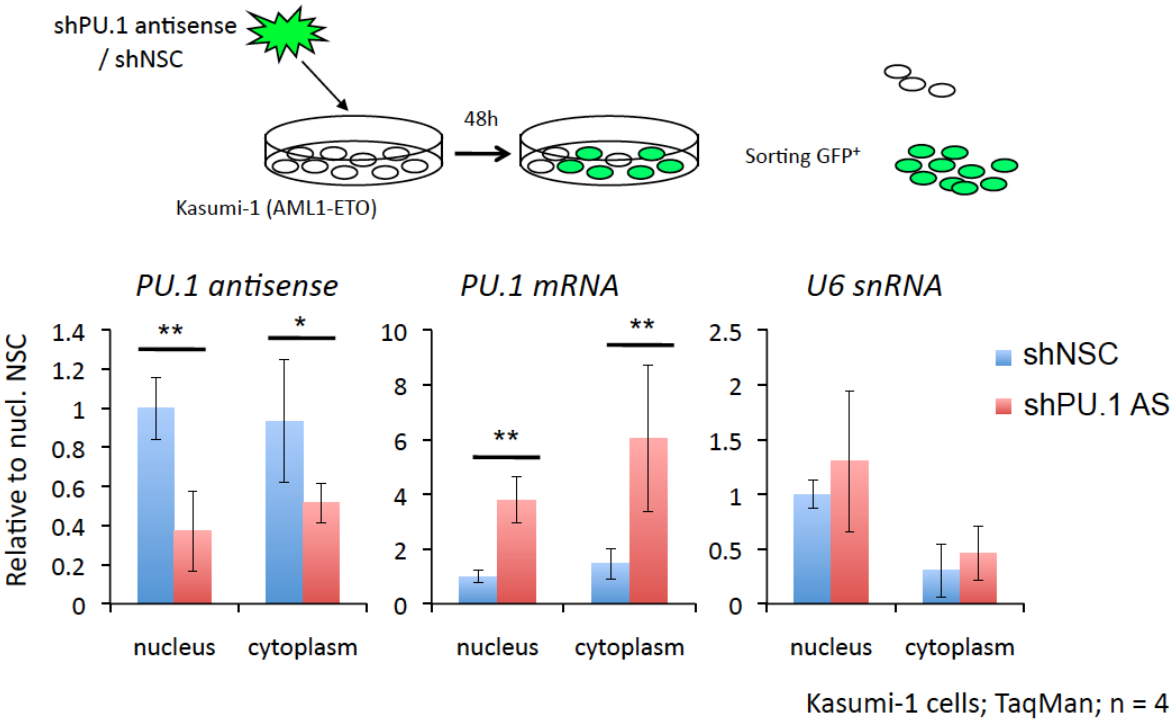

Figure 61. PU.1 mRNA and PU.1 As transcripts upon shRNA mediated knockdown of PU.1 antisense transcripts. (Realtime PCR; average values [avg.] + standard deviation [s.d.] relative ti nuclear NSC; n=4; *P<0.05, **P<0.01)

Cultured Kasumi-1 cells infected with shPU.1 AS differentiated into monocytes (detected morphologically and through induced cell surfaces expression of CD15 and CD11b) (Figure 62).

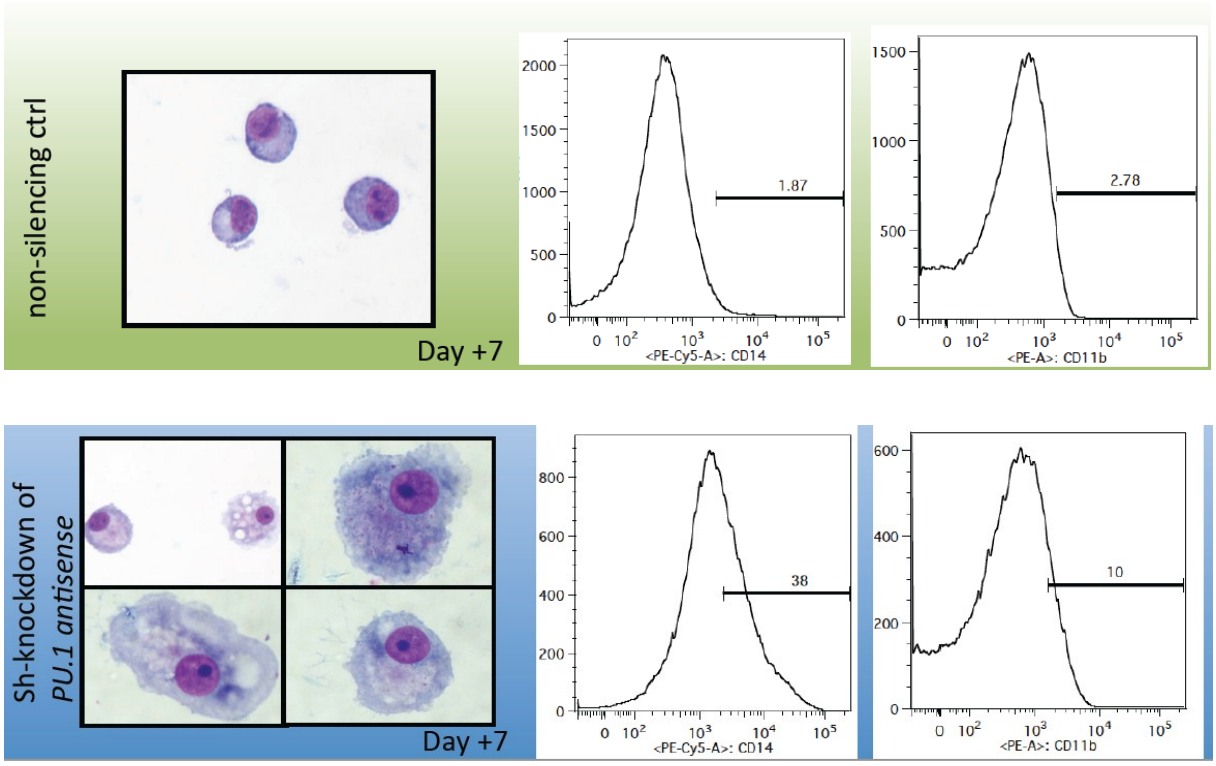

Figure 62. ShRNA mediated knockdown of PU.1 antisense transcripts induced monocyte differentiation of Kasumi-1 cells in vitro (as evidenced morphologically and via increased cell surface expression of myeloid markers CD11b and CD14).

Cell cycle analysis using Pyronin Y / Hoechst staining demonstrated that PU.1 As knockdown decreased cell cycle activity (Figure 63).

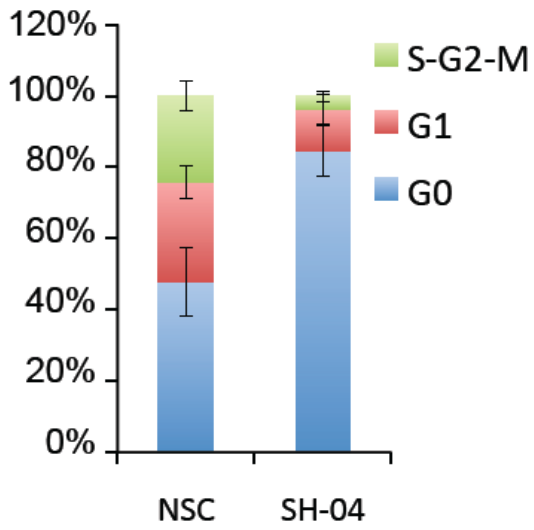

Figure 63. Increased fraction of Kasumi-1 cells in silent G0 cell cycle phase after knockdown of PU.1 As RNA (SH-04) compared to non silencing control (NSC).

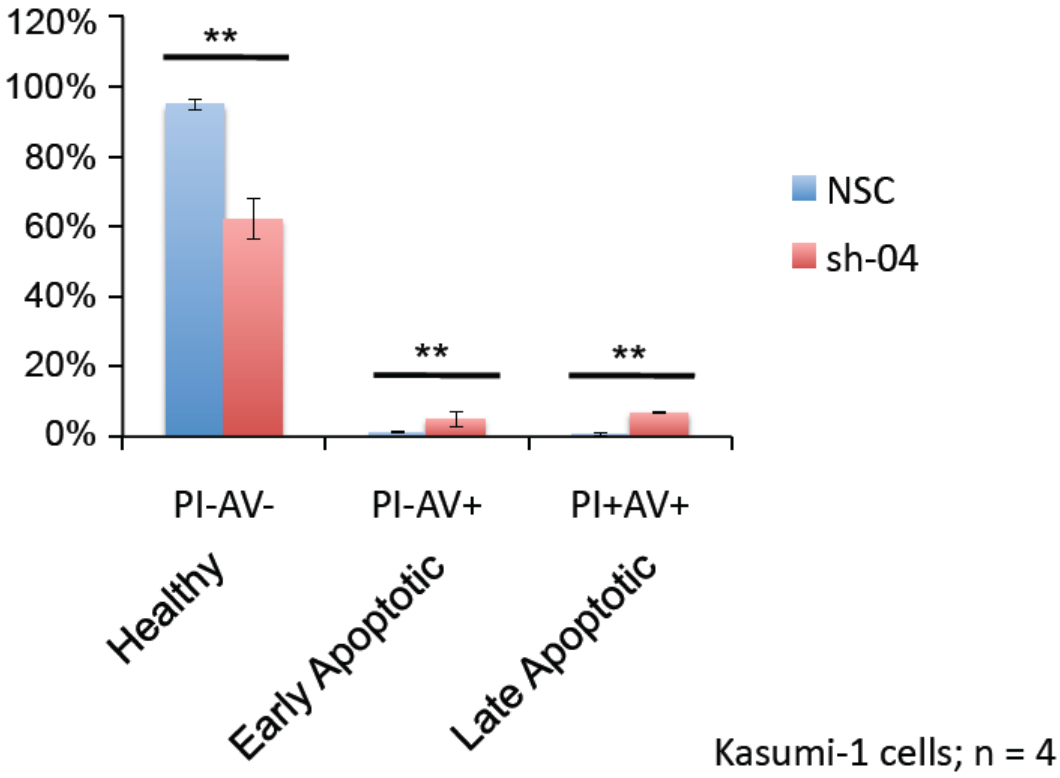

Figure 64. ShRNA mediated knockdown of PU.1 antisense transcripts (SH-04) induced apoptosis (indicated by Propidium iodide (PI) / Annexin V) in leukemic Kasumi-1 cells compared to non-sielencing control (NSC).

To analyze the effect of PU.1 As silencing on T-cell differentiation, we isolated murine progenitor cells (LSK) and transfected them with lentiviral shRNAs either NSC or anti-PU.1 As (Sh-4). We then cultured infected cells in a co-culture system with op9-delta1 stromal cells under addition of flt3 ligand and IL-7. After 8 days we measured T-cell progenitor differentiation using surface markers CD25 and Thy1. Interestingly, knockdown of PU.1 As inhibited T-cell progenitors development (Figure 65).

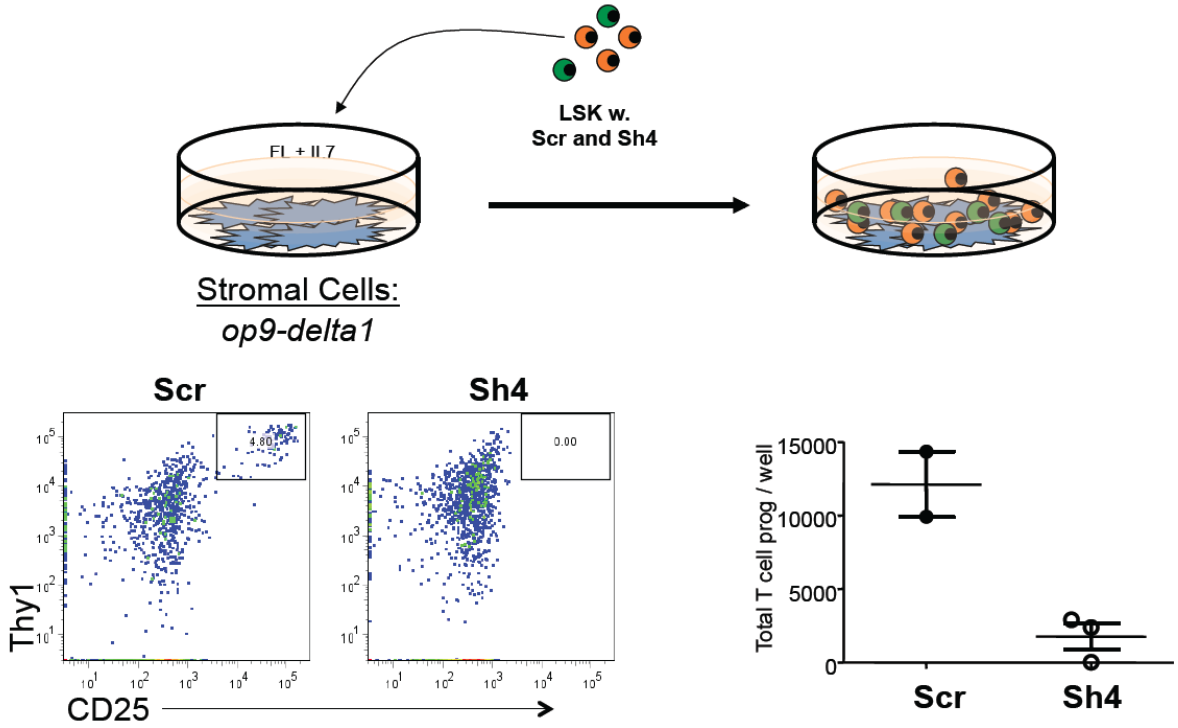

Figure 65. Co-culture system of NSC or Sh-4 transfected LSK cells with op9-delta1 stromal cells under addition of flt3 ligand and IL-7. After 8 days T-cell progenitor differentiation was analyzed by flow cytrometry using CD25 and Thy1 antibodies.

4.3.9 Targeting PU.1 AS by insertion of a transcriptional terminator *in vivo*

These data prompted us to initiate development of the following *in vivo* model system to further analyze the biological function of PU.1 As RNA. To analyze their role especially in the nucleus, we chose to insert transcriptional terminators into a human PU.1 BAC (Clone name: RP11-750A9) in antisense direction downstream of the antisense transcriptional start site in intron 3 (Intron 3 TerF BAC). Transcriptional terminator plasmids (TerF-FRT-Kan-FRT) were constructed through the insertion of the bacterial selection marker Kanamycin (Kan) flanked by FRT into the 2.2kb beta-globin transcription terminator (TerF) plasmid, kindly provided by Dr. Nick Proudfoot. We inserted TerF-FRT-Kan-FRT 3' to exon 3 within intron 3. After excision of Kan the construct was purified and linearized with P1-SceI and has been delivered to the Beth Israel Deaconess Medical Center (BIDMC) Transgenic Animal Core for direct pronuclear microinjection (Figure 66).Two founder lines of transgenic mice carrying the unmodified human PU.1 BAC (RP11-750A9) were kindly provided by Dr. Frank Rosenbauer. Since these mice appear normal and do not exhibit any hematologic

discrepancies they serve as serve as ideal controls. Interestingly, when crossed to PU.1 knockout mice expression of this human PU.1 transgene fully rescues the PU.1 knockout phenotype (Leddin et al., 2011).

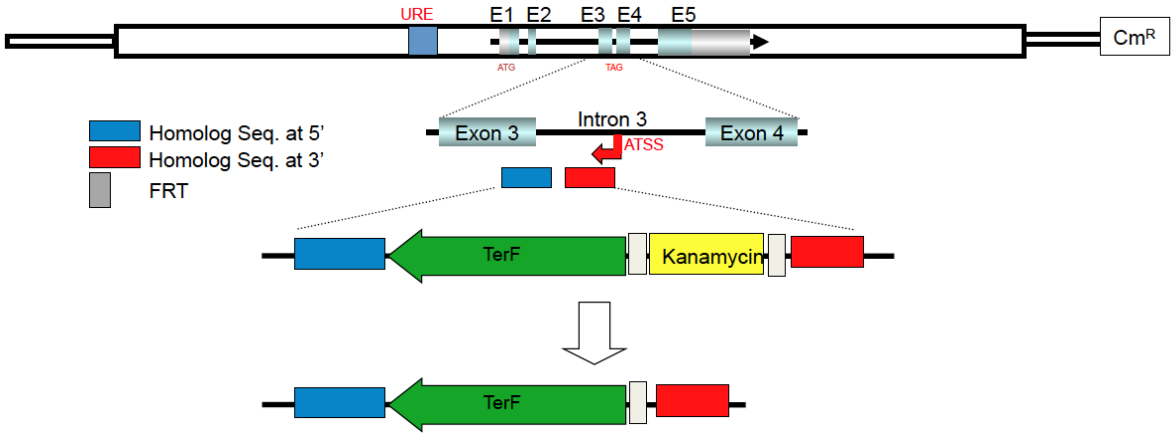

Figure 66. Schematic diagram of the strategy to insert the transcriptional terminator in intron 3.

For functional analyses of constructs we stably transfected 416B cells (murine myeloid progenitor cell line) with the modified human PU.1 BAC construct (Intron 3 TerF BAC) and as a control an unmodified human PU.1 BAC (RP11-750A9; Intact BAC) using co-transfection with PGK-puro. We obtained 9 positive founder lines per experimental group from which we picked 3 that showed comparable copy numbers of the inserted transgene as measured by TaqMan Real-Time PCR Assay (not shown). Interference of the insertion of the transcriptional terminator with splicing was thought to be ruled out using a human PU.1 specific RT-PCR spanning exon3 and exon4. Our studies on these stably transfected cell lines also revealed that insertion of a transcriptional terminator in intron 3 resulted in undetectable antisense expression levels (Figure 67).

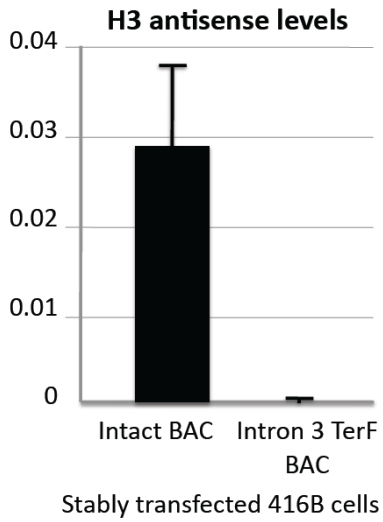

Figure 67. Abrogation of intron3 antisense transcription. 416B cells were transfected with either intact human PU.1 BAC or PU.1 BAC that was modified by insertion of a transcriptional terminator in antisense direction in intron 3. Bars show mean expression values (n = 3) of PU.1 antisense (intron3) expression normalized to PU.1 mRNA expression levels as measured by Taq-Man Real Time PCR. Error bars indicate s.e.m.

However, a detailed analysis on total bone marrow of the obtained transgenic animals demonstrated a profound interference of the transcriptional terminator with sense transcription and RNA splicing *in vivo* as indicated by Northern blotting (Figure 68).

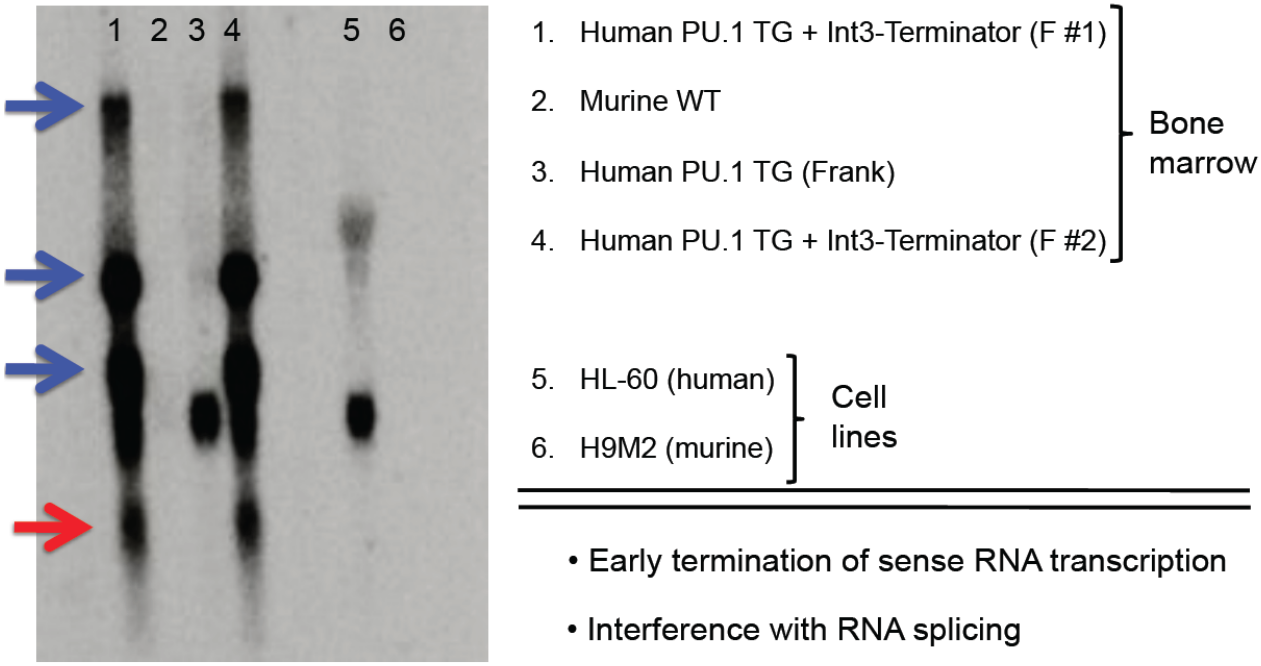

Figure 68. Northern blot using total bone marrow of transgenic mice with indicated genetic background indicated interference of the transcriptional terminator with sense transcription and RNA splicing.

We therefore concluded not to use the transcriptional terminator model for our further studies on the functional role of PU.1 As transcripts.

4.3.10 Functional effect of PU.1 AS silencing *in vivo*

Since we achieved a profound PU.1 As knockdown in Kasumi-1 cells using lentiviral shRNAs and since the transcriptional terminator mouse model did not work, we went on to study the effect of PU.1 As silencing in vivo using a xenograft model. We transplanted positive infected Kasumi-1 cells (eGFP+) into immune-compromised NOD-scid IL2Rgnull (NSCID) mice and assayed leukemia development and survival. PU.1 antisense knockdown reduced leukemic outgrow and prolonged survival (Figure 69).

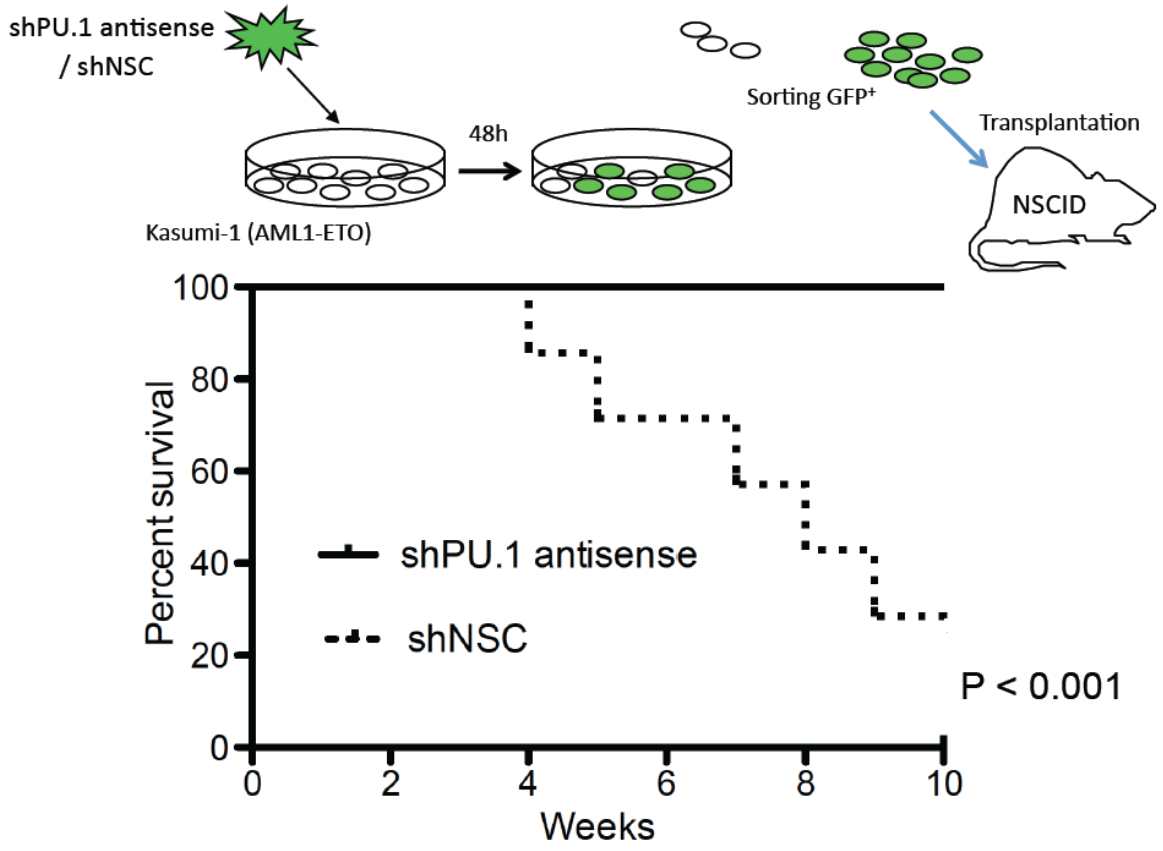

Figure 69. ShRNA mediated knockdown of PU.1 antisense transcripts reduces leukemic outgrow. $2x10^5$ eGFP+ cells were intravenously injected in NOD-scid IL2Rgnull (NSCID) mice. Recipients were monitored for leukemia development and survival (shown as Kaplan Meyer plot).

Leukemic populations were manifest as eGFP+ population in flowcytometry (not shown), splenomegaly, and white bone coloring (Figure 70).

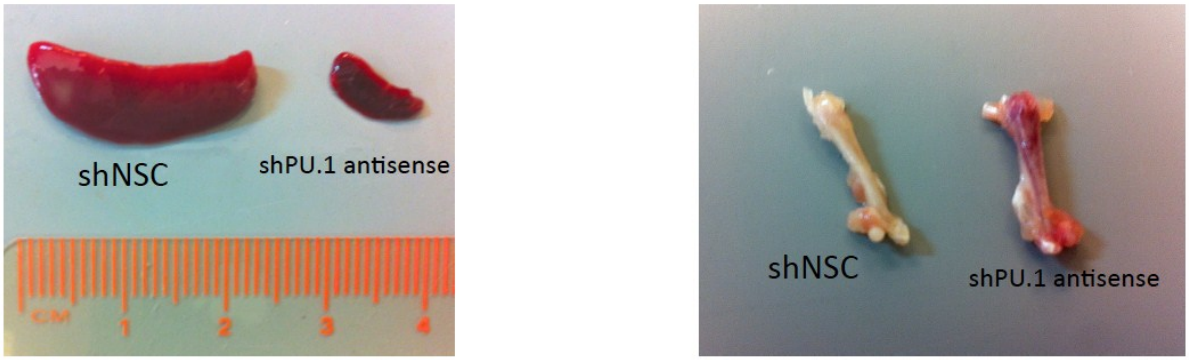

Figure 70. Moribund mice and controls were analyzed for signs of leukemia (eGFP+ population) splenomegly, color changes of bones

4.3.11 PU.1 AS transcripts induce PU.1 PrPr methylation

We next aimed to investigate if PU.1 AS transcripts might be involved in silencing PU.1 expression through methylation of CpG islands at its proximal promoter (PrPr). We utilized Combined Bisulfite Restriction Analysis (COBRA) in which "C" (Cytisin) is converted to "U" (uracil) by treatment with bisulfite. Consecutive PCR replaces "U" with "T" (tymidine). CpG methylation avoids "C" to "U/T" conversion and if a restriction enzyme is used that uses a CG sequence, cutting capability is preserved (Figure 71).

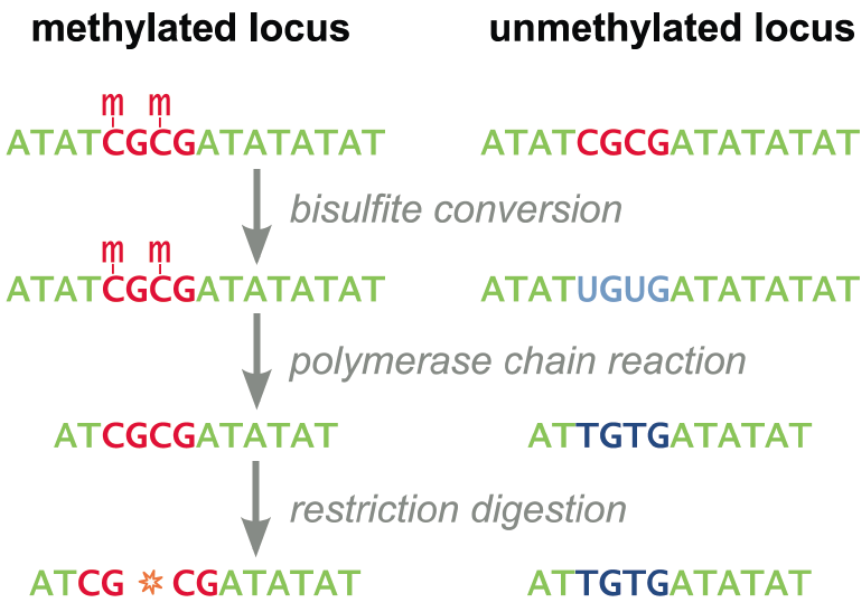

Figure 71. Scheme illustrating the principle of Combined Bisulfite Restriction Analysis (COBRA) (retrieved from Wikipedia: http://en.wikipedia.org/wiki/Combined_Bisulfite_Restriction_Analysis).

Using the pGHU6 lentiviral shRNA system we previously observed a knockdown of PU.1 AS transcripts even in the nucleus (Figure 61). We thus used that system to infect the AML-ETO leukemia cell line Kasumi-1 and the T-cell line Jurkat with pGHU6-shRNA- PU.1 AS and analyzed DNA of cell lysates with COBRA. The 530pb sequence including the PU.1 prPr contains 19 CpG islands, of which some are located within a restriction site of cutting enzymes, such as aTaq1: 2; Hpy166I:2; Hpy188III: 1. Using a restriction cocktail with these enzymes digested PCR products of bisulfite converted DNA of Kasumi-1 and Jurkat cells treated with the non silencing control (NSC), whereas after PU.1 AS knockdown methylation and digestion was lost (Figure 72).

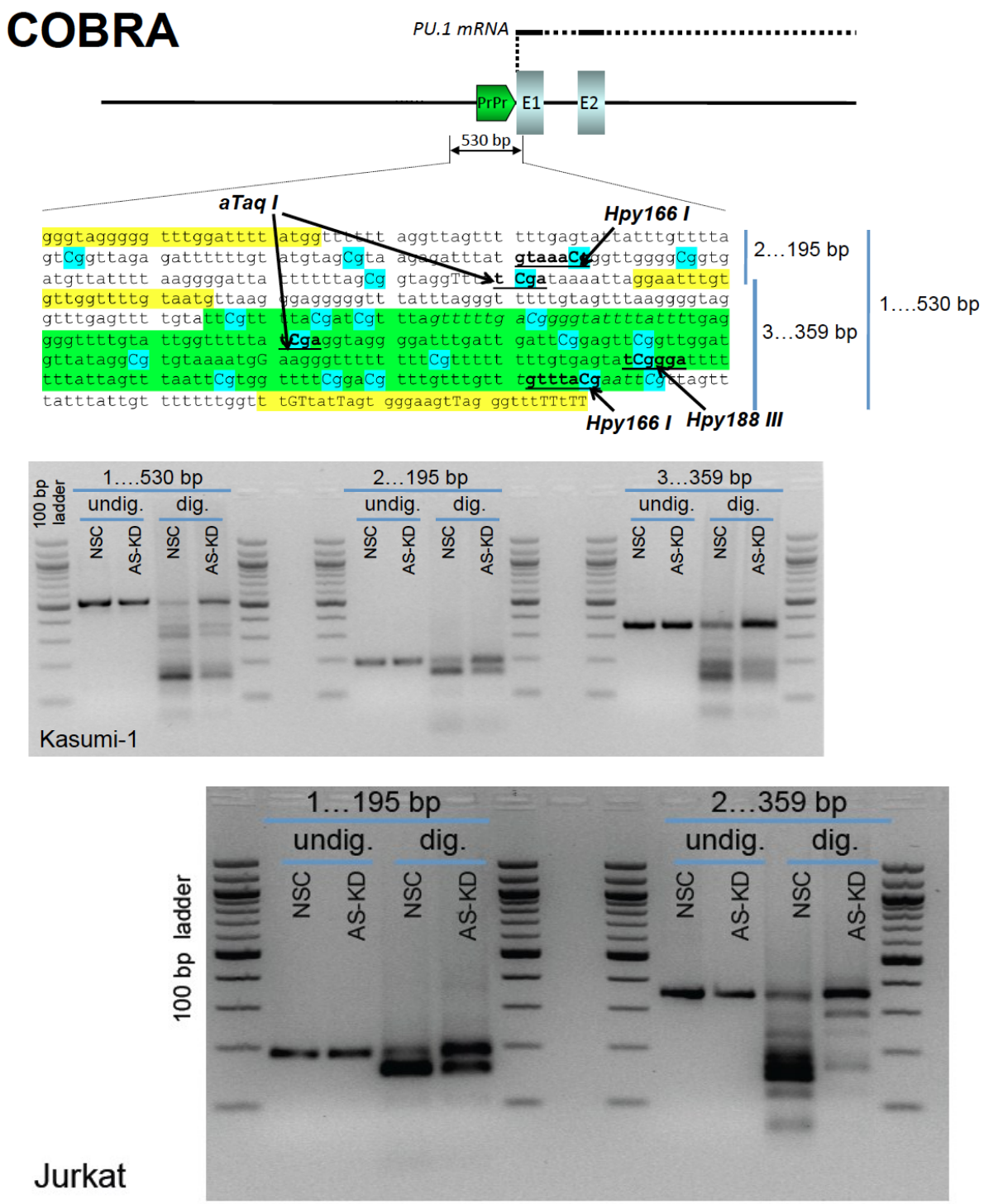

Figure 72. COBRA of Kasumi-1 and Jurkat cells after PU.1 AS knockdown demonstrates a loss of methylation sensitive digestion pattern compared to NSC. .

4.3.12 PU.1 AS transcripts interact with a DNA methyl transferase (DNMT)

To analyze if PU.1 AS noncoding transcripts mediate PU.1 prPr CpG methylation by shuttling of a DNA methyl transferase (DNMT) we tested a direct interaction using total RNA immunoprecipitation (RNA-IP or RIP) with antibodies directed against different DNMTs as indicated (Figure 73). Interestingly, RIP with DNMT3b revealed a clear positive signal in RT-PCR after IP (Figure 73). We thus, hypothesize that PU.1 AS mediates PU.1 prPr silencing by bringing the methylation initiating enzyme DNMT3b in close physical proximity.

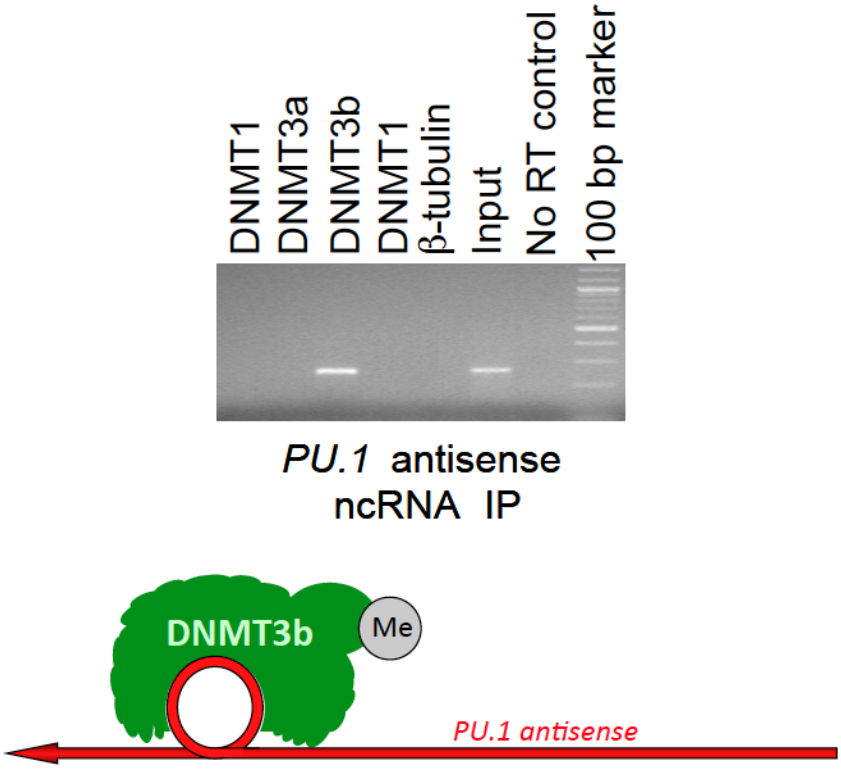

Figure 73. RNA immunoprecipitation (RNA-IP or RIP) with antibodies directed against different DNMTs.

5 Discussion

5.1 Chromatin structure and transcription factor binding

Our experiments functionally connect autoregulatory binding of PU.1 and binding of Runx factors to changes in chromosome structure and gene activity. Furthermore, we found that fusion oncoproteins of core binding factor (CBF) leukemias induce distinct structural chromosome changes. Among other reports using 3C assays to study enhancer-promoter interactions (for review see (Bulger and Groudine, 2011)), enhancer occupancy by the transcription factors Oct4, Nanog, and Sox2 and the cofactors mediator and cohesin was associated with enhancer-promoter co-localization of actively transcribed genes in embryonic stem cells (Kagey et al., 2010). While it can be suggested that binding of these factors actively mediates enhancer-promoter interaction, it is just as likely that they are consequences of independent events, thus leaving the mechanisms of action uncertain (Bulger and Groudine, 2011). A recent study identified a novel Igh V(D)J recombination control region harboring CTCF binding sites and reported loss of interaction with a long distance element in knockout lines for that region (Guo et al., 2011). However, these data were leaving the question unanswered if CTCF binding or other mechanisms would mediate loop formation. Importantly, we recently described that targeted mutations of RUNX binding sites in a downstream regulatory element (DRE) of a human CD34 transgene caused perturbation of the DRE-promoter interaction in transgenic mice (Levantini et al., 2011). Together with the functional models presented here, using specific disruption of transcription factor binding in the URE of the endogenous PU.1 locus, we now can distinguish between correlation and causation of transcription factor binding and chromosome looping necessary for gene activation (Figure 74).

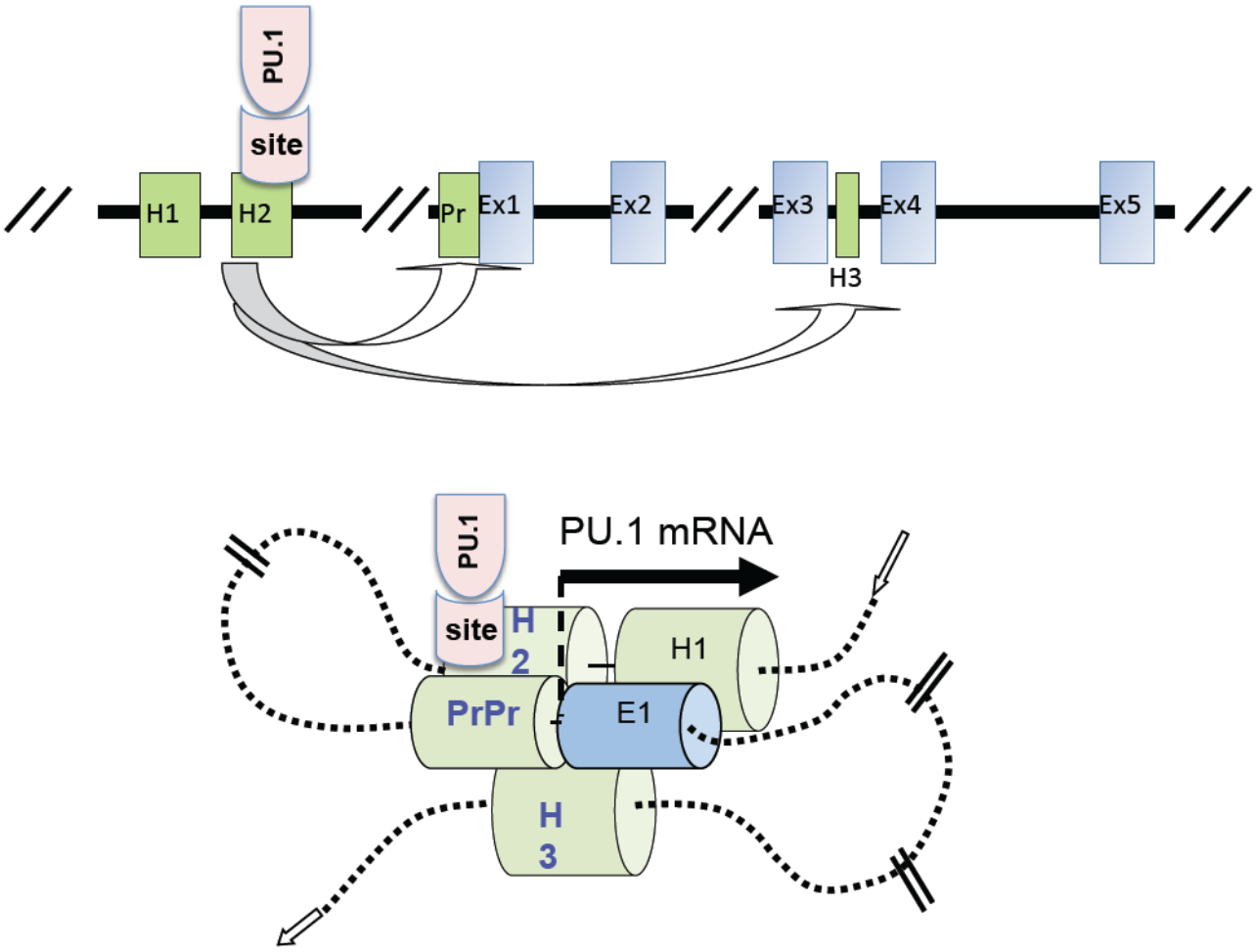

Figure 74. Cartoon illustrating transcription factor binding mediated folding of the PU.1 locus (H1 and H2 are the two homology regions of the URE).

In our 3C analysis of chromatin interactions of Kasumi-1 cells after AML1-ETO knockdown we found that the interaction of the URE with the antisense promoter changed to an URE-proximal promoter interaction after AML1-ETO depletion. This indicates that CBF fusion proteins mediate a specific chromosomal configuration of the PU.1 locus that is normally observed in T-cells. Thus, we conclude that CBF proteins hijack a T-cell specific mechanism of chromosome folding thereby establishing a chromosomal state that does support transcription of PU.1 AS, but not PU.1 mRNA (Figure 75).

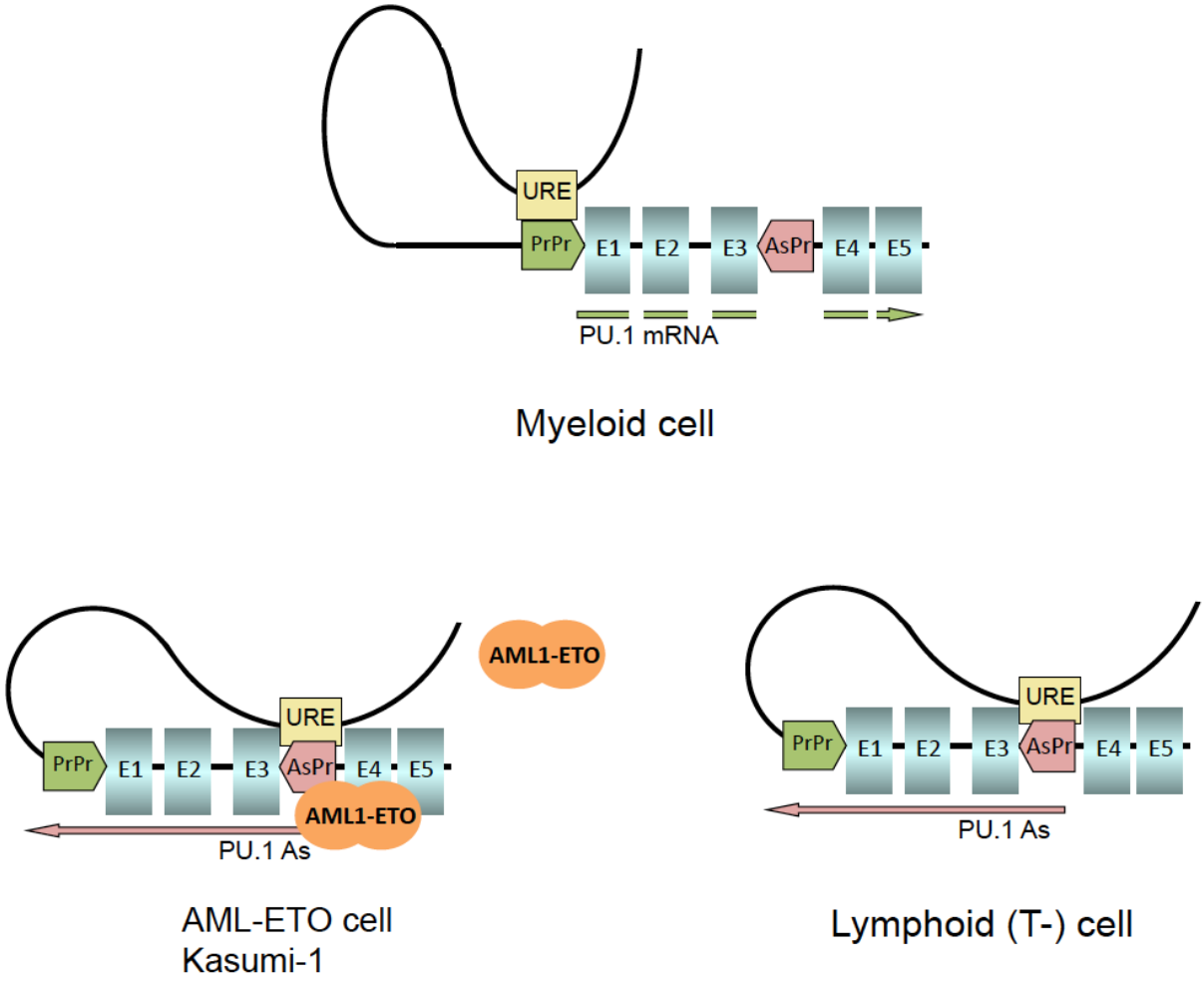

Figure 75. CBF proteins (AML1-ETO) hijacking a T-cell structure for myeloid leukemic cells.

5.2 PU.1 and stem cell proliferation

Our results demonstrate that PU.1acts as a key regulator of HSC proliferation by restraining cell cycle through multiple downstream targets. Limiting cell cycle activity is critical to maintain life-long HSC function and to prevent HSC exhaustion (Cheng et al., 2000, Hock et al., 2004, Zhang et al., 2006, Miyamoto et al., 2007, Matsumoto et al., 2011). It has been shown that PU.1 induces proliferation of erythroid progenitors (Fisher et al., 2004, Back et al., 2004). However, a previous study using inducible PU.1 over-expression suggested that PU.1 could reduce proliferation in HSCs (Fukuchi et al., 2008). As indicated by gene

expression and GO-analysis presented in this study, PU.1 significantly regulates pathways which have been associated with HSC maintenance and self-renewal, such as canonical Wnt, MAPK, and p53 signaling (Scheller et al., 2006, Kirstetter et al., 2006, Luis et al., 2009, Liu et al., 2009, Wang et al., 2011). Surprisingly, in HSCs PU.1 directly regulates various components of the cell cycle machinery by inhibiting cell cycle promoting factors like Cdk1, E2f1, and Cdc25a and inducing expression of inhibitors like Gfi1, Cdkn1a (p21), and Cdkn1c (p57). Similar to PU.1ki/ki hypomorphs, young Gfi1-/- mice demonstrate increased phenotypic HSCs, increased cell cycle activity, and decreased HSC maintenance and function (Zeng et al., 2004, Hock et al., 2004). PU.1 binds the promoter and a -35kb upstream regulatory element of Gfi1, which induces its expression in HSC/progenitor cells (Wilson et al., 2010a, Wilson et al., 2010b). Also, in concordance with the PU.1ki/ki model, mice deficient for the G1 checkpoint regulator Cdkn1a (p21) have increased HSC proliferation and susceptibility to exhaustion in stress conditions such as serial bone marrow transplantation and repetitive 5'FU injections (Cheng et al., 2000). Interestingly, HSCs of the b-catenin gain of function mouse model also demonstrated decreased p21 levels and a similar increase in HSC proliferation (S/G2/M: 3.5-fold in b-catenin gain of function mice; 2.5-fold in PU.1ki/ki mice) and consecutive exhaustion following serial transplantation (Scheller et al., 2006). Moreover, it has been reported recently that Mx1-Cre conditional deletion of Cdkn1c (p57) resulted in increased HSC cell cycle activity and exhaustion in adult mice (Matsumoto et al., 2011). Taken together, our data demonstrate that PU.1 levels control multiple components of the complex regulatory network that balances HSC quiescence and proliferation. Several of these components, which are under direct transcriptional control of PU.1 have been demonstrated to modify HSC proliferation and to impact HSC exhaustion (Figure 76, Figure 77).

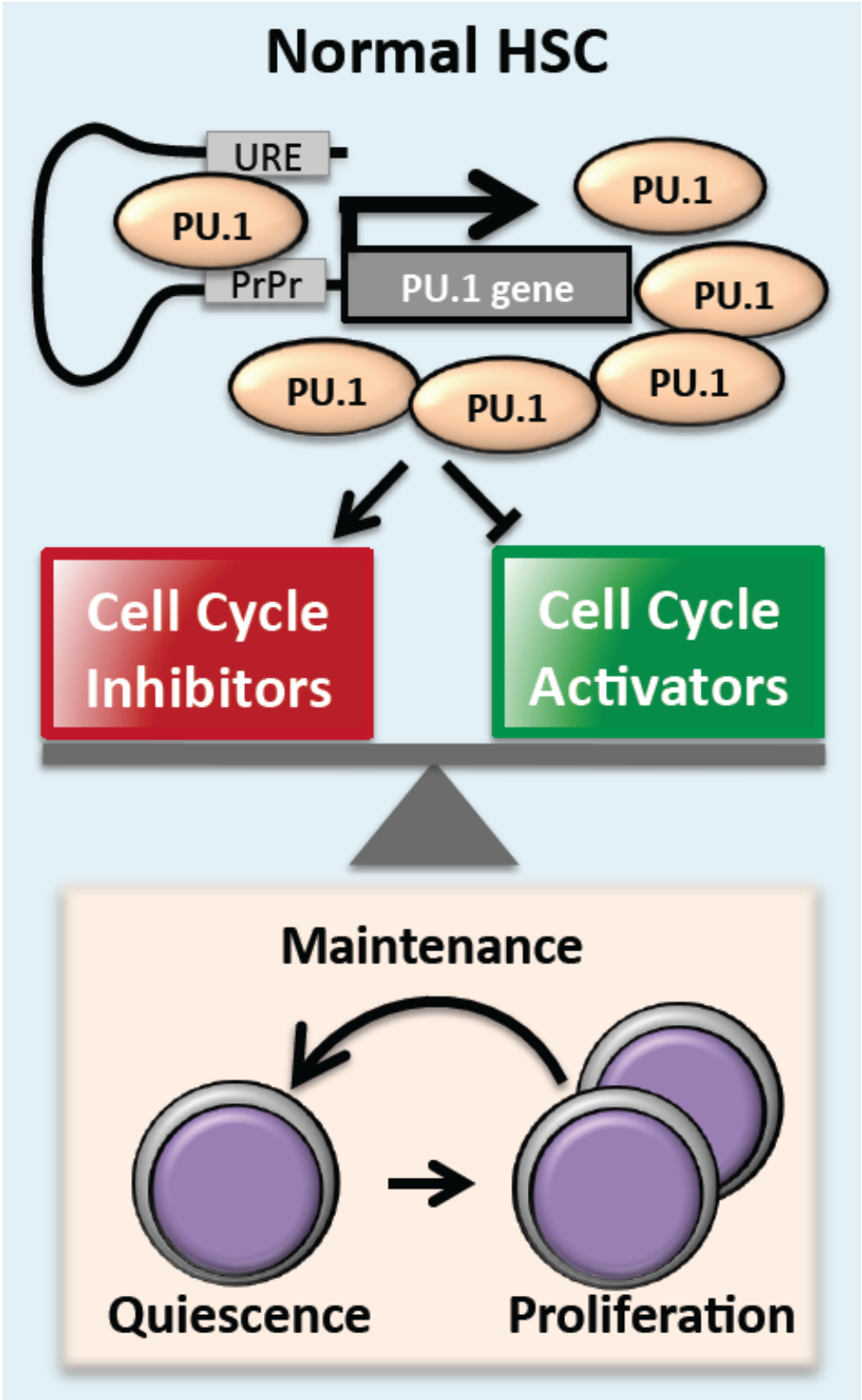

Figure 76. Positive autoregulation induces an active chromosome loop conformation resulting in sustained PU.1 levels which balance cell cycle inhibitors and activators thereby maintaining HSCs.

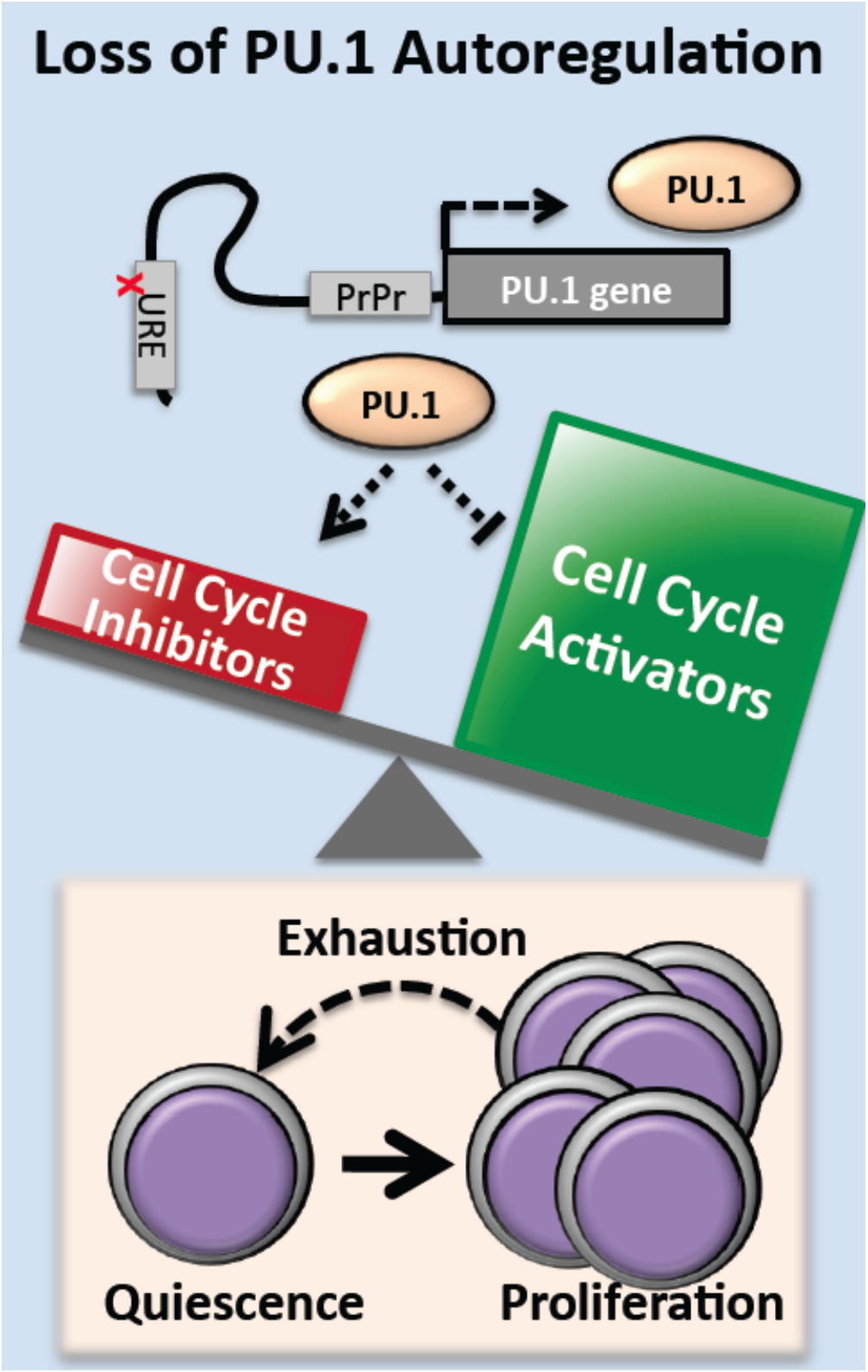

Figure 77. Disruption of positive autoregulation alters chromosome loop conformation resulting in reduced PU.1 levels, unbalanced cell cycle inhibitors and HSC exhaustion.

5.3 Transcription factor autoregulation in vivo

Our data demonstrate that positive autoregulation of a transcription factor occurs in vivo and that it has an essential function in an adult mammalian organism. Distinct cellular states are established and maintained by transcription factor networks, which can create cellular memory and stability (Xiong and Ferrell, 2003, Shykind et al., 2004, Acar et al., 2005). Autoregulation is suggested to play a critical role in fine-tuning the steady-state of transcription factor concentrations in these networks. In particular, positive transcriptional autoregulation is implicated to preserve stability and to enhance cellular memory by increasing concentration and response time to fluctuations of stimuli (Acar et al., 2005, Murugan and Kreiman, 2011). Synthetic circuits and in vitro culture based studies have been utilized to identify mechanisms of autoregulatory gene networks. Recently, genome-wide transcription factor occupancy studies have also emphasized a potentially fundamental role of autoregulation to maintain distinct cellular phenotypes such as embryonic stem cell state (Young, 2011). However, these studies are inherently descriptive, and are also limited in that they have not accounted for changes secondary to decreased transcription factor expression. Therefore, the natural occurrence and in vivo functional relevance of autoregulation in complex organisms such as mammals has remained unclear. Using a series of in vivo genetic models, including knockouts, transgenics, targeted deletions, and in particular models which maintain normal PU.1 expression, we can now demonstrate conclusively that PU.1 autoregulates its expression through a binding site in an upstream regulatory region.

5.4 Runx-PU.1 pathway in normal stem cells

This study uncovers a novel role of the Runx-PU.1 pathway in normal and leukemic stem cell biology. Previous reports of Runx1 function in HSCs have been inconsistent, probably due to partial compensatory effects of other Runx family members (Ichikawa et al., 2008, Jacob et al., 2010, Cai et al., 2011, Ichikawa et al., 2004). Here we show that Runx1 deletion led to Runx3 up-regulation in HSCs. Together with a recent study demonstrating a functional role of Runx3 in HSCs (Wang et al., 2013), this suggests that Runx3 partially substitutes for Runx1 function. The functional redundancy of Runx factors was further supported by a report

showing Runx2 up-regulation in MLL-AF9 leukemia (Bernt et al., 2011). By disrupting the common binding sequences of all Runx family members in the PU.1 URE, we could evaluate the Runx-PU.1 axis without compensatory effects. We found that Runx factors mediate folding of the PU.1 locus to a loop formation and induce PU.1 transcription in HSCs, which is fundamental to preserve HSC function by preventing exhaustion. Using PU.1 hypomorphic mice, we recently provided experimental evidence that PU.1 prevents HSC exhaustion (Staber et al., 2013). In HSCs, PU.1 directly regulates various components of the cell-cycle machinery by inhibiting cell-cycle-promoting factors, such as Cdk1, E2f1, and Cdc25a and inducing the expression of inhibitors such as Gfi1, Cdkn1a (p21), and Cdkn1c (p57) (Staber et al., 2013). Similarly, PU.1 slows down the cell cycle of HSCs/progenitors (Kueh et al., 2013). Thus, our data provide functional evidence that by inducing PU.1, Runx factors prevent HSC exhaustion through the regulatory function of PU.1 on the cell cycle machinery.

5.5 Runx-PU.1 pathway in leukemic stem cells

Acute leukemia is characterized by a block in hematopoietic differentiation. Since PU.1 strongly promotes myeloid differentiation, it has been thought to be a leukemia-suppressive gene (Tenen, 2003). Reducing PU.1 levels can induce AML in mice (Rosenbauer et al., 2004), and low PU.1 levels have also been implicated mechanistically in specific forms of leukemia such as Acute Promyelocytic Leukemia (Walter et al., 2005, Mueller et al., 2006) and Core-Binding Factor Leukemia (Vangala et al., 2003, Goyama and Mulloy, 2011, Huang et al., 2011, Huang et al., 2008, Okuda et al., 1998). However, the observation that the Runx-PU.1 pathway is essential in HSC biology led us to to investigate whether normal and leukemic stem cells might share the requirement of Runx induced PU.1 for their stemness. As proof of principle, we disrupted the Runx-PU.1 axis in AML/ETO9a induced leukemia and observed a dramatic decrease in leukemic stem cell function. This finding demonstrates the requirement of Runx-PU.1 for leukemic stem cell function, likely through the requirement of at least some level of PU.1 to prevent stem cell exhaustion. Using a mouse model with the combined loss of Runx1/CBFB a recent study reported the requirement of Runx for the survival of MLL-AF9 fusion leukemia cells (Goyama et al., 2013). Another recent report indicated a key role of Runx1 in MLL-AF4 leukemia (Wilkinson et al., 2013). Our data are

consistent with these reports. Furthermore, we here present experimental evidence that Runx factors are required to maintain the stemness of leukemic cells through their downstream target PU.1.

5.6 PU.1 antisense mediated silencing of PU.1 promoter

We have demonstrated that Runx induced PU.1 levels and the URE-prPr interaction have a crucial function in normal HSCs. Despite the fact that PU.1 is an anti-leukemic gene we further showed that at least some PU.1 levels through Runx mediated URE-prPr interaction is also required in A/E9a leukemic stem cells. It therefore appears surprising that AML-ETO fusion oncoprotein themselves mediate a specific structure that favors the interaction of the URE with the AsPr in contrast to the URE-prPr interaction. In AML-ETO leukemia with intact Runx sites URE-prPr interactions occur to a to a higher degree than in Runx site mutants, in which URE-prPr interaction was below the detection threshold. We therefore hypothesize that low PU.1 levels are critical for leukemia development since proliferation potential is increased and myeloid differentiation is disrupted. However, a decrease of PU.1 levels over a critical threshold affects the stemness of both normal HSCs and leukemic stem cells.

This work achieved three major innovations: First, we demonstrated how a higher-order chromosome architecture regulates gene transcription through activating either a proximal promoter or a non-coding antisense promoter in a competitive / dualistic manner ("competitive promoter model"). Second, we showed that fusion proteins of core-binding factor (CBF) leukemias t(8;21) and inv(16) arrange a specific three-dimensional chromosome structure, which facilitates excessive PU.1 antisense transcription resulting in PU.1 silencing as a driving event of these leukemias. Third, we found a direct interaction of PU.1 As transcripts with DNMT3b and described a noncoding dependent methylation of the PU. 1 promoter. These experiments established a novel mechanism linking a distinct higher-order chromatin structure with transcription of a non-coding RNA and tumor suppressor gene methylation as specific cause of a large subgroup of acute myeloid leukemia (Figure 78).

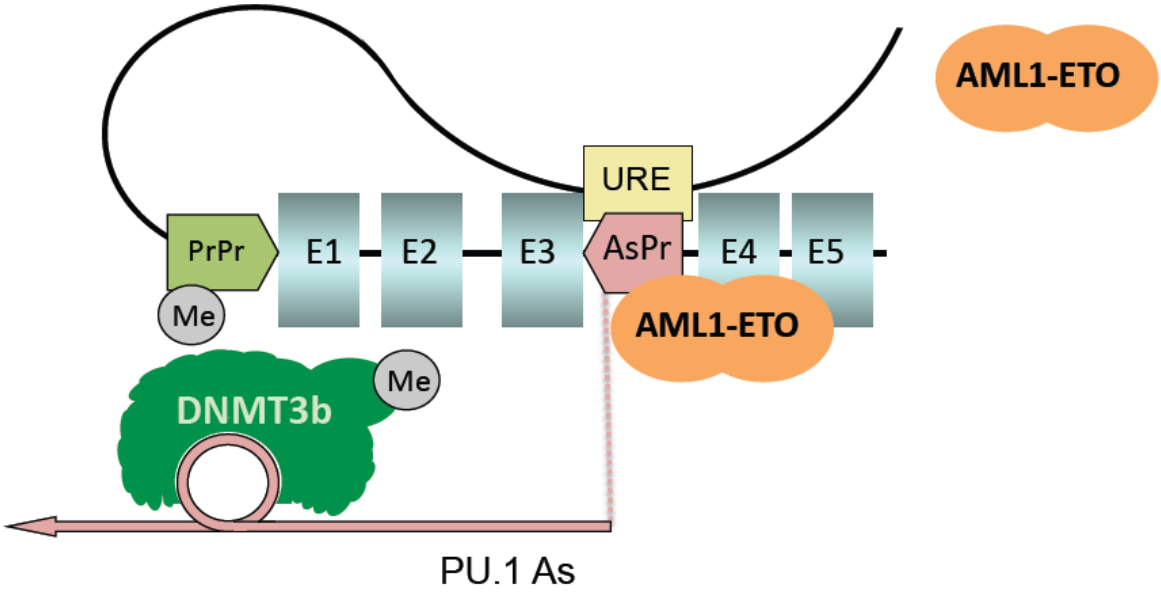

Figure 78. Scheme illustrating the mechanism linking a distinct higher-order chromatin structure with transcription of a non-coding RNA and PU.1 promoter methylation in CBF AML.

Hematopoietic stem cells (HSC) ensure a life-long replenishment of all blood lineages and maintain a sufficient HSC pool (Leary et al., 1985). The decision of an individual HSC to commit to the myeloid lineage requires a timed and strictly stage dependent expression of the master transcription factors Runx1 and PU.1 (Rosenbauer and Tenen, 2007, Hoogenkamp et al., 2009, Huang et al., 2008, Staber et al., 2013, Kueh et al., 2013). The interplay between these two factors may also be of significance in human leukemia, as Runx function is frequently affected in various types of the disease such as the core-binding factor leukemias t(8;21) and inv(16) or through direct mutations of Runx1 (Meyers et al., 1995, Lukasik et al., 2002, Silva et al., 2009, Peterson et al., 2007). Leukemia is the most frequent cancer related cause of death in adults between the age of 30 and 40 and also a frequent cause of death of children. The prognosis for these patients is poor, because to date, except for the small subgroup of t(15;17) leukemia cases, no causative therapy exists and our understanding about the mechanism of disease has remained limited (Swerdlow, 2008).

Emerging regulatory mechanisms include long non-coding RNA (ncRNA) molecules and higher order chromatin interactions (Lee and Bartolomei, 2013, Rinn and Chang, 2012,

Sexton and Cavalli, 2013, Staber et al., 2013). The biological characterization and functional analyses of PU.1 non-coding transcripts is a centerpiece of this thesis. We established the functional link between Runx and CBF fusion proteins, three dimensional chromatin arrangements and non-coding transcription thus breaking new grounds in our understanding of gene regulation. Insights in this novel mechanism deepened our knowledge of hematopoietic stem cell differentiation and CBF leukemia development and will provide a basis for the development of novel ncRNA directed causative drug therapies in hematologic disorders.

6. Abbreviations and bibliography

Abbreviations

PU.1 (encoded as SPI1/Sfpi1): Transcription factor binds to a purine-rich sequence known as the PU-box; Runt-related transcription factor (RUNX), ETS (E26 transformation-specific or E-twenty-six) family is one of the largest families of transcription factors, acute myeloid leukemia 1 protein (AML1), embryonic stem cells (ESC), induced pluripotent stem cells (iPSC), Hematopoietic stem cells (HSC), core-binding factor (CBF) leukemia, acute myeloid leukemia (AML), upstream regulatory element (URE), proximal promoter (PrPr), antisense promoter (AsPr), antisense transcription start site (ATSS), chromosome conformation capture (3C), enhanced green fluorescent protein (eGFP), antisense (AS), Non Silencing Control (NSC), small hairpin RNA (shRNA), Electro-Mobility-Shift-Assay (EMSA), Chromatin Immuno-precipitation (ChIP), polyinosinic-polycytidylic acid (pIpC),

Bibliography

ACAR, M., BECSKEI, A. & VAN OUDENAARDEN, A. 2005. Enhancement of cellular memory by reducing stochastic transitions. *Nature,* 435**,** 228-32.

ADLI, M., ZHU, J. & BERNSTEIN, B. E. 2010. Genome-wide chromatin maps derived from limited numbers of hematopoietic progenitors. *Nat Methods,* 7**,** 615-8.

AIKAWA, Y., KATSUMOTO, T., ZHANG, P., SHIMA, H., SHINO, M., TERUI, K., ITO, E., OHNO, H., STANLEY, E. R., SINGH, H., TENEN, D. G. & KITABAYASHI, I. 2010. PU.1-mediated upregulation of CSF1R is crucial for leukemia stem cell potential induced by MOZ-TIF2. *Nat Med,* 16**,** 580-5, 1p following 585.

APOSTOLOU, E., FERRARI, F., WALSH, R. M., BAR-NUR, O., STADTFELD, M., CHELOUFI, S., STUART, H. T., POLO, J. M., OHSUMI, T. K., BOROWSKY, M. L., KHARCHENKO, P. V., PARK, P. J. & HOCHEDLINGER, K. 2013. Genome-wide chromatin interactions of the Nanog locus in pluripotency, differentiation, and reprogramming. *Cell Stem Cell,* 12**,** 699-712.

BACK, J., DIERICH, A., BRONN, C., KASTNER, P. & CHAN, S. 2004. PU.1 determines the self-renewal capacity of erythroid progenitor cells. *Blood,* 103**,** 3615-23.

BAKRI, Y., SARRAZIN, S., MAYER, U. P., TILLMANNS, S., NERLOV, C., BONED, A. & SIEWEKE, M. H. 2005. Balance of MafB and PU.1 specifies alternative macrophage or dendritic cell fate. *Blood,* 105**,** 2707-16.

BERNT, K. M., ZHU, N., SINHA, A. U., VEMPATI, S., FABER, J., KRIVTSOV, A. V., FENG, Z., PUNT, N., DAIGLE, A., BULLINGER, L., POLLOCK, R. M., RICHON, V. M., KUNG, A. L. & ARMSTRONG, S. A. 2011. MLL-rearranged leukemia is dependent on aberrant H3K79 methylation by DOT1L. *Cancer Cell,* 20**,** 66-78.

BLYTH, K., CAMERON, E. R. & NEIL, J. C. 2005. The RUNX genes: gain or loss of function in cancer. *Nat Rev Cancer,* 5**,** 376-87.

BONIFER, C. 2005. Epigenetic plasticity of hematopoietic cells. *Cell Cycle,* 4**,** 211-4.

BULGER, M. & GROUDINE, M. 2011. Functional and mechanistic diversity of distal transcription enhancers. *Cell,* 144**,** 327-39.

BURCKSTUMMER, T., BANNING, C., HAINZL, P., SCHOBESBERGER, R., KERZENDORFER, C., PAULER, F. M., CHEN, D., THEM, N., SCHISCHLIK, F., REBSAMEN, M., SMIDA, M., FECE DE LA CRUZ, F., LAPAO, A., LISZT, M., EIZINGER, B., GUENZL, P. M., BLOMEN, V. A., KONOPKA, T., GAPP, B., PARAPATICS, K., MAIER, B., STOCKL, J., FISCHL, W., SALIC, S., TABA CASARI, M. R., KNAPP, S., BENNETT, K. L., BOCK, C., COLINGE, J., KRALOVICS, R., AMMERER, G., CASARI, G., BRUMMELKAMP, T. R., SUPERTI-FURGA, G. & NIJMAN, S. M. 2013. A reversible gene trap collection empowers haploid genetics in human cells. *Nat Methods,* 10**,** 965-71.

CAI, X., GAUDET, J. J., MANGAN, J. K., CHEN, M. J., DE OBALDIA, M. E., OO, Z., ERNST, P. & SPECK, N. A. 2011. Runx1 loss minimally impacts long-term hematopoietic stem cells. *PLoS One,* 6**,** e28430.

CARNINCI, P. 2009. Molecular biology: The long and short of RNAs. *Nature,* 457**,** 974-5.

CARNINCI, P., KASUKAWA, T., KATAYAMA, S., GOUGH, J., FRITH, M. C., MAEDA, N., OYAMA, R., RAVASI, T., LENHARD, B., WELLS, C., KODZIUS, R., SHIMOKAWA, K., BAJIC, V. B., BRENNER, S. E., BATALOV, S., FORREST, A. R., ZAVOLAN, M., DAVIS, M. J., WILMING, L. G., AIDINIS, V., ALLEN, J. E., AMBESI-IMPIOMBATO, A., APWEILER, R., ATURALIYA, R. N., BAILEY, T. L., BANSAL, M., BAXTER, L., BEISEL, K. W., BERSANO, T., BONO, H., CHALK, A. M., CHIU, K. P., CHOUDHARY, V., CHRISTOFFELS, A., CLUTTERBUCK, D. R., CROWE, M. L., DALLA, E., DALRYMPLE, B. P., DE BONO, B., DELLA GATTA, G., DI BERNARDO, D., DOWN, T., ENGSTROM, P., FAGIOLINI, M., FAULKNER, G., FLETCHER, C. F., FUKUSHIMA, T., FURUNO, M., FUTAKI, S., GARIBOLDI, M., GEORGII-HEMMING, P., GINGERAS, T. R., GOJOBORI, T., GREEN, R. E., GUSTINCICH, S., HARBERS, M., HAYASHI, Y., HENSCH, T. K., HIROKAWA, N., HILL, D., HUMINIECKI, L., IACONO, M., IKEO, K., IWAMA, A., ISHIKAWA, T., JAKT, M., KANAPIN, A., KATOH, M., KAWASAWA, Y., KELSO, J., KITAMURA, H., KITANO, H., KOLLIAS, G., KRISHNAN, S. P., KRUGER, A., KUMMERFELD, S. K., KUROCHKIN, I. V., LAREAU, L. F., LAZAREVIC, D., LIPOVICH, L., LIU, J., LIUNI, S., MCWILLIAM, S., MADAN BABU, M., MADERA, M., MARCHIONNI, L., MATSUDA, H., MATSUZAWA, S., MIKI, H., MIGNONE, F., MIYAKE, S., MORRIS, K., MOTTAGUI-TABAR, S., MULDER, N., NAKANO, N., NAKAUCHI, H., NG, P., NILSSON, R., NISHIGUCHI, S., NISHIKAWA, S., et al. 2005. The transcriptional landscape of the mammalian genome. *Science,* 309**,** 1559-63.

CAROTTA, S., DAKIC, A., D'AMICO, A., PANG, S. H., GREIG, K. T., NUTT, S. L. & WU, L. 2010. The transcription factor PU.1 controls dendritic cell development and Flt3 cytokine receptor expression in a dose-dependent manner. *Immunity,* 32**,** 628-41.

CASTILLA, L. H., WIJMENGA, C., WANG, Q., STACY, T., SPECK, N. A., ECKHAUS, M., MARIN-PADILLA, M., COLLINS, F. S., WYNSHAW-BORIS, A. & LIU, P. P. 1996. Failure of embryonic hematopoiesis and lethal hemorrhages in mouse embryos heterozygous for a knocked-in leukemia gene CBFB-MYH11. *Cell,* 87**,** 687-96.

CHEN, H. M., ZHANG, P., VOSO, M. T., HOHAUS, S., GONZALEZ, D. A., GLASS, C. K., ZHANG, D. E. & TENEN, D. G. 1995. Neutrophils and monocytes express high levels of PU.1 (Spi-1) but not Spi-B. *Blood,* 85**,** 2918-28.

CHEN, M. J., YOKOMIZO, T., ZEIGLER, B. M., DZIERZAK, E. & SPECK, N. A. 2009. Runx1 is required for the endothelial to haematopoietic cell transition but not thereafter. *Nature,* 457**,** 887-91.

CHENG, J., KAPRANOV, P., DRENKOW, J., DIKE, S., BRUBAKER, S., PATEL, S., LONG, J., STERN, D., TAMMANA, H., HELT, G., SEMENTCHENKO, V., PICCOLBONI, A., BEKIRANOV, S., BAILEY, D. K., GANESH, M., GHOSH, S., BELL, I., GERHARD, D. S. & GINGERAS, T. R. 2005. Transcriptional maps of 10 human chromosomes at 5-nucleotide resolution. *Science,* 308**,** 1149-54.

CHENG, T., RODRIGUES, N., SHEN, H., YANG, Y., DOMBKOWSKI, D., SYKES, M. & SCADDEN, D. T. 2000. Hematopoietic stem cell quiescence maintained by p21cip1/waf1. *Science,* 287**,** 1804-8.

CHUA, S. W., VIJAYAKUMAR, P., NISSOM, P. M., YAM, C. Y., WONG, V. V. & YANG, H. 2006. A novel normalization method for effective removal of systematic variation in microarray data. *Nucleic Acids Res,* 34**,** e38.

COOK, W. D., MCCAW, B. J., HERRING, C., JOHN, D. L., FOOTE, S. J., NUTT, S. L. & ADAMS, J. M. 2004. PU.1 is a suppressor of myeloid leukemia, inactivated in mice by gene deletion and mutation of its DNA binding domain. *Blood,* 104**,** 3437-44.

DAHL, R., WALSH, J. C., LANCKI, D., LASLO, P., IYER, S. R., SINGH, H. & SIMON, M. C. 2003. Regulation of macrophage and neutrophil cell fates by the PU.1:C/EBPalpha ratio and granulocyte colony-stimulating factor. *Nat Immunol,* 4**,** 1029-36.

DAKIC, A., METCALF, D., DI RAGO, L., MIFSUD, S., WU, L. & NUTT, S. L. 2005. PU.1 regulates the commitment of adult hematopoietic progenitors and restricts granulopoiesis. *J Exp Med,* 201**,** 1487-502.

DEKKER, J., RIPPE, K., DEKKER, M. & KLECKNER, N. 2002. Capturing chromosome conformation. *Science,* 295**,** 1306-11.

DEKOTER, R. P. & SINGH, H. 2000. Regulation of B lymphocyte and macrophage development by graded expression of PU.1. *Science,* 288**,** 1439-41.

DI RUSCIO, A., EBRALIDZE, A. K., BENOUKRAF, T., AMABILE, G., GOFF, L. A., TERRAGNI, J., FIGUEROA, M. E., DE FIGUEIREDO PONTES, L. L., ALBERICH-JORDA, M., ZHANG, P., WU, M., D'ALO, F., MELNICK, A., LEONE, G., EBRALIDZE, K. K., PRADHAN, S., RINN, J. L. & TENEN, D. G. 2013. DNMT1-interacting RNAs block gene-specific DNA methylation. *Nature,* 503**,** 371-6.

DIXON, J. R., SELVARAJ, S., YUE, F., KIM, A., LI, Y., SHEN, Y., HU, M., LIU, J. S. & REN, B. 2012. Topological domains in mammalian genomes identified by analysis of chromatin interactions. *Nature,* 485**,** 376-80.

DOSTIE, J. & DEKKER, J. 2007. Mapping networks of physical interactions between genomic elements using 5C technology. *Nat Protoc,* 2**,** 988-1002.

DUAN, Z., ANDRONESCU, M., SCHUTZ, K., MCILWAIN, S., KIM, Y. J., LEE, C., SHENDURE, J., FIELDS, S., BLAU, C. A. & NOBLE, W. S. 2010. A three-dimensional model of the yeast genome. *Nature,* 465**,** 363-7.

EBRALIDZE, A. K., GUIBAL, F. C., STEIDL, U., ZHANG, P., LEE, S., BARTHOLDY, B., JORDA, M. A., PETKOVA, V., ROSENBAUER, F., HUANG, G., DAYARAM, T., KLUPP, J., O'BRIEN, K. B., WILL, B., HOOGENKAMP, M., BORDEN, K. L., BONIFER, C. & TENEN, D. G. 2008. PU.1 expression is modulated by the balance of functional sense and antisense RNAs regulated by a shared cis-regulatory element. *Genes Dev,* 22**,** 2085-92.

EILKEN, H. M., NISHIKAWA, S. & SCHROEDER, T. 2009. Continuous single-cell imaging of blood generation from haemogenic endothelium. *Nature,* 457**,** 896-900.

ENGEL, J. D. & TANIMOTO, K. 2000. Looping, linking, and chromatin activity: new insights into beta-globin locus regulation. *Cell,* 100**,** 499-502.

FISHER, R. C., LOVELOCK, J. D. & SCOTT, E. W. 1999. A critical role for PU.1 in homing and long-term engraftment by hematopoietic stem cells in the bone marrow. *Blood,* 94**,** 1283-90.

FISHER, R. C., SLAYTON, W. B., CHIEN, C., GUTHRIE, S. M., BRAY, C. & SCOTT, E. W. 2004. PU.1 supports proliferation of immature erythroid progenitors. *Leuk Res,* 28**,** 83-9.

FUKUCHI, Y., ITO, M., SHIBATA, F., KITAMURA, T. & NAKAJIMA, H. 2008. Activation of CCAAT/enhancer-binding protein alpha or PU.1 in hematopoietic stem cells leads to their reduced self-renewal and proliferation. *Stem Cells,* 26**,** 3172-81.

GAIDZIK, V. I., BULLINGER, L., SCHLENK, R. F., ZIMMERMANN, A. S., ROCK, J., PASCHKA, P., CORBACIOGLU, A., KRAUTER, J., SCHLEGELBERGER, B., GANSER, A., SPATH, D., KUNDGEN, A., SCHMIDT-WOLF, I. G., GOTZE, K., NACHBAUR, D., PFREUNDSCHUH, M., HORST, H. A., DOHNER, H. & DOHNER, K. 2011. RUNX1 mutations in acute myeloid leukemia: results from a comprehensive genetic and clinical analysis from the AML study group. *J Clin Oncol,* 29**,** 1364-72.

GOYAMA, S. & MULLOY, J. C. 2011. Molecular pathogenesis of core binding factor leukemia: current knowledge and future prospects. *Int J Hematol,* 94**,** 126-33.

GOYAMA, S., SCHIBLER, J., CUNNINGHAM, L., ZHANG, Y., RAO, Y., NISHIMOTO, N., NAKAGAWA, M., OLSSON, A., WUNDERLICH, M., LINK, K. A., MIZUKAWA, B., GRIMES, H. L., KUROKAWA, M., LIU, P. P., HUANG, G. & MULLOY, J. C. 2013. Transcription factor RUNX1 promotes survival of acute myeloid leukemia cells. *J Clin Invest,* 123**,** 3876-88.

GROWNEY, J. D., SHIGEMATSU, H., LI, Z., LEE, B. H., ADELSPERGER, J., ROWAN, R., CURLEY, D. P., KUTOK, J. L., AKASHI, K., WILLIAMS, I. R., SPECK, N. A. & GILLILAND, D. G. 2005. Loss of Runx1 perturbs adult hematopoiesis and is associated with a myeloproliferative phenotype. *Blood,* 106**,** 494-504.

GUO, C., YOON, H. S., FRANKLIN, A., JAIN, S., EBERT, A., CHENG, H. L., HANSEN, E., DESPO, O., BOSSEN, C., VETTERMANN, C., BATES, J. G., RICHARDS, N., MYERS, D., PATEL, H., GALLAGHER, M., SCHLISSEL, M. S., MURRE, C., BUSSLINGER, M., GIALLOURAKIS, C. C. & ALT, F. W. 2011. CTCF-binding elements mediate control of V(D)J recombination. *Nature,* 477**,** 424-30.

GUTTMAN, M., AMIT, I., GARBER, M., FRENCH, C., LIN, M. F., FELDSER, D., HUARTE, M., ZUK, O., CAREY, B. W., CASSADY, J. P., CABILI, M. N., JAENISCH, R., MIKKELSEN, T. S., JACKS, T., HACOHEN, N., BERNSTEIN, B. E., KELLIS, M., REGEV, A., RINN, J. L. & LANDER, E. S. 2009. Chromatin signature reveals over a thousand highly conserved large non-coding RNAs in mammals. *Nature,* 458**,** 223-7.

HEINZ, S., BENNER, C., SPANN, N., BERTOLINO, E., LIN, Y. C., LASLO, P., CHENG, J. X., MURRE, C., SINGH, H. & GLASS, C. K. 2010. Simple combinations of lineage-determining transcription factors prime cis-regulatory elements required for macrophage and B cell identities. *Mol Cell,* 38**,** 576-89.

HOCK, H., HAMBLEN, M. J., ROOKE, H. M., SCHINDLER, J. W., SALEQUE, S., FUJIWARA, Y. & ORKIN, S. H. 2004. Gfi-1 restricts proliferation and preserves functional integrity of haematopoietic stem cells. *Nature,* 431**,** 1002-7.

HOOGENKAMP, M., KRYSINSKA, H., INGRAM, R., HUANG, G., BARLOW, R., CLARKE, D., EBRALIDZE, A., ZHANG, P., TAGOH, H., COCKERILL, P. N., TENEN, D. G. & BONIFER, C. 2007. The Pu.1 locus is differentially regulated at the level of chromatin structure and noncoding transcription by alternate mechanisms at distinct developmental stages of hematopoiesis. *Mol Cell Biol,* 27**,** 7425-38.

HOOGENKAMP, M., LICHTINGER, M., KRYSINSKA, H., LANCRIN, C., CLARKE, D., WILLIAMSON, A., MAZZARELLA, L., INGRAM, R., JORGENSEN, H., FISHER, A., TENEN, D. G., KOUSKOFF, V., LACAUD, G. & BONIFER, C. 2009. Early chromatin

unfolding by RUNX1: a molecular explanation for differential requirements during specification versus maintenance of the hematopoietic gene expression program. *Blood,* 114**,** 299-309.

HUANG, G., ZHANG, P., HIRAI, H., ELF, S., YAN, X., CHEN, Z., KOSCHMIEDER, S., OKUNO, Y., DAYARAM, T., GROWNEY, J. D., SHIVDASANI, R. A., GILLILAND, D. G., SPECK, N. A., NIMER, S. D. & TENEN, D. G. 2008. PU.1 is a major downstream target of AML1 (RUNX1) in adult mouse hematopoiesis. *Nat Genet,* 40**,** 51-60.

HUANG, G., ZHAO, X., WANG, L., ELF, S., XU, H., SASHIDA, G., ZHANG, Y., LIU, Y., LEE, J., MENENDEZ, S., YANG, Y., YAN, X., ZHANG, P., TENEN, D. G., OSATO, M., HSIEH, J. J. & NIMER, S. D. 2011. The ability of MLL to bind RUNX1 and methylate H3K4 at PU.1 regulatory regions is impaired by MDS/AML-associated RUNX1/AML1 mutations. *Blood,* 118**,** 6544-52.

ICHIKAWA, M., ASAI, T., SAITO, T., SEO, S., YAMAZAKI, I., YAMAGATA, T., MITANI, K., CHIBA, S., OGAWA, S., KUROKAWA, M. & HIRAI, H. 2004. AML-1 is required for megakaryocytic maturation and lymphocytic differentiation, but not for maintenance of hematopoietic stem cells in adult hematopoiesis. *Nat Med,* 10**,** 299-304.

ICHIKAWA, M., GOYAMA, S., ASAI, T., KAWAZU, M., NAKAGAWA, M., TAKESHITA, M., CHIBA, S., OGAWA, S. & KUROKAWA, M. 2008. AML1/Runx1 negatively regulates quiescent hematopoietic stem cells in adult hematopoiesis. *J Immunol,* 180**,** 4402-8.

IRIZARRY, R. A., BOLSTAD, B. M., COLLIN, F., COPE, L. M., HOBBS, B. & SPEED, T. P. 2003. Summaries of Affymetrix GeneChip probe level data. *Nucleic Acids Res,* 31**,** e15.

ITO, Y. 2008. RUNX genes in development and cancer: regulation of viral gene expression and the discovery of RUNX family genes. *Adv Cancer Res,* 99**,** 33-76.

IWASAKI, H., SOMOZA, C., SHIGEMATSU, H., DUPREZ, E. A., IWASAKI-ARAI, J., MIZUNO, S., ARINOBU, Y., GEARY, K., ZHANG, P., DAYARAM, T., FENYUS, M. L., ELF, S., CHAN, S., KASTNER, P., HUETTNER, C. S., MURRAY, R., TENEN, D. G. & AKASHI, K. 2005. Distinctive and indispensable roles of PU.1 in maintenance of hematopoietic stem cells and their differentiation. *Blood,* 106**,** 1590-600.

JACOB, B., OSATO, M., YAMASHITA, N., WANG, C. Q., TANIUCHI, I., LITTMAN, D. R., ASOU, N. & ITO, Y. 2010. Stem cell exhaustion due to Runx1 deficiency is prevented by Evi5 activation in leukemogenesis. *Blood,* 115**,** 1610-20.

KAGEY, M. H., NEWMAN, J. J., BILODEAU, S., ZHAN, Y., ORLANDO, D. A., VAN BERKUM, N. L., EBMEIER, C. C., GOOSSENS, J., RAHL, P. B., LEVINE, S. S., TAATJES, D. J., DEKKER, J. & YOUNG, R. A. 2010. Mediator and cohesin connect gene expression and chromatin architecture. *Nature,* 467**,** 430-5.

KATAYAMA, S., TOMARU, Y., KASUKAWA, T., WAKI, K., NAKANISHI, M., NAKAMURA, M., NISHIDA, H., YAP, C. C., SUZUKI, M., KAWAI, J., SUZUKI, H., CARNINCI, P., HAYASHIZAKI, Y., WELLS, C., FRITH, M., RAVASI, T., PANG, K. C., HALLINAN, J., MATTICK, J., HUME, D. A., LIPOVICH, L., BATALOV, S., ENGSTROM, P. G., MIZUNO, Y., FAGHIHI, M. A., SANDELIN, A., CHALK, A. M., MOTTAGUI-TABAR, S., LIANG, Z., LENHARD, B. & WAHLESTEDT, C. 2005. Antisense transcription in the mammalian transcriptome. *Science,* 309**,** 1564-6.

KHALIL, A. M., GUTTMAN, M., HUARTE, M., GARBER, M., RAJ, A., RIVEA MORALES, D., THOMAS, K., PRESSER, A., BERNSTEIN, B. E., VAN OUDENAARDEN, A., REGEV, A., LANDER, E. S. & RINN, J. L. 2009. Many human large intergenic noncoding RNAs associate with chromatin-modifying complexes and affect gene expression. *Proc Natl Acad Sci U S A,* 106**,** 11667-72.

KIEL, M. J., YILMAZ, O. H., IWASHITA, T., TERHORST, C. & MORRISON, S. J. 2005. SLAM family receptors distinguish hematopoietic stem and progenitor cells and reveal endothelial niches for stem cells. *Cell,* 121**,** 1109-21.

KIM, H. G., DE GUZMAN, C. G., SWINDLE, C. S., COTTA, C. V., GARTLAND, L., SCOTT, E. W. & KLUG, C. A. 2004. The ETS family transcription factor PU.1 is necessary for the maintenance of fetal liver hematopoietic stem cells. *Blood,* 104**,** 3894-900.

KIRSTETTER, P., ANDERSON, K., PORSE, B. T., JACOBSEN, S. E. & NERLOV, C. 2006. Activation of the canonical Wnt pathway leads to loss of hematopoietic stem cell repopulation and multilineage differentiation block. *Nat Immunol,* 7**,** 1048-56.

KUEH, H. Y., CHAMPHEKHAR, A., NUTT, S. L., ELOWITZ, M. B. & ROTHENBERG, E. V. 2013. Positive feedback between PU.1 and the cell cycle controls myeloid differentiation. *Science,* 341**,** 670-3.

KUO, Y. H., LANDRETTE, S. F., HEILMAN, S. A., PERRAT, P. N., GARRETT, L., LIU, P. P., LE BEAU, M. M., KOGAN, S. C. & CASTILLA, L. H. 2006. Cbf beta-SMMHC induces distinct abnormal myeloid progenitors able to develop acute myeloid leukemia. *Cancer Cell,* 9**,** 57-68.

LANCRIN, C., SROCZYNSKA, P., STEPHENSON, C., ALLEN, T., KOUSKOFF, V. & LACAUD, G. 2009. The haemangioblast generates haematopoietic cells through a haemogenic endothelium stage. *Nature,* 457**,** 892-5.

LEARY, A. G., STRAUSS, L. C., CIVIN, C. I. & OGAWA, M. 1985. Disparate differentiation in hemopoietic colonies derived from human paired progenitors. *Blood,* 66**,** 327-32.

LEDDIN, M., PERROD, C., HOOGENKAMP, M., GHANI, S., ASSI, S., HEINZ, S., WILSON, N. K., FOLLOWS, G., SCHONHEIT, J., VOCKENTANZ, L., MOSAMMAM, A. M., CHEN, W., TENEN, D. G., WESTHEAD, D. R., GOTTGENS, B., BONIFER, C. & ROSENBAUER, F. 2011. Two distinct auto-regulatory loops operate at the PU.1 locus in B cells and myeloid cells. *Blood,* 117**,** 2827-38.

LEE, J. T. 2012. Epigenetic regulation by long noncoding RNAs. *Science,* 338**,** 1435-9.

LEE, J. T. & BARTOLOMEI, M. S. 2013. X-inactivation, imprinting, and long noncoding RNAs in health and disease. *Cell,* 152**,** 1308-23.

LEVANTINI, E., LEE, S., RADOMSKA, H. S., HETHERINGTON, C. J., ALBERICH-JORDA, M., AMABILE, G., ZHANG, P., GONZALEZ, D. A., ZHANG, J., BASSERES, D. S., WILSON, N. K., KOSCHMIEDER, S., HUANG, G., ZHANG, D. E., EBRALIDZE, A. K., BONIFER, C., OKUNO, Y., GOTTGENS, B. & TENEN, D. G. 2011. RUNX1 regulates the CD34 gene in haematopoietic stem cells by mediating interactions with a distal regulatory element. *EMBO J,* 30**,** 4059-70.

LI, Y., OKUNO, Y., ZHANG, P., RADOMSKA, H. S., CHEN, H., IWASAKI, H., AKASHI, K., KLEMSZ, M. J., MCKERCHER, S. R., MAKI, R. A. & TENEN, D. G. 2001. Regulation of the PU.1 gene by distal elements. *Blood,* 98**,** 2958-65.

LIU, Y., ELF, S. E., MIYATA, Y., SASHIDA, G., HUANG, G., DI GIANDOMENICO, S., LEE, J. M., DEBLASIO, A., MENENDEZ, S., ANTIPIN, J., REVA, B., KOFF, A. & NIMER, S. D. 2009. p53 regulates hematopoietic stem cell quiescence. *Cell Stem Cell,* 4**,** 37-48.

LUIS, T. C., WEERKAMP, F., NABER, B. A., BAERT, M. R., DE HAAS, E. F., NIKOLIC, T., HEUVELMANS, S., DE KRIJGER, R. R., VAN DONGEN, J. J. & STAAL, F. J. 2009. Wnt3a deficiency irreversibly impairs hematopoietic stem cell self-renewal and leads to defects in progenitor cell differentiation. *Blood,* 113**,** 546-54.

LUKASIK, S. M., ZHANG, L., CORPORA, T., TOMANICEK, S., LI, Y., KUNDU, M., HARTMAN, K., LIU, P. P., LAUE, T. M., BILTONEN, R. L., SPECK, N. A. & BUSHWELLER, J. H. 2002. Altered affinity of CBF beta-SMMHC for Runx1 explains its role in leukemogenesis. *Nat Struct Biol,* 9**,** 674-9.

MATSUMOTO, A., TAKEISHI, S., KANIE, T., SUSAKI, E., ONOYAMA, I., TATEISHI, Y., NAKAYAMA, K. & NAKAYAMA, K. I. 2011. p57 is required for quiescence and maintenance of adult hematopoietic stem cells. *Cell Stem Cell,* 9**,** 262-71.

MENDENHALL, E. M. & BERNSTEIN, B. E. 2008. Chromatin state maps: new technologies, new insights. *Curr Opin Genet Dev,* 18**,** 109-15.

MEYERS, S., LENNY, N. & HIEBERT, S. W. 1995. The t(8;21) fusion protein interferes with AML-1B-dependent transcriptional activation. *Mol Cell Biol,* 15**,** 1974-82.

MIYAMOTO, K., ARAKI, K. Y., NAKA, K., ARAI, F., TAKUBO, K., YAMAZAKI, S., MATSUOKA, S., MIYAMOTO, T., ITO, K., OHMURA, M., CHEN, C., HOSOKAWA, K., NAKAUCHI, H., NAKAYAMA, K., NAKAYAMA, K. I., HARADA, M., MOTOYAMA, N., SUDA, T. & HIRAO, A. 2007. Foxo3a is essential for maintenance of the hematopoietic stem cell pool. *Cell Stem Cell,* 1**,** 101-12.

MIYOSHI, H., SHIMIZU, K., KOZU, T., MASEKI, N., KANEKO, Y. & OHKI, M. 1991. t(8;21) breakpoints on chromosome 21 in acute myeloid leukemia are clustered within a limited region of a single gene, AML1. *Proc Natl Acad Sci U S A,* 88**,** 10431-4.

MOOTHA, V. K., LINDGREN, C. M., ERIKSSON, K. F., SUBRAMANIAN, A., SIHAG, S., LEHAR, J., PUIGSERVER, P., CARLSSON, E., RIDDERSTRALE, M., LAURILA, E., HOUSTIS, N., DALY, M. J., PATTERSON, N., MESIROV, J. P., GOLUB, T. R., TAMAYO, P., SPIEGELMAN, B., LANDER, E. S., HIRSCHHORN, J. N., ALTSHULER, D. & GROOP, L. C. 2003. PGC-1alpha-responsive genes involved in oxidative phosphorylation are coordinately downregulated in human diabetes. *Nat Genet,* 34**,** 267-73.

MOREAU-GACHELIN, F., TAVITIAN, A. & TAMBOURIN, P. 1988. Spi-1 is a putative oncogene in virally induced murine erythroleukaemias. *Nature,* 331**,** 277-80.

MUELLER, B. U., PABST, T., FOS, J., PETKOVIC, V., FEY, M. F., ASOU, N., BUERGI, U. & TENEN, D. G. 2006. ATRA resolves the differentiation block in t(15;17) acute myeloid leukemia by restoring PU.1 expression. *Blood,* 107**,** 3330-8.

MURUGAN, R. & KREIMAN, G. 2011. On the minimization of fluctuations in the response times of autoregulatory gene networks. *Biophys J,* 101**,** 1297-306.

NAGANO, T., MITCHELL, J. A., SANZ, L. A., PAULER, F. M., FERGUSON-SMITH, A. C., FEIL, R. & FRASER, P. 2008. The Air noncoding RNA epigenetically silences transcription by targeting G9a to chromatin. *Science,* 322**,** 1717-20.

OKAZAKI, Y., FURUNO, M., KASUKAWA, T., ADACHI, J., BONO, H., KONDO, S., NIKAIDO, I., OSATO, N., SAITO, R., SUZUKI, H., YAMANAKA, I., KIYOSAWA, H., YAGI, K., TOMARU, Y., HASEGAWA, Y., NOGAMI, A., SCHONBACH, C., GOJOBORI, T., BALDARELLI, R., HILL, D. P., BULT, C., HUME, D. A., QUACKENBUSH, J., SCHRIML, L. M., KANAPIN, A., MATSUDA, H., BATALOV, S., BEISEL, K. W., BLAKE, J. A., BRADT, D., BRUSIC, V., CHOTHIA, C., CORBANI, L. E., COUSINS, S., DALLA, E., DRAGANI, T. A., FLETCHER, C. F., FORREST, A., FRAZER, K. S., GAASTERLAND, T., GARIBOLDI, M., GISSI, C., GODZIK, A., GOUGH, J., GRIMMOND, S., GUSTINCICH, S., HIROKAWA, N., JACKSON, I. J., JARVIS, E. D., KANAI, A., KAWAJI, H., KAWASAWA, Y., KEDZIERSKI, R. M., KING, B. L., KONAGAYA, A., KUROCHKIN, I. V., LEE, Y., LENHARD, B., LYONS, P. A., MAGLOTT, D. R., MALTAIS, L., MARCHIONNI, L., MCKENZIE, L., MIKI, H., NAGASHIMA, T., NUMATA, K., OKIDO, T., PAVAN, W. J., PERTEA, G., PESOLE, G., PETROVSKY, N., PILLAI, R., PONTIUS, J. U., QI, D., RAMACHANDRAN, S., RAVASI, T., REED, J. C., REED, D. J., REID, J., RING, B. Z., RINGWALD, M., SANDELIN, A., SCHNEIDER, C., SEMPLE, C. A., SETOU, M., SHIMADA, K., SULTANA, R., TAKENAKA, Y., TAYLOR, M. S., TEASDALE, R. D., TOMITA, M., VERARDO, R., WAGNER, L., WAHLESTEDT, C., WANG, Y., WATANABE, Y., WELLS, C., WILMING, L. G., WYNSHAW-BORIS, A., YANAGISAWA, M., et al. 2002. Analysis of the mouse transcriptome based on functional annotation of 60,770 full-length cDNAs. *Nature,* 420**,** 563-73.

OKUDA, T., CAI, Z., YANG, S., LENNY, N., LYU, C. J., VAN DEURSEN, J. M., HARADA, H. & DOWNING, J. R. 1998. Expression of a knocked-in AML1-ETO leukemia gene inhibits the establishment of normal definitive hematopoiesis and directly generates dysplastic hematopoietic progenitors. *Blood,* 91**,** 3134-43.

OKUDA, T., VAN DEURSEN, J., HIEBERT, S. W., GROSVELD, G. & DOWNING, J. R. 1996. AML1, the target of multiple chromosomal translocations in human leukemia, is essential for normal fetal liver hematopoiesis. *Cell,* 84**,** 321-30.

OKUNO, Y., HUANG, G., ROSENBAUER, F., EVANS, E. K., RADOMSKA, H. S., IWASAKI, H., AKASHI, K., MOREAU-GACHELIN, F., LI, Y., ZHANG, P., GOTTGENS, B. & TENEN, D. G. 2005. Potential autoregulation of transcription factor PU.1 by an upstream regulatory element. *Mol Cell Biol,* 25**,** 2832-45.

OLIVARIUS, S., PLESSY, C. & CARNINCI, P. 2009. High-throughput verification of transcriptional starting sites by Deep-RACE. *Biotechniques,* 46**,** 130-2.

PETERSON, L. F., LO, M. C., OKUMURA, A. J. & ZHANG, D. E. 2007. Inability of RUNX1/AML1 to breach AML1-ETO block of embryonic stem cell definitive hematopoiesis. *Blood Cells Mol Dis,* 39**,** 321-8.

PHILLIPS-CREMINS, J. E., SAURIA, M. E., SANYAL, A., GERASIMOVA, T. I., LAJOIE, B. R., BELL, J. S., ONG, C. T., HOOKWAY, T. A., GUO, C., SUN, Y., BLAND, M. J., WAGSTAFF, W., DALTON, S., MCDEVITT, T. C., SEN, R., DEKKER, J., TAYLOR, J. & CORCES, V. G. 2013. Architectural protein subclasses shape 3D organization of genomes during lineage commitment. *Cell,* 153**,** 1281-95.

PLASS, C., OAKES, C., BLUM, W. & MARCUCCI, G. 2008. Epigenetics in acute myeloid leukemia. *Semin Oncol,* 35**,** 378-87.

PTASINSKA, A., ASSI, S. A., MANNARI, D., JAMES, S. R., WILLIAMSON, D., DUNNE, J., HOOGENKAMP, M., WU, M., CARE, M., MCNEILL, H., CAUCHY, P., CULLEN, M., TOOZE, R. M., TENEN, D. G., YOUNG, B. D., COCKERILL, P. N., WESTHEAD, D. R., HEIDENREICH, O. & BONIFER, C. 2012. Depletion of RUNX1/ETO in t(8;21) AML cells leads to genome-wide changes in chromatin structure and transcription factor binding. *Leukemia,* 26**,** 1829-41.

RADOMSKA, H. S., ALBERICH-JORDA, M., WILL, B., GONZALEZ, D., DELWEL, R. & TENEN, D. G. 2012. Targeting CDK1 promotes FLT3-activated acute myeloid leukemia differentiation through C/EBPalpha. *J Clin Invest,* 122**,** 2955-66.

RANDO, O. J. & AHMAD, K. 2007. Rules and regulation in the primary structure of chromatin. *Curr Opin Cell Biol,* 19**,** 250-6.

RINN, J. L. & CHANG, H. Y. 2012. Genome regulation by long noncoding RNAs. *Annu Rev Biochem,* 81**,** 145-66.

RINN, J. L., KERTESZ, M., WANG, J. K., SQUAZZO, S. L., XU, X., BRUGMANN, S. A., GOODNOUGH, L. H., HELMS, J. A., FARNHAM, P. J., SEGAL, E. & CHANG, H. Y. 2007. Functional demarcation of active and silent chromatin domains in human HOX loci by noncoding RNAs. *Cell,* 129**,** 1311-23.

ROSENBAUER, F., OWENS, B. M., YU, L., TUMANG, J. R., STEIDL, U., KUTOK, J. L., CLAYTON, L. K., WAGNER, K., SCHELLER, M., IWASAKI, H., LIU, C., HACKANSON, B., AKASHI, K., LEUTZ, A., ROTHSTEIN, T. L., PLASS, C. & TENEN, D. G. 2006. Lymphoid cell growth and transformation are suppressed by a key regulatory element of the gene encoding PU.1. *Nat Genet,* 38**,** 27-37.

ROSENBAUER, F. & TENEN, D. G. 2007. Transcription factors in myeloid development: balancing differentiation with transformation. *Nat Rev Immunol,* 7**,** 105-17.

ROSENBAUER, F., WAGNER, K., KUTOK, J. L., IWASAKI, H., LE BEAU, M. M., OKUNO, Y., AKASHI, K., FIERING, S. & TENEN, D. G. 2004. Acute myeloid leukemia induced by graded reduction of a lineage-specific transcription factor, PU.1. *Nat Genet,* 36**,** 624-30.

ROTHENBERG, E. V. & ANDERSON, M. K. 2002. Elements of transcription factor network design for T-lineage specification. *Dev Biol,* 246**,** 29-44.

SADO, T., HOKI, Y. & SASAKI, H. 2005. Tsix silences Xist through modification of chromatin structure. *Dev Cell,* 9**,** 159-65.

SCHARDIN, M., CREMER, T., HAGER, H. D. & LANG, M. 1985. Specific staining of human chromosomes in Chinese hamster x man hybrid cell lines demonstrates interphase chromosome territories. *Hum Genet,* 71**,** 281-7.

SCHELLER, M., HUELSKEN, J., ROSENBAUER, F., TAKETO, M. M., BIRCHMEIER, W., TENEN, D. G. & LEUTZ, A. 2006. Hematopoietic stem cell and multilineage defects generated by constitutive beta-catenin activation. *Nat Immunol,* 7**,** 1037-47.

SCHNITTGER, S., DICKER, F., KERN, W., WENDLAND, N., SUNDERMANN, J., ALPERMANN, T., HAFERLACH, C. & HAFERLACH, T. 2011. RUNX1 mutations are frequent in de novo AML with noncomplex karyotype and confer an unfavorable prognosis. *Blood,* 117**,** 2348-57.

SCHOENFELDER, S., SEXTON, T., CHAKALOVA, L., COPE, N. F., HORTON, A., ANDREWS, S., KURUKUTI, S., MITCHELL, J. A., UMLAUF, D., DIMITROVA, D. S., ESKIW, C. H., LUO, Y., WEI, C. L., RUAN, Y., BIEKER, J. J. & FRASER, P. 2010. Preferential associations between co-regulated genes reveal a transcriptional interactome in erythroid cells. *Nat Genet,* 42**,** 53-61.

SCHUBELER, D. & ELGIN, S. C. 2005. Defining epigenetic states through chromatin and RNA. *Nat Genet,* 37**,** 917-8.

SEXTON, T. & CAVALLI, G. 2013. The 3D genome shapes up for pluripotency. *Cell Stem Cell,* 13**,** 3-4.

SEXTON, T., YAFFE, E., KENIGSBERG, E., BANTIGNIES, F., LEBLANC, B., HOICHMAN, M., PARRINELLO, H., TANAY, A. & CAVALLI, G. 2012. Three-dimensional folding and functional organization principles of the Drosophila genome. *Cell,* 148**,** 458-72.

SHYKIND, B. M., ROHANI, S. C., O'DONNELL, S., NEMES, A., MENDELSOHN, M., SUN, Y., AXEL, R. & BARNEA, G. 2004. Gene switching and the stability of odorant receptor gene choice. *Cell,* 117**,** 801-15.

SILVA, F. P., MOROLLI, B., STORLAZZI, C. T., ANELLI, L., WESSELS, H., BEZROOKOVE, V., KLUIN-NELEMANS, H. C. & GIPHART-GASSLER, M. 2003. Identification of RUNX1/AML1 as a classical tumor suppressor gene. *Oncogene,* 22**,** 538-47.

SILVA, F. P., SWAGEMAKERS, S. M., ERPELINCK-VERSCHUEREN, C., WOUTERS, B. J., DELWEL, R., VRIELING, H., VAN DER SPEK, P., VALK, P. J. & GIPHART-GASSLER, M. 2009. Gene expression profiling of minimally differentiated acute myeloid leukemia: M0 is a distinct entity subdivided by RUNX1 mutation status. *Blood,* 114**,** 3001-7.

SPLINTER, E., HEATH, H., KOOREN, J., PALSTRA, R. J., KLOUS, P., GROSVELD, F., GALJART, N. & DE LAAT, W. 2006. CTCF mediates long-range chromatin looping and local histone modification in the beta-globin locus. *Genes Dev,* 20**,** 2349-54.

STABER, P. B., ZHANG, P., YE, M., WELNER, R. S., NOMBELA-ARRIETA, C., BACH, C., KERENYI, M., BARTHOLDY, B. A., ZHANG, H., ALBERICH-JORDA, M., LEE, S., YANG, H., NG, F., ZHANG, J., LEDDIN, M., SILBERSTEIN, L. E., HOEFLER, G., ORKIN, S. H., GOTTGENS, B., ROSENBAUER, F., HUANG, G. & TENEN, D. G. 2013. Sustained PU.1 levels balance cell-cycle regulators to prevent exhaustion of adult hematopoietic stem cells. *Mol Cell,* 49**,** 934-46.

STEIDL, U., ROSENBAUER, F., VERHAAK, R. G., GU, X., EBRALIDZE, A., OTU, H. H., KLIPPEL, S., STEIDL, C., BRUNS, I., COSTA, D. B., WAGNER, K., AIVADO, M., KOBBE, G., VALK, P. J., PASSEGUE, E., LIBERMANN, T. A., DELWEL, R. & TENEN, D. G. 2006. Essential role of Jun family transcription factors in PU.1 knockdown-induced leukemic stem cells. *Nat Genet,* 38**,** 1269-77.

SWERDLOW, S. H., CAMPO, E., HARRIS, N.L., JAFFE, E.S., PILERI, S.A., STEIN, H., THIELE, J., VARDIMAN, J.W 2008. WHO Classification of Tumours of Haematopoietic and Lymphoid Tissues, Fourth Edition. *IARC*.

TANG, J. L., HOU, H. A., CHEN, C. Y., LIU, C. Y., CHOU, W. C., TSENG, M. H., HUANG, C. F., LEE, F. Y., LIU, M. C., YAO, M., HUANG, S. Y., KO, B. S., HSU, S. C.,

WU, S. J., TSAY, W., CHEN, Y. C., LIN, L. I. & TIEN, H. F. 2009. AML1/RUNX1 mutations in 470 adult patients with de novo acute myeloid leukemia: prognostic implication and interaction with other gene alterations. *Blood,* 114**,** 5352-61.

TENEN, D. G. 2003. Disruption of differentiation in human cancer: AML shows the way. *Nat Rev Cancer,* 3**,** 89-101.

TSAI, M. C., MANOR, O., WAN, Y., MOSAMMAPARAST, N., WANG, J. K., LAN, F., SHI, Y., SEGAL, E. & CHANG, H. Y. 2010. Long noncoding RNA as modular scaffold of histone modification complexes. *Science,* 329**,** 689-93.

VANGALA, R. K., HEISS-NEUMANN, M. S., RANGATIA, J. S., SINGH, S. M., SCHOCH, C., TENEN, D. G., HIDDEMANN, W. & BEHRE, G. 2003. The myeloid master regulator transcription factor PU.1 is inactivated by AML1-ETO in t(8;21) myeloid leukemia. *Blood,* 101**,** 270-7.

VOSO, M. T., BURN, T. C., WULF, G., LIM, B., LEONE, G. & TENEN, D. G. 1994. Inhibition of hematopoiesis by competitive binding of transcription factor PU.1. *Proc Natl Acad Sci U S A,* 91**,** 7932-6.

WALTER, M. J., PARK, J. S., RIES, R. E., LAU, S. K., MCLELLAN, M., JAEGER, S., WILSON, R. K., MARDIS, E. R. & LEY, T. J. 2005. Reduced PU.1 expression causes myeloid progenitor expansion and increased leukemia penetrance in mice expressing PML-RARalpha. *Proc Natl Acad Sci U S A,* 102**,** 12513-8.

WANG, C. Q., MOTODA, L., SATAKE, M., ITO, Y., TANIUCHI, I., TERGAONKAR, V. & OSATO, M. 2013. Runx3 deficiency results in myeloproliferative disorder in aged mice. *Blood,* 122**,** 562-6.

WANG, Y., KELLNER, J., LIU, L. & ZHOU, D. 2011. Inhibition of p38 mitogen-activated protein kinase promotes ex vivo hematopoietic stem cell expansion. *Stem Cells Dev,* 20**,** 1143-52.

WEI, Z., GAO, F., KIM, S., YANG, H., LYU, J., AN, W., WANG, K. & LU, W. 2013. Klf4 organizes long-range chromosomal interactions with the oct4 locus in reprogramming and pluripotency. *Cell Stem Cell,* 13**,** 36-47.

WILKINSON, A. C., BALLABIO, E., GENG, H., NORTH, P., TAPIA, M., KERRY, J., BISWAS, D., ROEDER, R. G., ALLIS, C. D., MELNICK, A., DE BRUIJN, M. F. & MILNE, T. A. 2013. RUNX1 is a key target in t(4;11) leukemias that contributes to gene activation through an AF4-MLL complex interaction. *Cell Rep,* 3**,** 116-27.

WILSON, N. K., FOSTER, S. D., WANG, X., KNEZEVIC, K., SCHUTTE, J., KAIMAKIS, P., CHILARSKA, P. M., KINSTON, S., OUWEHAND, W. H., DZIERZAK, E., PIMANDA, J. E., DE BRUIJN, M. F. & GOTTGENS, B. 2010a. Combinatorial transcriptional control in blood stem/progenitor cells: genome-wide analysis of ten major transcriptional regulators. *Cell Stem Cell,* 7**,** 532-44.

WILSON, N. K., TIMMS, R. T., KINSTON, S. J., CHENG, Y. H., ORAM, S. H., LANDRY, J. R., MULLENDER, J., OTTERSBACH, K. & GOTTGENS, B. 2010b. Gfi1 expression is controlled by five distinct regulatory regions spread over 100 kilobases, with Scl/Tal1, Gata2, PU.1, Erg, Meis1, and Runx1 acting as upstream regulators in early hematopoietic cells. *Mol Cell Biol,* 30**,** 3853-63.

XIONG, W. & FERRELL, J. E., JR. 2003. A positive-feedback-based bistable 'memory module' that governs a cell fate decision. *Nature,* 426**,** 460-5.

YAN, M., KANBE, E., PETERSON, L. F., BOYAPATI, A., MIAO, Y., WANG, Y., CHEN, I. M., CHEN, Z., ROWLEY, J. D., WILLMAN, C. L. & ZHANG, D. E. 2006. A previously unidentified alternatively spliced isoform of t(8;21) transcript promotes leukemogenesis. *Nat Med,* 12**,** 945-9.

YE, M., ERMAKOVA, O. & GRAF, T. 2005. PU.1 is not strictly required for B cell development and its absence induces a B-2 to B-1 cell switch. *J Exp Med,* 202**,** 1411-22.

YE, T., KREBS, A. R., CHOUKRALLAH, M. A., KEIME, C., PLEWNIAK, F., DAVIDSON, I. & TORA, L. 2011. seqMINER: an integrated ChIP-seq data interpretation platform. *Nucleic Acids Res,* 39**,** e35.

YERGEAU, D. A., HETHERINGTON, C. J., WANG, Q., ZHANG, P., SHARPE, A. H., BINDER, M., MARIN-PADILLA, M., TENEN, D. G., SPECK, N. A. & ZHANG, D. E. 1997. Embryonic lethality and impairment of haematopoiesis in mice heterozygous for an AML1-ETO fusion gene. *Nat Genet,* 15**,** 303-6.

YOUNG, R. A. 2011. Control of the embryonic stem cell state. *Cell,* 144**,** 940-54.

ZENG, H., YUCEL, R., KOSAN, C., KLEIN-HITPASS, L. & MOROY, T. 2004. Transcription factor Gfi1 regulates self-renewal and engraftment of hematopoietic stem cells. *EMBO J,* 23**,** 4116-25.

ZHANG, H., JIAO, W., SUN, L., FAN, J., CHEN, M., WANG, H., XU, X., SHEN, A., LI, T., NIU, B., GE, S., LI, W., CUI, J., WANG, G., SUN, J., FAN, X., HU, X., MRSNY, R. J., HOFFMAN, A. R. & HU, J. F. 2013. Intrachromosomal looping is required for activation of endogenous pluripotency genes during reprogramming. *Cell Stem Cell,* 13**,** 30-5.

ZHANG, J., GRINDLEY, J. C., YIN, T., JAYASINGHE, S., HE, X. C., ROSS, J. T., HAUG, J. S., RUPP, D., PORTER-WESTPFAHL, K. S., WIEDEMANN, L. M., WU, H. & LI, L. 2006. PTEN maintains haematopoietic stem cells and acts in lineage choice and leukaemia prevention. *Nature,* 441**,** 518-22.

ZHAO, J., SUN, B. K., ERWIN, J. A., SONG, J. J. & LEE, J. T. 2008. Polycomb proteins targeted by a short repeat RNA to the mouse X chromosome. *Science,* 322**,** 750-6.

ZHAO, Z., TAVOOSIDANA, G., SJOLINDER, M., GONDOR, A., MARIANO, P., WANG, S., KANDURI, C., LEZCANO, M., SANDHU, K. S., SINGH, U., PANT, V., TIWARI, V., KURUKUTI, S. & OHLSSON, R. 2006. Circular chromosome conformation capture (4C) uncovers extensive networks of epigenetically regulated intra- and interchromosomal interactions. *Nat Genet,* 38**,** 1341-7.

7. Annex

Outgoing host laboratory:

Daniel G. Tenen, M.D.
Harvard Medical School,
Beth Israel Deaconess Medical Center,
Division of Hematology and Oncology,
Tel: +1 (617) 667-5561
Fax: +1 (617) 667-3299
Email: dtenen@bidmc.harvard.edu
Internet: http://www.bidmc.harvard.edu/display.asp?node_id=1600

Results of 4.1 have been published in Mol Cell: (Staber et al., 2013)
Results of 4.2 are currently in review in *Blood*.
Results of 4.3: Manuscript in preparation.